DISSERTATION

THE ECOLOGICAL LEGACIES OF DROUGHT, FIRE, AND INSECT DISTURBANCE IN WESTERN NORTH AMERICAN FORESTS

Submitted by

Timothy J. Assal

Graduate Degree Program in Ecology

In partial fulfillment of the requirements

For the Degree of Doctor of Philosophy

Colorado State University

Fort Collins, Colorado

Fall 2015

Doctoral Committee:

Advisor: Jason S. Sibold

Zachary H. Bowen
Geneva W. Chong
Richard L. Knight
Jeffrey T. Morisette

Copyright by Timothy J. Assal 2015

All Rights Reserved

ABSTRACT

THE ECOLOGICAL LEGACIES OF DROUGHT, FIRE, AND INSECT DISTURBANCE IN WESTERN NORTH AMERICAN FORESTS

Temperate forest ecosystems are subject to various disturbances including insect agents, drought and fire, which can have profound effects on the structure of the ecosystem for many years after the event. Impacts of disturbance can vary widely, therefore an understanding of the legacies of an event are critical in the interpretation of contemporary forest patterns and those of the near future. The primary objective of this dissertation was to investigate the ecological legacies of drought, beetle outbreak and ensuing wildfire in two different ecosystems. A secondary objective of my research, data development, was motivated by a lack of available data which precluded ecological investigation of each disturbance.

I studied the effects of drought on deciduous and coniferous forest along a forest-shrubland ecotone in the southern portion of the Wyoming Basin Ecoregion. The results show that forests in the region have experienced high levels of cumulative drought related mortality over the last decade. Negative trends were not consistent across forest type or distributed randomly across the study area. The patterns of long-term trends highlight areas of forest that are resistant, persistent or vulnerable to severe drought.

In the second thread of my dissertation, I used multiple lines of evidence to retrospectively characterize a landscape scale mountain pine beetle disturbance from the 1970s in Glacier National Park. The lack of spatially explicit data on this disturbance was a major data gap since wildfire had removed some of the evidence from the landscape. I used this information to assess the influence of beetle severity on the burn severity of subsequent wildfires in the

decades after the outbreak. Although many factors contribute to burn severity, my results indicate that beetle severity can positively influence burn severity of wildfire. This is likely due to the change in forest structure in the decades after the outbreak and not as a direct result of tree mortality from the outbreak. The long-term perspective of this study suggests that ecological legacies of high severity disturbance may continue to influence subsequent disturbance for many years after the initial event. This work also provides insight on future disturbance interactions associated with the recent mountain pine beetle outbreak that has impacted tens of millions of hectares in western North America over the last two decades.

ACKNOWLEDGEMENTS

As I reflect on my graduate studies at Colorado State University, I am humbled by all the people who have supported me throughout my journey. I would like to extend my gratitude to my dissertation committee for sharing their time and expertise during my graduate studies. My advisor, Jason Sibold, encouraged me to explore many potential avenues of research, all with an eye to push me to become a better ecologist. I like to think that he accomplished his goal. I thank my supervisor, Zachary Bowen, for the opportunity to pursue a doctoral degree while working at the US Geological Survey. Geneva Chong, Jeff Morisette, and Rick Knight each provided support, great insight and constructive comments on draft manuscripts. Finally, Robin Reich lent me invaluable assistance in my research and instilled confidence in my statistical abilities as I move forward in my career.

The research in Wyoming and Colorado (Chapters 2 and 3) was supported by the USGS Fort Collins Science Center and the Wyoming Landscape Conservation Initiative. Logistical support was provided by the Wyoming Game and Fish Department Green River Office and Bureau of Land Management Rock Springs Field Office. I thank Ali Urza, Marie Dematatis, and Darlene Kilpatrick for assistance in the field, and Anne and Jim Assal for their contributions to data entry. The research in Glacier National Park (Chapters 4 and 5) was supported by a National Park Service grant through the Rocky Mountains Cooperative Ecosystem Studies Unit (IMR H1200090004), with logistical support provided by the USGS Fort Collins Science Center. I thank Dennis Divoky, Mike McClellan and Sheree West for provision of data, Dan Manier and Brian Cade for thoughtful discussion on research direction, and Michael Wimberly for a sample R script for the SAR analysis. I gratefully acknowledge the USGS Earth Resources Observation Systems Data Center for provision of much of the satellite data utilized in this dissertation. The

planning for the first Landsat satellite began in the mid-1960s and I am greatly indebted to all of the people that made this program a reality, those that have maintained it, and those who had the foresight to make the archive open access data.

I had the opportunity to participate in two unique fellowships during my graduate studies. A fellowship in the School of Global Environmental Sustainability at Colorado State University changed the way I communicate science. An open science fellowship with the National Center for Ecological Analysis and Synthesis at the University of California, Santa Barbara changed the way I do science. I extend my gratitude to both of these organizations for their support which greatly influenced my research and led to new friendships and collaborations.

I thank my classmates, colleagues and friends in the CSU ecology community; it is a privilege to be a part of your fraternity. I extend a special thanks to my lab mates in the CSU Biogeography Lab, especially, Ali Urza, Lucy Burris, Carlyn Perovich and Sayat Temirbekov. Your ideas, discussions and camaraderie enriched my time in the lab. Although it was a challenge to continue working at the USGS during my graduate studies, it also afforded me unique opportunities to interact with many experts in my field. I would like to thank my colleagues (far too many to name) for their assistance, support and ideas. In particular, I thank Mike O'Donnell for his world-class expertise in geospatial analysis and Pat Anderson for his support and encouragement throughout this entire process. Finally, I am most grateful to all of my family and friends who supported me and preserved my sanity during my studies. Last, but certainly, not least, I thank Erin whose unwavering love and support was the foundation that made this dissertation a reality.

TABLE OF CONTENTS

LIST OF TABLES

LIST OF FIGURES

CHAPTER 1: Introduction

1.1 DISTURBANCE IN FOREST ECOSYSTEMS

A disturbance is considered a relatively discrete event that changes the resource availability or physical environment and in turn disrupts the structure of an ecosystem, community or population (White and Pickett, 1985). Such an event can be abiotic (e.g. drought, desiccation stress), biotic (e.g. insect or fungal agent) or some combination of the two (e.g. fire), and result in punctuated killing, displacement or damaging of one or more individuals of an ecosystem (Sousa, 1984). The spatial and temporal dynamics of disturbances over a period of time that affect a given area or ecosystem are known as the disturbance regime (Turner, 2010). The disturbance regime includes characteristics of multiple disturbances such as the spatial distribution, frequency, return interval, rotation period, as well as characteristics of individual disturbances such as size, intensity and severity (Sousa, 1984; Turner, 2010).

Disturbances are key drivers of spatial and temporal heterogeneity at various scales because they can alter ecosystem components and subsequent trajectory (Turner, 2010). The ensuing landscape pattern influences the rate and pattern of energy flow, nutrient cycling, wildlife and human responses, and susceptibility to subsequent disturbance (Turner and Dale, 1998; Veblen et al., 1994). Disturbance can result in changes in species composition and ecotone boundaries (Allen and Breshears, 1998) and accelerate potential transitions to no-analog communities in the future (Williams and Jackson, 2007). Such changes could have large implications on the quantity, quality and distribution of habitat leading to impacts on species biogeography (Turner, 2010).

Large, infrequent disturbances are a key mechanism for landscape pattern in forests (Turner and Dale, 1998) due to the enduring legacies of physical and biological structure

produced from such disturbances (Foster et al., 1998). In addition to the area impacted by the disturbance, the biotic remnants or disturbance residuals contribute to the vegetation pattern in forested landscapes (Bebi et al., 2003; Turner and Dale, 1998). Much of the literature focuses on large disturbances, but legacies can persist at some level regardless of the size or frequency of the disturbance (Turner et al., 1998). An understanding of specific disturbance impact on pattern and legacy forms the foundation of basic landscape ecology research (Turner, 1989). Furthermore, this information becomes critical when evaluating characteristics of ecosystem recovery from different types of disturbance (Foster et al., 1998). Given that legacies can persist for decades to centuries, past disturbance is important in explaining the present landscape. However, contemporary and recent disturbance, coupled with global climate change will likely be key mechanisms of ecological dynamics well into the future (Turner, 2010).

Temperate forest ecosystems are subject to various disturbances such as insect agents, drought and fire (Allen, 2009; Foster et al., 1998; Logan et al., 2003). These disturbances contribute to ecological legacies that can have profound effects on the structure of the ecosystem for many years after the event (Turner and Dale, 1998). However, impacts and legacies of disturbance can vary widely in extent, duration and severity over space and time. Superimposed on this concept is global climate change which is expected to increase rates of forest disturbance (Dale et al., 2001; Overpeck et al., 1990). Therefore an understanding of disturbance events and legacies are critical in the interpretation of contemporary forest patterns (Foster et al., 1998) and those of the near future (~ 50 years).

1.2 CLIMATE CHANGE AND DISTURBANCE EVENTS

Global climate change is expected to impact temperature and precipitation regimes and increase the frequency of extreme events (IPCC, 2007). Global mean surface temperature has

risen by 0.74 °C (+/- 0.18 °C) over the last 100 years; with the warming rate over the last 50 years nearly double that of earlier in the century. However, warming rates have not been steady nor uniform spatially (different locations) or temporally (different seasons). Variability in global precipitation has not been uniform, and changes have been observed in the amount, intensity, frequency and type of precipitation. Radiative forcing affects evaporation and sensible heating rates which influence the amount, frequency, intensity, duration, and type of precipitation of a localized area (Trenberth et al., 2003). Extreme events (values exceeded 1, 5, or 10% of the time) are an expression of increased climate variability leading to changes in the frequency and intensity of events. Decreased land precipitation and increased temperatures have enhanced evapotranspiration and the intensity, duration and spatial extent of drought has increased (particularly in the last three decades) (IPCC, 2007). The Palmer Drought Severity Index (Palmer, 1965) indicates that very dry areas have more than doubled since the 1970s (Dai et al., 2004). The El Niño – Southern Oscillation (ENSO) was responsible in part for the precipitation decrease in the early 1980s, but surface warming is cited as the primary cause after the mid-1980s (Dai et al., 2004). In the late 1990s and early 2000s, over half of the coterminous United States experienced moderate to severe drought conditions with record (or near-record) breaking precipitation deficits throughout the western part of the country (Cook et al., 2004). This event brought attention to drought vulnerability in the semi-arid western United States. Warming accelerates land surface drying which increases drought potential (IPCC, 2007), therefore an increase in warming could result in elevated aridity in western North America (Cook et al., 2004).

Regional climate models (RCMs) project that all of North America is likely to warm during this century, with annual mean warming surpassing the global mean rate of warming in

most areas (IPCC, 2007). Global and regional simulations predict that a 1 to 2.5 °C increase in temperature by mid-century will have a strong impact on snowpack in the western United States (Leung et al., 2004), as a result of delayed autumn snowfall, earlier spring snowmelt and changes in precipitation form (IPCC, 2007). Even small changes in temperature and precipitation can magnify impacts to snowpack and runoff on monthly and seasonal time scales due to various surface hydrological and land-atmosphere feedback processes (Leung et al., 2004). RCMs using the A2 emission scenario project that the increase in atmospheric concentrations of greenhouse gases will result in a dramatic increase in extreme heat events, decreases in extreme cold events and increases in extreme precipitation events (Diffenbaugh et al., 2005). Although large-scale climate dynamics govern these changes, fine-scale climate-system modifiers will also play a part, especially in the topographically complex terrain of the western United States (Diffenbaugh et al., 2005).

Many disturbances have a significant climate forcing and research over the last couple of decades has demonstrated that disturbance regimes are in a phase of rapid change (Turner, 2010). Three major disturbance types that are of interest for my research are bark beetle outbreaks, severe drought and fire. Bark beetles (Dendroctonae) are directly vulnerable to disruption by climate change due to impacts on developmental timing, cold tolerance and habitat constraints (Bentz et al., 2010; Hicke et al., 2006; Logan et al., 2003). Indirect effects of climate include host-tree vigor and other community associates (Bentz et al., 2010). Severe drought in the early part of the last decade contributed to stress, dieback and mortality across diverse forest types (Allen, 2009; Breshears et al., 2005; Gitlin et al., 2006; Michaelian et al., 2011). The frequency of large fires in the western United States has increased due to warming temperatures, earlier snowmelt, and longer fire seasons (Littell et al., 2009; Westerling et al., 2006). Future

predictions indicate that fires may become more frequent and severe, leading to novel fire-climate-vegetation relationships (Lutz et al., 2009; Westerling et al., 2011). Research on interactions among disturbances has increased in recent years (Simard et al., 2011), yet understanding interactions remains a key challenge in ecology (Turner, 2010).

1.3 RESOURCE MANAGEMENT AND FOREST DISTURBANCE

Climatic means and variability shape patterns in vegetation through the seasonal balance between energy supply and moisture (Stephenson, 1990). Climate exerts top-down control on ecosystem pattern and process and vegetation is vulnerable to water stress from drought and warm temperatures (Allen, 2009). If water for growth is not available, the energy acts to heat and stress the plant (Stephenson, 1990). Severe drought in the early part of the last decade was the mechanism for disturbance through tree stress, dieback and mortality across diverse forest types (Allen, 2009; Breshears et al., 2005; Gitlin et al., 2006; Michaelian et al., 2011). Drought has indirect effects on other disturbances including bark beetles and fire. Drought reduces host-tree vigor which increases insect attack probability (Bentz et al., 2010). Drought contributes to flammability of fuels and decreased snowpack, resulting in longer fire seasons (Littell et al., 2009; Westerling et al., 2006). Therefore in this framework, drought is considered both an indirect mechanism for other disturbance types as well as a disturbance under severe drought circumstances.

Current forest managers are faced with increasing levels of uncertainty given that future landscapes will likely be different from both the past and present (Millar et al., 2007). The use of historical range and variability (HRV) has often been employed by land managers (Keane et al., 2009), but this idea may no longer be appropriate where future, no-analog communities do not reflect historic conditions (Williams and Jackson, 2007). A contrasting approach to gain

insight into future landscapes uses predictive models. Predictive models have provided valuable information on future impacts, but have been criticized in the use of assumptions and limited knowledge (Sinclair et al., 2010). The study of recent events falls somewhere between HRV and predictive models and has the potential to reduce levels of uncertainty as we move into the future. Analyzing recent events may provide resource managers the most realistic view of landscapes over the next 50 years.

1.4 REMOTE SENSING OF FOREST DISTURBANCE

Remote sensing is the collection of information about an object, without being in direct contact with the object. Disturbance alters ecosystem structure by both abrupt, conspicuous change and by gradual, slow change over some period of time. Such impacts allow remote sensing to capture the pre- and post-disturbance landscape, and in some cases, the duration of the event. The need to measure change over space is clear, but the ability to measure change over time is paramount to remote sensing of forest disturbance. Consideration of spatial and temporal scale is a prominent theme in the work presented in this dissertation. Disturbance such as wildfire or land cover change may occur very quickly and result in conspicuous change. However, the impact of disturbances such as drought or insect outbreaks may not be realized until the timeframe of study is expanded.

The remote sensing archive is a great resource for my work as much of the research presented in this dissertation has a focus on retrospective analysis of events that occurred over the last 40 years. Available imagery represents tradeoffs between spatial, temporal and spectral resolution. Multispectral imagery combined with temporal trend analysis provides high utility to assess impacts to forest vegetation from drought, fire, and insect damage. Aerial photography is a valuable research tool that provides detailed records of forest landscapes over the last half

century. Although limited in spatial extent, such records can provide a snapshot of disturbance at one or multiple points in time. This information can be scaled up to lower spatial resolution, but increased spatial extent of satellite imagery. Scale is an integral part of ecological research (Levin, 1992), and the ability to scale up from local areas to regional landscapes is critical to our understanding of ecosystems (Turner, 2010; Wilson et al., 2010).

Various types of open or freely shared remotely sensed data are utilized in this dissertation: traditional landscape photos, digital and hardcopy aerial photos, and a number of satellite imagery platforms (Landsat Multispectral Scanner (MSS), Landsat Thematic Mapper (TM), Landsat Enhanced Thematic Mapper (ETM+), Landsat Operational Land Imager (OLI), Système Pour l'Observation de la Terre (SPOT 5), and Moderate Resolution Imaging Spectroradiometer (MODIS)). The value of historic records should never be underestimated and the opportunistic scientist might find value where others do not. Had it not been for the heroic actions of one Park Service employee during an office cleanup, a very important set of aerial photos would have been discarded and never found its way into Chapter 4 of this dissertation.

1.5 RESEARCH MOTIVATION AND OBJECTIVES

Numerous studies highlight the value of spatially explicit research as disturbance impacts are not uniform over time and space. For example, the 1988 fires in Yellowstone National Park burned a very large area (250,000 ha) but 75% of the burned area was less than 200 m from unburned forest which has large implications for post-fire regeneration (Turner et al., 1994). In northern New Mexico, the ecotone between ponderosa pine forest and pinyon-juniper woodland seen on the landscape today shifted by upwards of two kilometers following a drought in the 1950s. Such information is valuable to a wide audience spanning local resource managers to national policy makers. My work aims to contribute to this field through several lines of research

addressed in this discussion. The overall goal of this dissertation is to uncover the ecological legacies that recent drought, insect outbreaks and fire have on forested ecosystems. These disturbances are major issues in the two regions of study and will continue to be as we move into an uncertain future. It is my hope that the research contributes to an ecological understanding of the subject matter, but also provides a framework for retrospective study of ecosystem disturbance than can be applied to other ecosystems. My research is further motivated by a lack of available data that limit investigation of these questions. I use a combination of remote sensing, geospatial and statistical analysis to develop datasets that can then be used to investigate larger ecological questions. The two major threads of my dissertation research are summarized below.

Drought in the Forest-Shrubland Ecotone – Little Mountain Ecosystem

What are the spatial and temporal effects of recent drought in a forested ecosystem expected to be vulnerable to climate change?

In the southern part of the Wyoming Basin Ecoregion, referred to as the Little Mountain Ecosystem (LME), relatively small patches of deciduous and coniferous forest occur on moist sites in a matrix of sagebrush steppe. Multiple entities have identified the region as a priority area for conservation given the important habitat it provides many wildlife species. The area has experienced a relatively dry period since 2000, punctuated by two years of extreme drought. Lack of aspen regeneration due to high rates of herbivory is a local concern, yet little attention has been given to the effect of top down controls on the condition of the forest across the region. Recent drought-related mortality of aspen has been documented in western North America (Michaelian et al., 2011; Worrall et al., 2008) and multiple studies have also documented an increase in mortality rates of coniferous species throughout the western United States over the

later part of the 20th century (Allen and Breshears, 1998; Breshears et al., 2005; van Mantgem et al., 2009). These events are driven by increased water deficit associated with drought, but secondary agents such as bark beetle outbreaks have also contributed to mortality in some areas (van Mantgem et al., 2009). Mortality has been observed in the LME, but the extent and timing has not been documented. The effects of climate change are expected to be most rapid and extreme at ecotones in semi-arid areas (Allen and Breshears, 1998; Gosz, 1992) and the current climate profile for several of the dominant tree species are predicted to be greatly limited or no longer present over the course of the next century (Crookston et al., 2010; Rehfeldt et al., 2009). Ecotones are important barometers of climate change (NEON, 2000) and stress, dieback and mortality are expected to accompany severe drought in this arid landscape. Several recent studies have found the use of a temporal remotely sensed data to be effective in monitoring drought induced changes in arid forests (Lloret et al., 2007; Maselli, 2004; Vogelmann et al., 2009; Volcani et al., 2005). My primary objective is to quantify the spatial and temporal effects of drought on the forests of the Little Mountain Ecosystem. Regional climate is mediated by local topography, and I am also interested in the influence of these bottom-up controls during drought periods across the complex terrain of this semi-arid area. However, regional land cover data did not provide adequate details on forest cover to address our objective. Therefore, my initial objective was to develop new data which accurately portrayed the amount and pattern of forest cover in the area, which I used to address the primary objective.

Mountain Pine Beetle Outbreak and Wildfire – Glacier National Park

Did the severity associated with the 1970s mountain pine beetle outbreak affect the burn severity of subsequent wildfires in Glacier National Park?

The influence of mountain pine beetle on past fire activity (Lynch et al., 2007) and future fire probability (Simard et al., 2011) has been explored in Yellowstone National Park and other areas of western North America, yet similar work has not been conducted in Glacier National Park (GNP). The 1970s mountain pine beetle outbreak in GNP was a high severity disturbance that covered 1400 km^2 (28% of the park) by the end of the decade. However, the aerial survey data from that time did not contain any measure of severity so we cannot determine heterogeneity of the disturbance. In the decades after the outbreak, fire was frequent on the landscape as 27% of the forest in the park burned between 1984 and 2006. The lack of spatially explicit data on the beetle outbreak represents a major data gap and inhibits our ability to investigate the influence of beetle severity on subsequent fire. Recent research has garnered positive results tracking the recent (~1996-2006) beetle outbreak using temporal Landsat TM data (Goodwin et al., 2008; Huang et al., 2010; Meigs et al., 2011). A major challenge of this analysis is to reconstruct the extent of a disturbance in which most of the evidence has been erased through subsequent disturbance. The initial objective was to reconstruct the extent and severity of the beetle outbreak. In the second phase of analysis, I used the model of outbreak severity developed in the first phase to assess the influence of beetle severity on the burn severity of succeeding wildfires.

1.6 DISSERTATION LAYOUT

This dissertation consists of six chapters. This chapter (chapter one) introduces the concept of ecological disturbance in forest ecosystems. Further discussion outlines the influence of climate change on forest disturbance and implications to resource management. I outline the utility of remote sensing in forest disturbance research and the motivation behind my dissertation research. There are two analysis chapters devoted to each geographic area of study covered in

this dissertation. The first chapter (two and four) of each geographic area has a primary focus on modeling an ecological variable of interest then the new datasets are used to address the primary ecological questions of each study area (chapters three and five).

In Chapter two, I present a framework that incorporates aerial photos and satellite imagery to model dominant forest cover at local scales across a forest-shrubland ecotone in the southern portion of the Wyoming Basin Ecoregion (Assal et al., 2015). I developed probability of occurrence models for forest type and combined the outputs into a synthesis map that captures the functional type, size, and distribution pattern of forest cover in a spatially heterogeneous landscape. The output addressed an important research need and provides managers with an important tool to support conservation and monitoring efforts across management unit boundaries. To explore the utility of my findings, I compared my results with basic metrics of forest cover derived from several regional land cover datasets. This information is presented in Appendix A of the dissertation. In the third chapter, I assessed the relationship between remotely sensed indices and field measured forest characteristics. Then I used the index in trend analysis of a long-term satellite dataset to uncover the location, direction and timing of forest change associated with drought. The analysis identifies spatially explicit patterns of long-term trends anchored with ground based evidence to highlight areas of forest that are resistant, persistent or vulnerable to severe drought. The results provide a long-term perspective for the resource management of this area and can be applied to similar ecosystems throughout western North America.

The fourth chapter and fifth chapters are devoted to questions related to mountain pine beetle and wildfire disturbance in Glacier National Park. In chapter four, I present an approach that incorporates multiple lines of evidence to retrospectively characterize the landscape scale

mountain pine beetle disturbance of the late 1970s and early 1980s (Assal et al., 2014). Then I use this dataset in chapter five to determine if beetle severity had a measureable influence on burn severity in wildfires in the ensuing decades after the outbreak. The long-term perspective of the study shows that ecological legacies of a prior high severity beetle outbreak may continue to influence subsequent disturbance for many years after the initial event. The findings of the dissertation are summarized in chapter six.

LITERATURE CITED

Allen, C.D., 2009. Climate-induced forest dieback: an escalating global phenomenon? Unasylva 60, 43–49.

Allen, C.D., Breshears, D.D., 1998. Drought-induced shift of a forest-woodland ecotone: rapid landscape response to climate variation. Proc. Natl. Acad. Sci. 95, 14839–42.

Assal, T., Anderson, P., Sibold, J., 2015. Mapping forest functional type in a forest-shrubland ecotone using SPOT imagery and predictive habitat distribution modelling. Remote Sens. Lett. 6, 755–764. doi:10.1080/2150704X.2015.1072289

Assal, T.J., Sibold, J., Reich, R., 2014. Modeling a Historical Mountain Pine Beetle Outbreak Using Landsat MSS and Multiple Lines of Evidence. Remote Sens. Environ. 155, 275–288. doi:10.1016/j.rse.2014.09.002

Baker, W.L., Flaherty, P.H., Lindemann, J.D., Veblen, T.T., Eisenhart, K., 2002. Effect of vegetation on the impact of a severe blowdown in the southern Rocky Mountains, USA. For. Ecol. Manage. 168, 63–75. doi:10.1016/S0378-1127(01)00730-7

Bebi, P., Kulakowski, D., Veblen, T.T., 2003. Interactions between Fire and Spruce Beetles in a Subalpine Rocky Mountain Forest Landscape. Ecology 84, 362–371.

Bentz, B.J., Régnière, J., Fettig, C.J., Hansen, E.M., Hayes, J.L., Hicke, J.A., Kelsey, R.G., Negrón, J.F., Seybold, S.J., 2010. Climate Change and Bark Beetles of the Western United States and Canada: Direct and Indirect Effects. Bioscience 60, 602–613. doi:10.1525/bio.2010.60.8.6

Breshears, D.D., Cobb, N.., Rich, P.M., Price, K.P., Allen, C.D., Balice, R.G., Romme, W.H., Kastens, J.H., Floyd, M.L., Belnap, J., Anderson, J.J., Myers, O.B., Meyer, C.W., 2005. Regional vegetation die-off in response to global-change-type drought. Proc. Natl. Acad. Sci. U. S. A. 102, 15144–8. doi:10.1073/pnas.0505734102

Cook, E.R., Woodhouse, C.A., Eakin, C.M., Meko, D.M., Stahle, D.W., 2004. Long-term aridity changes in the western United States. Science 306, 1015–8. doi:10.1126/science.1102586

Crookston, N.L., Rehfeldt, G.E., Dixon, G.E., Weiskittel, A.R., 2010. Addressing climate change in the forest vegetation simulator to assess impacts on landscape forest dynamics. For. Ecol. Manage. 260, 1198–1211. doi:10.1016/j.foreco.2010.07.013

Dai, A., Trenberth, K.E., Qian, T., 2004. A Global Dataset of Palmer Drought Severity Index for 1870 – 2002: Relationship with Soil Moisture and Effects of Surface Warming. J. Hydrometeorol. 5, 1117–1130.

Dale, V.H., Joyce, L.A., Mcnulty, S., Neilson, R.P., Ayres, M.P., Flannigan, M.D., Hanson, P.J., Irland, L.C., Lugo, A.E., Peterson, C.J., Simberloff, D., Swanson, F.J., Stocks, B.J., Wotton, B.M., 2001. Climate Change and Forest Disturbances. Bioscience 51, 723–734. doi:10.1641/0006-3568(2001)051

Diffenbaugh, N.S., Pal, J.S., Trapp, R.J., Giorgi, F., 2005. Fine-scale processes regulate the response of extreme events to global climate change. Proc. Natl. Acad. Sci. U. S. A. 102, 15774–8. doi:10.1073/pnas.0506042102

Foster, D.R., Knight, D.H., Franklin, J.F., 1998. Landscape Patterns and Legacies Resulting from Large, Infrequent Forest Disturbances. Ecosystems 1, 497–510. doi:10.1007/s100219900046

Gitlin, A.R., Sthultz, C.M., Bowker, M.A., Stumpf, S., Paxton, K.L., Kennedy, K., Muñoz, A., Bailey, J.K., Whitham, T.G., 2006. Mortality gradients within and among dominant plant populations as barometers of ecosystem change during extreme drought. Conserv. Biol. 20, 1477–86. doi:10.1111/j.1523-1739.2006.00424.x

Goodwin, N.R., Coops, N.C., Wulder, M.A., Gillanders, S., Schroeder, T.A., Nelson, T., 2008. Estimation of insect infestation dynamics using a temporal sequence of Landsat data. Remote Sens. Environ. 112, 3680–3689. doi:10.1016/j.rse.2008.05.005

Gosz, J.R., 1992. Gradient analysis of ecological change in time and space: implications for forest management. Ecol. Appl. 2, 248–261.

Hicke, J.A., Logan, J.A., Powell, J., Ojima, D.S., 2006. Changing temperatures influence suitability for modeled mountain pine beetle (Dendroctonus ponderosae) outbreaks in the western United States. J. Geophys. Res. 111, 1–12. doi:10.1029/2005JG000101

Huang, C., Goward, S.N., Masek, J.G., Thomas, N., Zhu, Z., Vogelmann, J.E., 2010. An automated approach for reconstructing recent forest disturbance history using dense Landsat time series stacks. Remote Sens. Environ. 114, 183–198. doi:10.1016/j.rse.2009.08.017

IPCC, I.P. on C.C., 2007. Fourth Assessment Report.

Keane, R.E., Hessburg, P.F., Landres, P.B., Swanson, F.J., 2009. The use of historical range and variability (HRV) in landscape management. For. Ecol. Manage. 258, 1025–1037. doi:10.1016/j.foreco.2009.05.035

Leung, L.R., Qian, Y., Bian, X., Washington, W.M., Han, J., Roads, J.O., 2004. Mid-Century Ensemble Regional Climate Change Scenarios for the Western United States. Clim. Change 62, 75–113.

Levin, S.A., 1992. The Problem of Pattern and Scale in Ecology. Ecology 73, 1943–1967.

Littell, J.S., McKenzie, D., Peterson, D.L., Westerling, A.L., 2009. Climate and wildfire area burned in western U.S. ecoprovinces, 1916-2003. Ecol. Appl. 19, 1003–1021.

Lloret, F., Lobo, a, Estevan, H., Maisongrande, P., Vayreda, J., Terradas, J., 2007. Woody plant richness and NDVI response to drought events in Catalonian (northeastern Spain) forests. Ecology 88, 2270–9.

Logan, J.A., Régnière, J., Powell, J.A., 2003. Assessing the impacts of global warming on forest pest dynamics. Front. Ecol. Environ. 1, 130–137.

Lutz, J.A., van Wagtendonk, J.W., Thode, A.E., Miller, J.D., Franklin, J.F., 2009. Climate, lightning ignitions, and fire severity in Yosemite National Park, California, USA. Int. J. Wildl. Fire 18, 765–774. doi:10.1071/WF08117

Lynch, H.J., Renkin, R.A., Crabtree, R.L., Moorcroft, P.R., 2007. The Influence of Previous Mountain Pine Beetle (Dendroctonus ponderosae) Activity on the 1988 Yellowstone Fires. Ecosystems 9, 1318–1327. doi:10.1007/s10021-006-0173-3

Maselli, F., 2004. Monitoring forest conditions in a protected Mediterranean coastal area by the analysis of multiyear NDVI data. Remote Sens. Environ. 89, 423–433. doi:10.1016/j.rse.2003.10.020

Meigs, G.W., Kennedy, R.E., Cohen, W.B., 2011. A Landsat time series approach to characterize bark beetle and defoliator impacts on tree mortality and surface fuels in conifer forests. Remote Sens. Environ. 115, 3707–3718. doi:10.1016/j.rse.2011.09.009

Michaelian, M., Hogg, E.H., Hall, R.J., Arsenault, E., 2011. Massive mortality of aspen following severe drought along the southern edge of the Canadian boreal forest. Glob. Chang. Biol. 17, 2084–2094. doi:10.1111/j.1365-2486.2010.02357.x

Millar, C.I., Stephenson, N.L., Stephens, S.L., 2007. Climate change and forests of the future: managing in the face of uncertainty. Ecol. Appl. 17, 2145–51.

NEON, 2000. Report on first Workshop on the National Ecological Observatory Network (NEON). Lake Placid, Florida.

Overpeck, J.T., Rind, D., Goldberg, R., 1990. Climate-induced changes in forest disturbance and vegetation. Nature 343, 51–53.

Palmer, W.C., 1965. Meteorological Drought. Weather Bur. Res. Pap. 45.

Rehfeldt, G.E., Ferguson, D.E., Crookston, N.L., 2009. Aspen, climate, and sudden decline in western USA. For. Ecol. Manage. 258, 2353–2364. doi:10.1016/j.foreco.2009.06.005

Rousse, J.W., Hass, R.H., Schell, J.A., Deering, D.W., Harlan, J.C., 1974. Monitoring the vernal advancement of retrogradation of natural vegetation, Type III, Final Report. Greenbelt, Maryland.

Simard, M., Romme, W.H., Griffin, J.M., Turner, M.G., 2011. Do mountain pine beetle outbreaks change the probability of active crown fire in lodgepole pine forests? Ecol. Monogr. 81, 3–24.

Sinclair, S.J., White, M.D., Newell, G.R., 2010. How Useful Are Species Distribution Models for Managing Biodiversity under Future Climates? Ecol. Soc. 15.

Sousa, W.P., 1984. The Role of Disturbance in Natural Communities. Annu. Rev. Ecol. Syst. 15, 353–391.

Stephenson, N.L., 1990. Climatic Control of Vegetation Distribution : The Role of the Water Balance. Am. Nat. 135, 649–670.

Trenberth, K.E., Dai, A., Rasmussen, R.M., Parsons, D.B., 2003. The Changing Character of Precipitation. Bull. Am. Meteorol. Soc. 84, 1205–1217. doi:10.1175/BAMS-84-9-1205

Turner, M.G., 2010. Disturbance and landscape dynamics in a changing world. Ecology 91, 2833–2849. doi:10.1080/03630242.2010.516702

Turner, M.G., 1989. Landscape Ecology: The Effect of Pattern on Process. Annu. Rev. Ecol. Syst. 20, 171–197. doi:10.1146/annurev.es.20.110189.001131

Turner, M.G., Baker, W.L., Peterson, C.J., Peet, R.K., 1998. Factors Influencing Succession: Lessons from Large, Infrequent Natural Disturbances. Ecosystems 511–523.

Turner, M.G., Dale, V.H., 1998. Comparing Large, Infrequent Disturbances: What Have We Learned? Ecosystems 1, 493–496.

Turner, M.G., Hargrove, W.W., Gardner, R.H., Romme, W.H., 1994. Effects of Fire on Landscape Heterogeneity in Yellowstone National Park, Wyoming. J. Veg. Sci. 5, 731–742.

Van Mantgem, P.J., Stephenson, N.L., Byrne, J.C., Daniels, L.D., Franklin, J.F., Fulé, P.Z., Harmon, M.E., Larson, A.J., Smith, J.M., Taylor, A.H., Veblen, T.T., 2009. Widespread increase of tree mortality rates in the western United States. Science (80-.). 323, 521–524. doi:10.1126/science.1165000

Veblen, T.T., Hadley, K.S., Nel, E.M., Kitzberger, T., Reid, M., Villalba, R., 1994. Disturbance regime and disturbance interactions in a Rocky Mountain subalpine forest. J. Ecol. 82, 125–135.

Vogelmann, J.E., Tolk, B., Zhu, Z., 2009. Monitoring forest changes in the southwestern United States using multitemporal Landsat data. Remote Sens. Environ. 113, 1739–1748. doi:10.1016/j.rse.2009.04.014

Volcani, A., Karnieli, A., Svoray, T., 2005. The use of remote sensing and GIS for spatio-temporal analysis of the physiological state of a semi-arid forest with respect to drought years. For. Ecol. Manage. 215, 239–250. doi:10.1016/j.foreco.2005.05.063

Westerling, A.L., Hidalgo, H.G., Cayan, D.R., Swetnam, T.W., 2006. Warming and earlier spring increase western U.S. forest wildfire activity. Science (80-.). 313, 94094–3. doi:10.1126/science.1128834

Westerling, A.L., Turner, M.G., Smithwick, E.A.H., Romme, W.H., Ryan, M.G., 2011. Continued warming could transform Greater Yellowstone fire regimes by mid-21st century. Proc. Natl. Acad. Sci. 108, 13165–13170. doi:10.1073/pnas.1110199108

White, P.S., Pickett, S.T.A., 1985. Natural disturbance and patch dynamics: an introduction, in: The Ecology of Natural Disturbance and Patch Dynamics. Academic Press, New York, New York., pp. 3–13.

Williams, J.W., Jackson, S.T., 2007. Novel climates, no-analog communities, and ecological surprises. Front. Ecol. Environ. 5, 475–482. doi:10.1890/070037

Wilson, A.M., Silander, J.A., Gelfand, A., Glenn, J.H., 2010. Spatial Ecology Scaling up: linking field data and remote sensing with a hierarchical model. Int. J. Geogr. Inf. Sci. 14, 1–13. doi:10.1080/1365881YYxxxxxxxx

Worrall, J.J., Egeland, L., Eager, T., Mask, R.A., Johnson, E.W., Kemp, P.A., Shepperd, W.D., 2008. Rapid mortality of Populus tremuloides in southwestern Colorado, USA. For. Ecol. Manage. 255, 686–696. doi:10.1016/j.foreco.2007.09.071

CHAPTER 2: Mapping Forest Functional Type in a Forest-Shrubland Ecotone using SPOT Imagery and Predictive Habitat Distribution Modeling[1]

2.1 SUMMARY

The availability of land cover data at local scales is an important component in forest management and monitoring efforts. Regional land cover data seldom provide detailed information needed to support local management needs. Here we present a transferable framework to model forest cover by major plant functional type using aerial photos, multi-date Système Pour l'Observation de la Terre (SPOT) imagery, and topographic variables. We developed probability of occurrence models for deciduous broad-leaved forest and needle-leaved evergreen forest using logistic regression in the southern portion of the Wyoming Basin Ecoregion. The model outputs were combined into a synthesis map depicting deciduous and coniferous forest cover type. We evaluated the models and synthesis map using a field validated, independent data source. Results showed strong relationships between forest cover and model variables and the synthesis map was accurate with an overall correct classification rate of 0.87 and Cohen's kappa value of 0.81. The results suggest our method adequately captures the functional type, size and distribution pattern of forest cover in a spatially heterogeneous landscape.

[1] A version of this chapter was published in *Remote Sensing Letters* on 21 August 2015, available online: http://www.tandfonline.com/doi/full/10.1080/2150704X.2015.1072289: Assal, T., Anderson, P., Sibold, J., 2015. Mapping forest functional type in a forest-shrubland ecotone using SPOT imagery and predictive habitat distribution modelling. Remote Sens. Lett. 6, 755–764. doi:10.1080/2150704X.2015.1072289

2.2 INTRODUCTION

Land cover data provides the foundation for a wide variety of geographical analysis and science applications. There have been several national and regional land cover mapping initiatives over the last two decades, most notably the National Land Cover Database (NLCD) (Jin et al., 2013), LANDFIRE (Rollins, 2009), and ReGAP (Davidson et al., 2009). These products have provided tremendous utility in studies documenting land cover change (Radeloff et al., 2005), effects of climate change (Wylie et al., 2014), vegetation change (Bradley and Fleishman, 2008) and conservation planning (Stoms, 2000). However, in some heterogeneous ecosystems, they lack the spatial resolution needed to adequately characterize the extent and juxtaposition of land cover. In the Wyoming Basin ecoregion, small areas of forest are found within sagebrush shrubland at higher elevations which are difficult to adequately characterize using regional land cover data.

Plant functional types (PFTs) are groups of species that share similar structural, physiological and phenological traits (Barbour et al., 1999). PFTs provide a framework to consider how species utilize resource availability and respond to environmental change and management. At the stand scale, multispectral remote sensing can be used to delineate the relationship between vegetation structure and physiology of PFTs, linking biophysical properties to ecological theory (Ustin and Gamon, 2010). Predictive habitat distribution modeling offers the potential to assess the current extent of species as well as effects of global climate change and other change agents. However, a challenge is to better link remote sensing data to underlying ecological relationships and describe the distribution of species along environmental gradients (Zimmermann et al., 2007). Incorporating remote sensing variables in the modeling process allows us to take full

advantage of continuous gradients to delineate biophysical properties of vegetation such as leaf shape, structure, longevity and chlorophyll content (Jones and Vaughan, 2010).

We explored the potential of fine-scale remotely sensed spectral data in predictive habitat distribution modeling of forest cover type across a forest-shrubland ecotone. The two PFTs of interest in the study area are deciduous broad-leaved forest (referred to as deciduous forest) and montane needle-leaved evergreen forest (referred to as coniferous forest). We hypothesized that the delineation between forest functional type would be aided with the addition of multitemporal remote sensing predictors due to differences in phenology between deciduous and coniferous species (Bergen and Dronova, 2007; Zimmermann et al., 2007). The major goal of the study was to develop an operational mapping framework using aerial photos coupled with fine-scale satellite imagery to efficiently model dominant forest cover. The specific objectives were to: 1) develop probability of occurrence models for deciduous and coniferous forest; and 2) to combine model outputs into a field-validated synthesis map depicting forest cover type.

2.3 STUDY AREA

The study area, managed largely by the U.S. Bureau of Land Management, is located in the southern part of the Wyoming Basin ecoregion, spanning parts of southwestern Wyoming, northwestern Colorado, and northeastern Utah (Figure 2.1). Several prominent ridges form a transition zone between basins and mountainous areas (Knight, 1994), where several species of trees exist at the xeric fringes of their respective ranges. Forests are dominated by either aspen (*Populus tremuloides*) or several coniferous species, namely subalpine fir (*Abies lasiocarpa*), Douglas-fir (*Pseudotsuga menziesii*), and lodgepole pine (*Pinus contorta*), that occur as relatively small patches on moist sites in a matrix of mountain sagebrush (*Artemisia tridendata* spp. *vaseyana*) or mixed-species shrublands. Scattered juniper (*Juniperus communis* var.

depressa) and limber pine (*Pinus flexilis*) woodlands, distinct from the montane conifer forest, are found on rocky slopes at lower elevations and small patches of manzanita (*Arctostaphylos patula*) are found in the southern part of the study area. The area has a midlatitude steppe climate with a substantial portion of the annual precipitation occurring as snow. Multiple state and federal agencies, along with the Wyoming Landscape Conservation Initiative (wlci.gov), have identified the region as a priority area for conservation given the important habitat it provides for many wildlife species. Drought-related mortality of aspen is a concern in western North America (Worrall et al., 2008), and lack of aspen regeneration due to high rates of herbivory is a concern locally. Active management seeks to address these concerns and locally accurate maps of forest cover type are critical to support conservation and monitoring efforts.

2.4 METHODS

2.4.1 Explanatory Variables

We identified a contiguous area (1,088 km^2) greater than 2,300 m in elevation known to encompass the forest communities of the study area (Figure 2.1). We explored the relationship of topographic and multi-date remotely sensed variables to forest presence that have had utility in other SDMs (Turner et al., 2003; Zimmermann et al., 2007; Jarnevich et al., 2014; Engler et al., 2013). Topographic variables were derived from a 10 m National Elevation Dataset and remotely sensed variables were derived from terrain corrected Level 1 T SPOT 5 HRG satellite imagery, acquired at no cost (USGS, 2014) (Table 2.1). We obtained two cloud-free dates during leaf-on (07 September 2010) and leaf-off (19 October 2010) conditions from two SPOT scenes (KJ grid 555-267; 555-286). Each of the four images were geometrically registered to National Agriculture Imagery Program (NAIP) aerial photos using 20-25 ground control points with a root mean square error of less than 0.5 pixel. A top-of-atmosphere correction was applied to each

image to account for differences in sensor and viewing angle (Wulder et al., 2006; Vogelmann et al., 2012; Sankey et al., 2008).

Remotely sensed spectral bands and derived vegetation indices often exhibit high levels of collinearity (Engler et al., 2013). Multi-collinearity among all potential explanatory variables was assessed prior to model calibration using the Pearson's correlation coefficient. Variables with a correlation coefficient greater than 0.8 or less than -0.8 were removed from consideration within the same model (Jarnevich et al., 2014). All of the analysis was conducted using the R statistical package (R Development Core Team 2013).

2.4.2 Sample Data

ReGAP land cover data was reclassified into eight land cover categories (including deciduous and coniferous forest), and we used a stratified random selection procedure to ensure an unbiased distribution of sample plots (10 m x 10 m, congruent with a SPOT pixel) across land cover types. Our objective was to capture fine-scale patterns in the study area, while minimizing the impact of spatial dependency between observations. We used a total of 545 plots, with a minimum distance of 250 m (25 pixels) between each plot, to develop presence and absence records. We interpreted recent aerial photographs (natural color and infrared NAIP) and classified each plot as deciduous forest, coniferous forest, or non-forest. Mixed forest is not found at broad scales in the study area, and it is difficult to reliably classify a 10 m NAIP plot as mixed forest. Absence records for deciduous forest included both non-forest and coniferous forest plots, whereas absence records for coniferous forest included non-forest and deciduous forest. We extracted the values of the 19 predictor variables (Table 2.1) at each sample location. The respective leaf-on and leaf-off periods for each band exhibited high collinearity. Leaf-on bands 1, 2, and 4 were also highly correlated along with leaf-on NDVI. We opted to use leaf-on

bands over leaf-off, although leaf-off data was incorporated into ΔNDVI (Table 2.1). We retained band 1 over band 2 since information from band 2 is incorporated into the NDVI variable. This selection process resulted in 13 variables for consideration (Table 2.1), including longitude and latitude to account for spatial autocorrelation (Knapp et al., 2003; Hu and Lo, 2007).

2.4.3 Data Analysis

Logistic regression is a widely used method to predict the probability of a dichotomous variable (i.e., presence, absence of a forest cover type) that has been used in species distribution modeling (SDM) (Engler et al., 2013; Jarnevich et al., 2014; Stohlgren et al., 2010) and other ecological studies (Turner et al., 2003; Wulder et al., 2006; Dubovyk et al., 2013). We used a multivariate generalized linear model (GLM, binomial distribution, logit link function) to create independent models of deciduous (DECID) and coniferous (CONIF) forest cover in the study area. We modeled each cover type independently to maximize information contained in the continuous gradient of biophysical characteristics of these systems. The full dataset (n = 545) was used for model calibration. To simplify the interpretation of the logistic model, we converted the regression coefficients into odds ratios, then calculated the percent change in odds (Wulder et al., 2006). This approach identifies the percent change in the probability of a pixel containing deciduous or coniferous forest relative to changes in independent variables.

We tested several models for each type of forest cover, using different combinations of predictor variables below the acceptable collinearity threshold. For each model a standard stepwise selection by Akaike's Information Criterion (AIC) was used to select the best subset of independent variables and we calculated variance inflation factors (VIF) to ensure all model variables had a value below 5 (Dubovyk et al., 2013). In logistic regression, spatial

autocorrelation violates the assumption that observations are independent and can cause unreliable estimates of the model parameters (Hu and Lo, 2007). We evaluated spatial autocorrelation using the Moran's *I* statistic on each model using Pearson residuals which are comparable to residuals of linear regression models. The neighborhood structure of the spatial weights matrix was defined using inverse distance (Assal et al., 2014).

The two selected models produced a continuous surface with values between zero and one corresponding to the probability of a pixel containing either deciduous or coniferous forest. We used an independent dataset (n=321) representing coniferous, deciduous and non-forest observations to evaluate each model. The reference dataset was compiled from observations of related studies that were visited in the field between 2010 and 2013. We randomly selected 100 presence and 100 absence points of the respective forest cover type for each model to calculate the receiver operator characteristic area under the curve (AUC). For each model, we selected a threshold where the sensitivity was equal to the specificity (Liu et al., 2005) (i.e. the number of false positives were equal to the number of false negatives) to convert each model output into a binary map of presence and absence.

2.4.4 Synthesis Map

The binary maps from the two models were combined into a synthesis map of deciduous and coniferous forest cover. If a pixel was predicted to contain both forest types, the values from each model above the presence threshold were linearly rescaled from 0 to 1. The cover type with the highest occurrence probability was then assigned to the pixel (Engler et al., 2013). Within each cover type, pixels were assigned to neighbors in all eight directions ('queen's move') to identify contiguous forest patches. Patches of three pixels and greater were retained in order to minimize small, likely incorrect classified areas. We used the full, validation dataset (n=321) to

build a confusion matrix to calculate the overall classification accuracy and Cohen's kappa coefficient on the synthesis map.

2.5 RESULTS

Forest cover type was best predicted by a combination of topographic and spectral variables, and the two models included several common variables selected through the model fitting process (Table 2.2). The residuals of both models exhibited very weak or no spatial autocorrelation (DECID; Moran's I=0.005, p=0.052; CONIF; Moran's I=0.001, p=0.38). Aspen, the only deciduous forest type present, have a clonal growth form which produces clustered patches of deciduous forest in the study area. Both of the models had high accuracy with AUC values of 0.92 for DECID and 0.99 for CONIF. The percentage changes in the odds ratio for model variables are shown in Table 2.2. The DECID model indicated that the presence of deciduous forest is mainly associated with high values in the NIR band (band3.leaf-on), north facing slopes, and high values of ΔNDVI. Deciduous forest is more likely to be found in areas higher in elevation, particularly moderate elevations (classes 3 and 2). The model also indicated that deciduous forest was less likely associated with higher values in the green band (band1.leaf-on) and higher TPI values, found along ridge lines and hilltops. The CONIF model indicated presence of coniferous forest is mainly associated with high values in NDVI (NDVI.leaf-on), TPI and elevation and less likely associated with high values in the NIR band (band3.leaf-on) and areas that experience a higher HLI.

A comparison of the output maps, derived from the binary models, revealed high separation between the two models. Less than 1% of all pixels in the study area were predicted to contain both deciduous and coniferous forest. The comparison indicated satisfactory agreement with an overall classification accuracy of 87% (Table 2.3) and a Cohen's kappa coefficient (Cohen,

1960) of 0.81. Our synthesis map identified 61.7 km^2 of forest (Figure 2.2). Deciduous forest accounts for 44% (27.2 km^2) of total forest cover, while the remaining 56% (34.5 km^2) is coniferous forest. There are over 7,000 patches of deciduous forest compared to less than 2,400 coniferous forest patches, and the mean patch size is much smaller for deciduous (0.004 km^2) compared to coniferous forest (0.015 km^2).

2.6 DISCUSSION

The spatial resolution (10 m) of the SPOT imagery appeared particularly appropriate for identifying the extent and pattern of forest cover in this highly heterogeneous ecosystem (Figure 2.3). The models performed well and had little overlap between forest functional types. Furthermore, we considered spatial autocorrelation in our framework which is often overlooked in SDMs. The inclusion of latitude and longitude in the model, as well as treating elevation as an indicator variable, accounted for spatial autocorrelation in the models. Consideration of plant physiology and species traits illuminates the ecological context of biophysical variables that were captured with leaf-on and leaf-off SPOT imagery. Due to differences in seasonal phenology, deciduous forests are more likely to be associated with areas that have a large ΔNDVI between leaf-on and leaf-off periods. Aspen leaves absorb more radiation (and reflect less) in the green region of the electromagnetic spectrum compared to sagebrush and grassland plants (Jones and Vaughan, 2010). Therefore, deciduous forest is associated with lower values in the green band (band1.leaf-on) compared to shrubland and grasslands. Coniferous forests have higher NDVI values than grassland and shrubland, especially late in the growing season when the leaf-on image was acquired. Although deciduous forests have a higher NDVI than coniferous forests, NDVI was not as important in DECID, which also included ΔNDVI and the NIR band (band3.leaf-on). Coniferous forests do not reflect as much radiation as aspen forest, grassland,

and sagebrush and, therefore, are more likely to be associated with lower values in the NIR (band3.leaf-on).

In our synthesis map, the non-forest class had the lowest producer's accuracy (the percentage of reference observations correctly mapped), due to Type 1 errors (i.e. false-positives) in the deciduous forest class (Table 2.3). The DECID model incorrectly classified some small areas of manzanita, non-forested riparian areas, narrow, linear bands of deciduous shrubs and one large herbaceous wetland. There is a trade-off between capturing small patches of deciduous forest and incorrectly classifying some small areas with similar spectral values to deciduous forest. In future work, our methodology could be improved with additional information that discriminates between herbaceous wetlands and deciduous forest. The deciduous forest class had the lowest user's accuracy (the percentage of map locations correctly identified) due to several type II errors (i.e. false-negatives). The higher rate of misclassification might be explained by the open canopy of aspen forests compared to closed, dense coniferous forest. Furthermore, some aspen stands observed in the field had a substantial amount of canopy dieback and tree mortality. Aspen forests with highly reduced leaf area at the time the satellite image was acquired have lower reflectance values and therefore tend to be mapped as non-forest. Although this can be a drawback, it highlights the value of our methodology to capture changes in aspen forest if fine-scale imagery is available over an appropriate time period. The CONIF model performed very strongly as needle-leaved species have a closed canopy that forms dense stands. A few exceptions include several conifer stands dominated by Douglas-fir that experienced high mortality in recent years due to infestation of the Douglas-fir beetle (*Dendroctonus pseudotsugae*).

2.7 CONCLUSIONS

We have presented a framework that incorporates aerial photos and satellite imagery to model dominant forest cover at local scales across a forest-shrubland ecotone. Our modeling process offers a powerful alternative to traditional image classification and our synthesis map provides managers with an important tool to support conservation and monitoring efforts across management unit boundaries. Our study highlights the advantages of using physiologically relevant remote sensing products in predictive modeling and addresses an important research need (e.g. high-resolution remote sensing of aspen distribution, (Kulakowski et al., 2013)). We conclude that our approach is suitable to characterize the extent and juxtaposition of forest cover in a highly heterogeneous ecosystem. Furthermore, our framework utilizes open access aerial photos and satellite data. In this way it is transferable to highly heterogeneous ecosystems to develop critical baseline tree cover data that can be updated at regular intervals to monitor the effects of disturbance and long-term ecosystem dynamics.

Any use of trade, firm, or product names is for descriptive purposes only and does not imply endorsement by the U.S. Government.

2.9 TABLES

Table 2.1. Description of the explanatory variables considered in the analysis.

Variable	Description
Spectral variables	
Band1.leaf-on*	Green band (0.50 µm - 0.59 µm)
Band2.leaf-on	Red band (0.61 µm - 0.68 µm)
Band3.leaf-on*	Near infrared band (0.79 µm - 0.89 µm)
Band4.leaf-on*	Short wave infrared band (1.58 µm - 1.75 µm)
Normalized difference vegetation index (NDVI.leaf-on*)	NDVI = (B3 reflectance – B2 reflectance)/(B3 reflectance + B2 reflectance) (Rousse et al., 1974)
Band1.leaf-off	Green band (0.50 µm - 0.59 µm)
Band2.leaf-off	Red band (0.61 µm - 0.68 µm)
Band3.leaf-off	Near infrared band (0.79 µm - 0.89 µm)
Band4.leaf-off	Short wave infrared band (1.58 µm - 1.75 µm)
Normalized difference vegetation index (NDVI.leaf-off)	NDVI = (B3 reflectance – B2 reflectance)/(B3 reflectance + B2 reflectance) (Rousse et al., 1974)
ΔNDVI*	$\Delta NDVI = NDVI_{leaf\text{-}on} - NDVI_{leaf\text{-}off}$
Topographic variables	
Elevation*	Derived from National elevation dataset
Slope*	Derived from National elevation dataset
North exposure*	Cosine transformation of aspect
East exposure*	Sine transformation of aspect
Heat load index (HLI)*	Potential direct incident radiation (McCune and Keon, 2002; equation 3)
Topographic position index (TPI)*	A measure of slope position and landform type with respect to adjacent grid cells
Longitude*	Longitude at cell centroid
Latitude*	Latitude at cell centroid

Notes: Leaf-on variables were acquired from the 07 September 2010 SPOT image; leaf-off variables were acquired from the 19 October 2010 SPOT image. All variables have a spatial resolution of 10 m. The native resolution for band 4 is 20 m, but it was resampled to 10 m using a nearest neighbour transformation.

*Indicates variable was utilized in the modeling process.

Table 2.2. Predictor variables used in the logistic regression models.

Explanatory variable	DECID model		CONIF model	
	Coefficient	**Change in odds (%)**	**Coefficient**	**Change in odds (%)**
Spectral variables				
NDVI.leaf-on	-	-	1.9164*	580
ΔNDVI	0.3327*	39	-0.2914	-25
Band1.leaf-on	-4.261*	-99	-	-
Band3.leaf-on	3.068*	2050	-3.7485*	-98
Topographic variables				
TPI	-0.5016*	-39	0.8194*	127
HLI	-	-	-0.7466*	-53
North exposure	0.8654*	138	-0.6963	-50
Longitude	$-6.86e^{-05}$*	-	-	-
Latitude	$-1.24e^{-04}$*	-	-	-
Elevation**				
Class 1 (low)	-	-	-	-
Class 2 (low to moderate)	5.053*	15549	0.3221	38
Class 3 (moderate to high)	5.591*	26700	1.7885	498
Class 4 (High)	4.409*	-8119	3.5633*	3428

Notes: Estimates of the model parameters are listed for each model accordingly. **p-values* are significant at 0.05 or lower. **Elevation is treated as an indicator variable; therefore the percent change in odds for each class can only be compared to the reference elevation class (Class 1).

Table 2.3. Confusion matrix for the synthesis forest cover map.

Field data	Classified as:			Producer's accuracy (%)
	Non-forest	**Deciduous forest**	**Coniferous forest**	
Non-forest	**95**	24	3	78
Deciduous forest	6	**86**	5	89
Conifer forest	0	2	**100**	98
User's accuracy (%)	94.1	76.8	92.6	**87**

Note: bold values in the matrix diagonal highlight the correctly predicted samples.

2.10 FIGURES

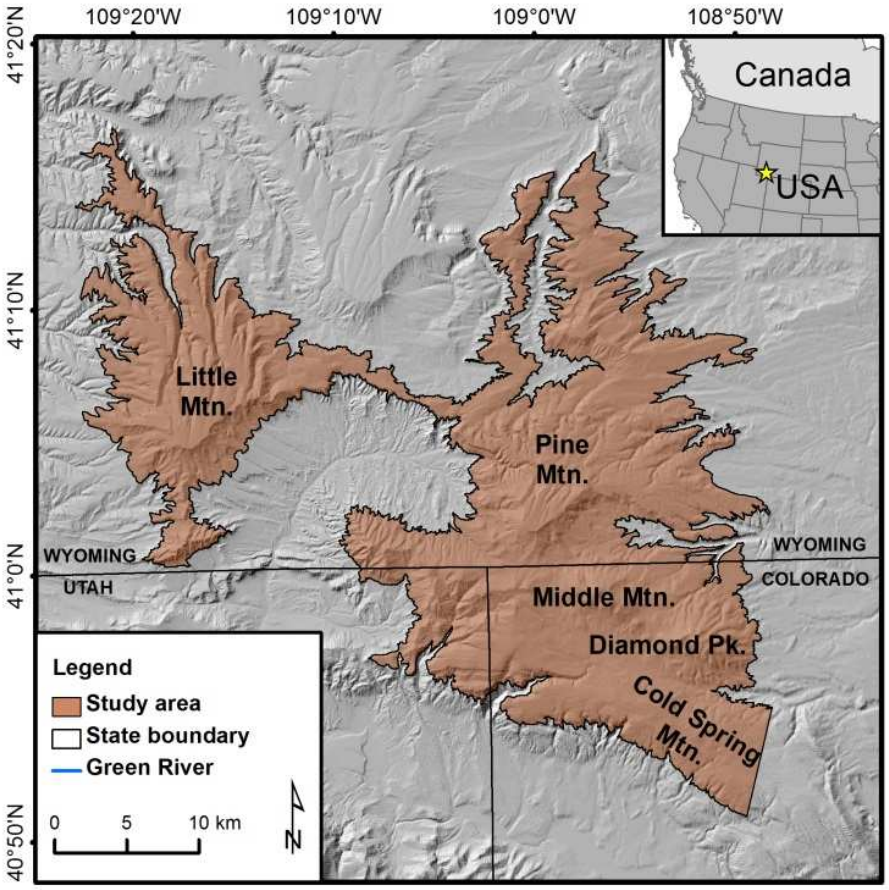

Figure 2.1. Location of study area. Note: approximately 50 km^2 of non-forest were omitted from the southeast corner of the study area due to the extent of the SPOT image.

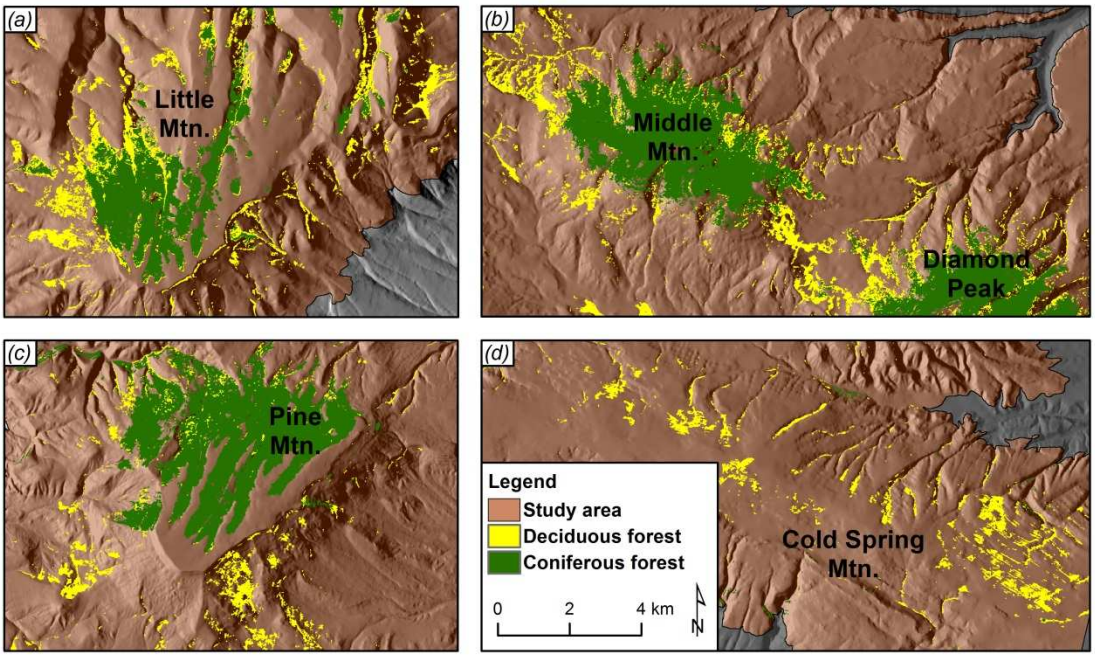

Figure 2.2. Results of the model outputs combined into the synthesis map. (a) Little Mountain, (b) Middle Mountain and portions of Diamond Peak, (c) Pine Mountain and (d) Cold Spring Mountain. Note: each map panel is displayed at the same scale.

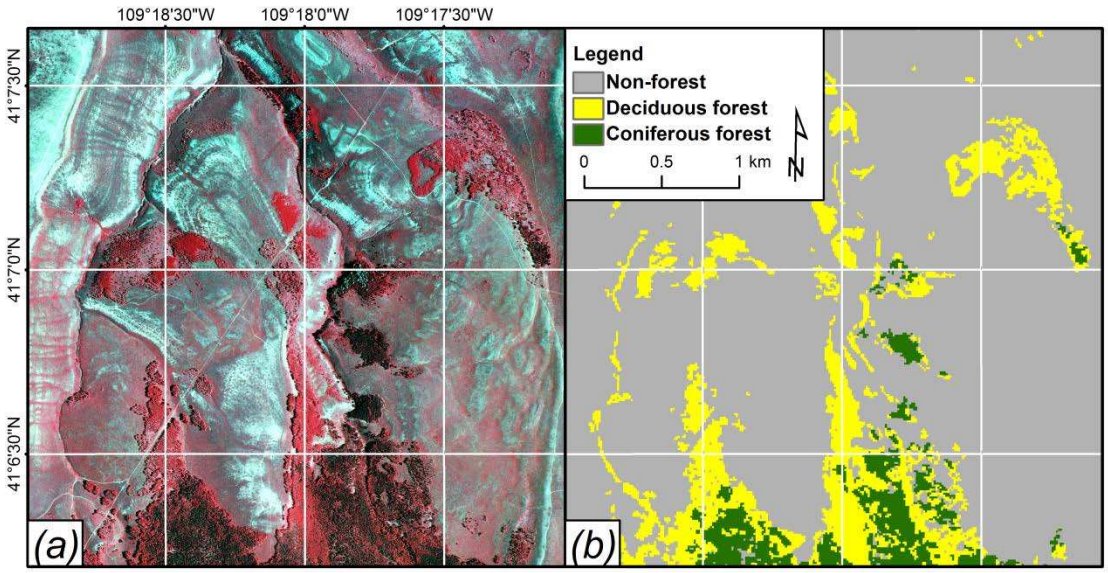

Figure 2.3. Comparison of forest type maps derived from each data source of a representative area of the landscape on Little Mountain. (a) 2009 color-infrared aerial photo (National Agriculture Imagery Program) where dark red/black hues indicate coniferous forest, red hues indicate deciduous forest, grey/light red/blue hues represent non-forest and (*b*) USGS synthesis map. Note: each map panel is displayed at the same scale and extent.

LITERATURE CITED

Assal, T.J., Sibold, J., Reich, R., 2014. Modeling a Historical Mountain Pine Beetle Outbreak Using Landsat MSS and Multiple Lines of Evidence. Remote Sens. Environ. 155, 275–288. doi:10.1016/j.rse.2014.09.002

Barbour, M.G., Burk, J.H., Pitts, W.D., Gilliam, F.S., Schwartz, M.W., 1999. Terrestrial Plant Ecology, Third. ed. Benjamin Cummings, New York, New York.

Bergen, K.M., Dronova, I., 2007. Observing succession on aspen-dominated landscapes using a remote sensing-ecosystem approach. Landsc. Ecol. 22, 1395–1410. doi:10.1007/s10980-007-9119-1

Bradley, B.A., Fleishman, E., 2008. Relationships between expanding pinyon–juniper cover and topography in the central Great Basin, Nevada. J. Biogeogr. 35, 951–964. doi:10.1111/j.1365-2699.2007.01847.x

Cohen, J., 1960. A coefficient of agreement for nominal scales. Educ. Psychol. Meas. 20, 37–46.

Davidson, A., Aycrigg, J., Grossmann, E., Kagan, J., Lennartz, S., McDonough, S., Miewald, T., Ohmann, J., Radel, A., Sajwaj, T., Tobalske, C., 2009. Digital Land Cover Map for the Northwestern United States.

Dubovyk, O., Menz, G., Conrad, C., Kan, E., Machwitz, M., Khamzina, A., 2013. Spatio-temporal analyses of cropland degradation in the irrigated lowlands of Uzbekistan using remote-sensing and logistic regression modeling. Environ. Monit. Assess. 185, 4775–90. doi:10.1007/s10661-012-2904-6

Engler, R., Waser, L.T., Zimmermann, N.E., Schaub, M., Berdos, S., Ginzler, C., Psomas, A., 2013. Combining ensemble modeling and remote sensing for mapping individual tree species at high spatial resolution. For. Ecol. Manage. 310, 64–73.

Hu, Z., Lo, C., 2007. Modeling urban growth in Atlanta using logistic regression. Comput. Environ. Urban Syst. 31, 667–688. doi:10.1016/j.compenvurbsys.2006.11.001

Jarnevich, C.S., Esaias, W.E., Ma, P.L.A., Morisette, J.T., Nickeson, J.E., Stohlgren, T.J., Holcombe, T.R., Nightingale, J.M., Wolfe, R.E., Tan, B., 2014. Regional distribution models with lack of proximate predictors: Africanized honeybees expanding north. Divers. Distrib. 20, 193–201. doi:10.1111/ddi.12143

Jin, S., Yang, L., Danielson, P., Homer, C., Fry, J., Xian, G., 2013. A comprehensive change detection method for updating the National Land Cover Database to circa 2011. Remote Sens. Environ. 132, 159–175.

Jones, H.G., Vaughan, R.H., 2010. Remote Sensing of Vegetation: Principles, Techniques, and Applications. Oxford University Press, Oxford, UK.

Knapp, R.A., Matthews, K.R., Preisler, H.K., Jellison, R., 2003. Developing Probabilistic Models to Predict Amphibian Site Occupancy in a Patchy Landscape. Ecol. Appl. 13, 1069–1082.

Knight, D.H., 1994. Mountains and Plains: The Ecology of Wyoming Landscapes. Yale University, New Haven, CT.

Liu, C., Berry, P.M., Dawson, T.P., Pearson, R.G., 2005. Selecting thresholds of occurrence in the prediction of species distributions. Ecography (Cop.). 28, 385–393.

McCune, B., Keon, D., 2002. Equations for potential annual direct incident radiation and heat load. J. Veg. Sci. 13, 603–606.

R Development Core Team, 2013. R: A language and environment for statistical computing.

Radeloff, V.C., Hammer, R.B., Stewart, S.I., Fried, J.S., Holcomb, S.S., McKeefry, J.F., 2005. The Wildland-Urban Interface in the United States. Ecol. Appl. 15, 799–805.

Rollins, M.G., 2009. LANDFIRE: a nationally consistent vegetation, wildland fire, and fuel assessment. Int. J. Wildl. Fire 18, 235–249.

Rousse, J.W., Hass, R.H., Schell, J.A., Deering, D.W., Harlan, J.C., 1974. Monitoring the vernal advancement of retrogradation of natural vegetation, Type III, Final Report. Greenbelt, Maryland.

Sankey, T.T., Moffet, C., Weber, K., 2008. Postfire Recovery of Sagebrush Communities: Assessment Using Spot-5 and Very Large-Scale Aerial Imagery. Rangel. Ecol. Manag. 61, 598–604. doi:10.2111/08-079.1

Stohlgren, T.J., Ma, P., Kumar, S., Rocca, M., Morisette, J.T., Jarnevich, C.S., Benson, N., 2010. Ensemble habitat mapping of invasive plant species. Risk Anal. 30, 224–235. doi:10.1111/j.1539-6924.2009.01343.x

Stoms, D.M., 2000. GAP management status and regional indicators of threats to biodiversity. Landsc. Ecol. 15, 21–33.

Turner, M.G., Romme, W.H., Reed, R.A., Tuskan, G.A., 2003. Post-fire aspen seedling recruitment across the Yellowstone (USA) Landscape. Landsc. Ecol. 18, 127–140.

USGS, 2014. EarthExplorer archive [WWW Document]. URL http://edcsns17.cr.usgs.gov/NewEarthExplorer/

Ustin, S.L., Gamon, J.A., 2010. Remote sensing of plant functional types. New Phytol. 186, 795–816. doi:10.1111/j.1469-8137.2010.03284.x

Vogelmann, J.E., Xian, G., Homer, C., Tolk, B., 2012. Monitoring gradual ecosystem change using Landsat time series analyses: Case studies in selected forest and rangeland ecosystems. Remote Sens. Environ. 122, 92–105. doi:10.1016/j.rse.2011.06.027

Worrall, J.J., Egeland, L., Eager, T., Mask, R.A., Johnson, E.W., Kemp, P.A., Shepperd, W.D., 2008. Rapid mortality of Populus tremuloides in southwestern Colorado, USA. For. Ecol. Manage. 255, 686–696. doi:10.1016/j.foreco.2007.09.071

Wulder, M.A., White, J.C., Bentz, B.J., Alvarez, M.F., Coops, N.C., 2006. Estimating the probability of mountain pine beetle red-attack damage. Remote Sens. Environ. 101, 150–166.

Wylie, B., Rigge, M., Brisco, B., Murnaghan, K., Rover, J., Long, J., 2014. Effects of Disturbance and Climate Change on Ecosystem Performance in the Yukon River Basin Boreal Forest. Remote Sens. 6, 9145–9169. doi:10.3390/rs6109145

Zimmermann, N.E., Edwards, T.C., Moisen, G.G., Frescino, T.S., Blackard, J.A., 2007. Remote sensing-based predictors improve distribution models of rare, early successional and broadleaf tree species in Utah. J. Appl. Ecol. 44, 1057–1067. doi:10.1111/j.1365-2664.2007.01348.x

CHAPTER 3: Spatial and Temporal Analysis of Drought Effects in a Heterogeneous Semi-Arid Forest Ecosystem[2]

3.1 SUMMARY

Drought has long been recognized as a driving mechanism in the forests of western North America and drought-induced mortality has been documented across genera in recent years. Given the frequency of these events are expected to increase in the future, understanding patterns of mortality and plant response to severe drought is important to resource managers. Drought can affect the functional, physiological, structural, and demographic properties of forest ecosystems. Remote sensing studies have documented changes in forest properties due to direct and indirect effects of drought; however, few studies have addressed this at local scales needed to characterize highly heterogeneous ecosystems in the forest-shrubland ecotone. We analyzed a 22-year Landsat time series (1985-2012) to determine changes in forest in an area that experienced a relatively dry decade punctuated by two years of extreme drought. We assessed the relationship between several vegetation indices and field measured characteristics (e.g. plant area index and canopy gap fraction) and applied this index to trend analysis to uncover the location, direction and timing of change. Finally, we assessed the interaction of climate and topography by forest functional type. The Normalized Difference Moisture Index (NDMI) had the strongest correlation with short-term field measures of plant area index ($R^2 = 0.64$) and canopy gap fraction ($R^2 = 0.65$). Over the entire time period, 25% of the forested area experienced a significant ($p < 0.05$) negative trend in NDMI, compared to less than 10% in a positive trend. Negative trends were not consistent across forest functional type as a larger amount of coniferous forest was impacted by negative trends than deciduous forest. Southern

[2] A version of this chapter was submitted to *Forest Ecology and Management.*

aspects were least likely to exhibit a negative trend and north aspects were most prevalent. Field plots with a negative trend had a lower live density, and higher amounts of standing dead and down trees compared to plots with no trend. Our analysis identifies spatially explicit patterns of long-term trends anchored with ground based evidence to highlight areas of forest that are resistant, persistent or vulnerable to severe drought. The results provide a long-term perspective for the resource management of this area and can be applied to similar ecosystems throughout western North America.

3.2 INTRODUCTION

Climate shapes patterns in vegetation through the balance between energy supply, moisture and the seasonal timing of the two (Stephenson, 1990). In this way, the climate of a region exerts top-down control on ecosystem pattern and process. Ecosystem disturbance, in particular large, infrequent disturbances (Turner and Dale, 1998), are also recognized as a key mechanism of landscape pattern in forests due to the enduring legacies of physical and biological structure that result from these events (Foster et al., 1998). However, disturbance also operates at less conspicuous scales and the range of disturbance impacts are best thought of along a continuum (Sousa, 1984), as legacies can persist at some level regardless of the size or frequency of the disturbance (Turner et al., 1998). Drought and desiccation stress are forms of ecosystem disturbance (Sousa, 1984), yet the spatial and temporal complexity of drought renders identification and quantification very difficult (Vicente-Serrano, 2007).

Vegetation is vulnerable to climate via water stress brought on by drought and warm temperatures (Allen, 2009). If water for growth is not available, the energy acts to heat and stress the plant (Stephenson, 1990). In the early 2000s, over half of the coterminous United States experienced moderate to severe drought conditions and record breaking precipitation deficits

throughout the western part of the country (Cook et al., 2004). This event brought attention to drought vulnerability in semi-arid forests of western North America. Portions of the intermountain west also experienced severe to extreme drought in 2012 (NOAA, 2012). Severe drought in the early part of the last decade has been identified as the driver of tree stress, dieback and mortality across diverse forest types (Allen et al., 2010; Breshears et al., 2005; Gitlin et al., 2006; Michaelian et al., 2011). Lag effects of drought may lead to tree mortality several years after the drought event (Bigler et al., 2007). Moreover, drought has indirect effects on other disturbances including insect agents, pathogens and fire. For example, reduced host-tree vigor from drought increases insect attack probability (Bentz et al., 2010). Drought contributes to flammability of fuels and decreased snowpack, resulting in longer fire seasons (Littell et al., 2009; Westerling et al., 2006).

Dominant tree species in Rocky Mountains forests including quaking aspen (*Populus tremuloides*), sub-alpine fir (*Abies lasiocarpa*), lodgepole pine (*Pinus contorta*), and Douglas-fir (*Pseudotsuga menziesii*) are susceptible to drought through stress and dieback, which impact the photosynthetic activity of the tree, as well as mortality. Although the clonal root system of aspen may provide an advantage during periods of lower moisture, droughts of long duration are likely to affect the growth of both suckers and mature trees alike (Hessl and Graumlich, 2002). Severe drought in the boreal forest and parkland of western Canada resulted in a two-fold increase in stem mortality and a 30% decrease in regional stem growth in persistent trees (Hogg et al., 2008). Decrease in growth is the result of high levels of twig and branch dieback in the crowns of living trees and productivity is limited by carbon dioxide fixation imposed by leaf stomatal resistance during soil or atmospheric water deficits (Hogg et al., 2000). Trees that are not killed are susceptible to other stressors such as insects and fungal agents that can amplify and prolong

the impact of drought (Hogg et al., 2008, 2005). A phenomenon known as sudden aspen decline (SAD) has been documented in regional aspen forests (Worrall et al., 2008). Rapid and sudden onset of mortality is primarily caused by high temperatures, acute drought and secondary biotic agents (Worrall et al., 2008).

Multiple studies have documented an increase in mortality rates of coniferous species throughout the western United States over the later part of the 20th century (Allen and Breshears, 1998; Breshears et al., 2005; van Mantgem et al., 2009). Increases in mortality rates have been reported across ecosystem type and elevation, among dominant genera and tree size, and at sites with diverse fire histories (Gitlin et al., 2006; van Mantgem et al., 2009). All of these mortality events are driven by increased water deficit associated with drought, but secondary agents such as bark beetle outbreaks have also contributed to mortality in some areas (van Mantgem et al., 2009).

Drought can induce direct or indirect tree mortality, however, less conspicuous effects such as loss of productivity can accompany drought as well. Forest response to drought is likely dependent on the spatial pattern of forest structure and function (Hope et al., 2014), and the duration of the drought is a key element in plant response. Water stress can lead to an increase in plant respiration (Jones and Vaughan, 2010), and plants cope with drought via stomatal closure and reduced leaf area index (LAI) (Hope et al., 2014). A reduction in leaf area leads to a lower photosynthetic capacity and a change in canopy structure. Collectively, these responses result in a decrease in chlorophyll and water content of plant leaves (Jones and Vaughan, 2010). Successive years of declining productivity associated with severe drought can also lead to delayed mortality (Bigler et al., 2007).

Disturbance alters ecosystem structure by both abrupt, obvious change and through gradual, slow change over some period of time (Assal et al., 2014). Remote sensing offers a powerful medium to capture the pre and post disturbance landscape and detect changes that might not be readily observed, such as drought stress. Spatial, temporal and spectral scales are an important consideration when using remote sensing in ecosystem disturbance studies. Two common multispectral remote sensing platforms used in drought studies are the Moderate Resolution Imaging Spectroradiometer (MODIS) (Abbas et al., 2014; Bastos et al., 2014; Hope et al., 2014) and the Landsat satellites (Huang and Anderegg, 2012; Maselli, 2004; Vogelmann et al., 2009; Volcani et al., 2005). Both platforms are well suited to study ecosystem dynamics at regional scales given the large coverage area per scene. However, subtle changes in forest structure and productivity are difficult to detect with satellite derived observations (Deshayes et al., 2006). Therefore, drought studies require a long term series of observations, which makes the high temporal resolution of these satellites well suited for this application. Although MODIS has a high-temporal resolution (16-day composite product compared to 16-day revisit time for Landsat), the lower spatial resolution (250-500 m compared to 30 m) preclude its use in highly heterogeneous forest-shrubland ecotones. Trend analysis utilizing time-series of Landsat data is useful to identify, monitor, and assess both abrupt and subtle forest change (Czerwinski et al., 2014; Dorman et al., 2013; Kennedy et al., 2010; Vogelmann et al., 2009).

Forest canopy reflectance is influenced by several biophysical parameters including crown closure, canopy and branch architecture, LAI, the chlorophyll and water content of leaves as well as the understory and exposed soil properties of the stand (Deshayes et al., 2006). Multispectral satellites have spectral bands spanning the visible and infrared wavelengths that can be combined into vegetation indices that are sensitive to differences in these biophysical

parameters (Jones and Vaughan, 2010). Living vegetation absorbs radiation in portions of the visible wavelengths and reflects in the near-infrared (NIR) and radiation in the shortwave-infrared (SWIR) is absorbed by water content of leaves (Jones and Vaughan, 2010). The NIR and SWIR are sensitive to variations in LAI and the SWIR band is sensitive to water stress during periods of drought (Deshayes et al., 2006). Numerous spectral vegetation indices (VIs) have been used in disturbance and drought studies, many of which utilize the NIR and/or the SWIR bands. The Normalized Difference Vegetation Index (NDVI) is the most widely used vegetation index to document and monitor drought and related impacts in forests (Breshears et al., 2005; Carreiras et al., 2006; DeRose et al., 2011; Lloret et al., 2007; Maselli, 2004; Volcani et al., 2005; Weiss et al., 2004). However, other vegetation indices have utility in disturbance related vegetation dynamics including the Enhanced Vegetation Index (EVI) (Hope et al., 2014; Tüshaus et al., 2014), the Normalized Difference Moisture Index (NDMI) (Goodwin et al., 2008; Meddens et al., 2013), the soil adjusted vegetation index (SAVI) (Tüshaus et al., 2014), and the Tasseled Cap (Czerwinski et al., 2014).

We sought to quantify the spatial and temporal effects of drought in an ecosystem that is expected to be vulnerable to drought stress and climate change. The effects of climate change and variability are expected to be most rapid and extreme at ecotones, especially in semi-arid areas (Allen and Breshears, 1998; Gosz, 1992). An understanding of the link between climate variability and tree mortality for species near ecotones is an important goal of current research (Kulakowski et al., 2013). Recent studies (Crookston et al., 2010; Rehfeldt et al., 2009) predict the current climate profile for several prominent tree species (e.g. aspen, subalpine fir and lodgepole pine) will be greatly limited or no longer present in isolated forests of the Rocky Mountains over the course of the next century. Ecotones are important barometers of climate

change (NEON, 2000) and stress, dieback and mortality are expected to accompany severe drought in this arid landscape. However, regional climate can be influenced by local terrain, a concept known as topoclimate (Thornthwaite, 1953). Slope and aspect influence air temperature, water balance, radiation, snowmelt patterns and wind exposure (Dobrowski, 2011). In this way, topography can potentially amplify the effects of drought, particularly in arid landscapes. The use of temporal remotely sensed data has been effective in monitoring drought induced changes in forests and woodlands (Maselli, 2004; Vogelmann et al., 2012). A primary challenge in spectral change analysis is to segregate long-term vegetation change from interannual phenology differences in response to climate variability. We hypothesize that the ecological consequences of drought create a landscape mosaic of drought effects and that trend analysis of vegetation indices can be used to document these impacts across a range of severities (Lloret et al., 2007). The gradient spans demographic (i.e. tree mortality), structural (i.e. crown partial dieback), functional (i.e. reduction in leaf area), and physiological (i.e. temporary/permanent reduction in photosynthetic activity) properties of the forest ecosystem that will result in different spectral trajectories. This study was undertaken because little is known about baseline condition in this ecosystem, and how climate, in particular drought, affects this topographically complex ecosystem. Finally, we are interested in providing managers with a long-term perspective of the forest dynamics of this ecosystem with respect to variability in precipitation patterns.

Our research objectives were to:

1) Identify an appropriate vegetation index for use in temporal trend analysis based on the relationship with field measured estimates of vegetation traits,
2) Analyze the spatial location, directional trend, and timing of change by forest type, and
3) Assess the drivers of change by forest type and the interaction of climate on topography.

3.3 METHODS

3.3.1 Study Area

Our study area is located in the southern part of the Wyoming Basin ecoregion, spanning parts of southwestern Wyoming, northwestern Colorado and northeastern Utah (Figure 3.1). Several prominent ridges form a transition zone between basins and mountainous areas (Knight, 1994), where several species of trees are found at the xeric fringes of their respective ranges. Forests dominated by aspen (*Populus tremuloides*) and several coniferous species (sub-alpine fir (*Abies lasiocarpa*), lodgepole pine (*Pinus contorta*), and Douglas-fir (*Pseudotsuga menziesii*)) occur as relatively small patches on moist sites in a matrix of sagebrush steppe (*Artemisia tridendata* spp. *vaseyana*) or mixed-species shrublands. Scattered juniper (*Juniperus communis var. depressa*) and limber pine (*Pinus flexilis*) woodlands, distinct from the montane conifer forest, are found on rocky slopes at lower elevations and small patches of manzanita (*Arctostaphylos patula*) are found in the southern part of the study area. Most of the area is under jurisdiction of the U.S. Bureau of Land Management, interspersed with small parcels of state and private land. The area has a midlatitude steppe climate with a substantial portion of the annual precipitation occurring as snow. Dominant land uses include livestock grazing, energy extraction and recreation. Multiple state and federal agencies, along with the Wyoming Landscape Conservation Initiative (wlci.gov), have identified the region as a priority area for conservation. The area provides important habitat for many wildlife species including big game, migratory and resident birds, as well as domestic livestock. Management has sought to rejuvenate decadent aspen stands and reduce conifer expansion in successional aspen stands through prescribed fire and mechanical thinning. Drought related mortality of aspen is a concern in western North

America (Worrall et al., 2008) and lack of aspen regeneration due to high rates of herbivory is a concern in the study area.

3.3.2 Drought Index Calculation

To understand the effects of drought at a local level, we needed to develop a localized index of drought severity. The most widely used drought index, the standardized precipitation index (SPI) (Vicente-Serrano, 2007), was used to quantify water deficit and surplus. We used the SPI instead of the regional Palmer Drought Severity Index to capture local differences in annual precipitation of the relatively small and isolated study area. The SPI indicates the number of standard deviations the precipitation deviates from the long-term mean during the measured period (Vicente-Serrano, 2007). The majority of the precipitation in the study area is received in the form of snow. The flexibility of the SPI enabled us to calculate a 12-month duration equivalent to the water year (Oct-Sept) between 1980 and 2014. We obtained 4 km^2 SPI data from the Western Regional Climate Center (http://www. wrcc.dri.edu; accessed 15 February 2015) and calculated the water year mean for a 50 km^2 area that encompasses the forested ridges of the study area.

3.3.3 Landsat Data

The growing season in the study area is short, with snow possible in mid-June and leaf senescence by late September. To select a consistent window of peak greenness, we calculated the average growing season phenology (2000-2012) of the forested portion of the study area using MODIS NDVI 16-day composite data (MOD13Q1). Predominantly cloud-free Landsat images were selected between July 01 and September 06 (day of year 182 to 249 in non-leap years). A total of 24 Landsat Thematic Mapper (TM), Enhanced Thematic Mapper Plus (ETM+), and Operational Land Imager (OLI) images (path 36, row 32) were acquired for analysis from

the USGS EarthExplorer Archive (USGS, 2014) between 1985 and 2014 (Table 3.1). The imagery was processed to surface reflectance using the Landsat Ecosystem Disturbance Adaptive Processing System (LEDAPS) (Masek et al., 2006) which has been successfully used in other ecosystem change studies (McManus et al., 2012). We used the LEDAPS quality mask layer to identify pixels with clouds, cloud shadows and other unacceptable pixels that were removed from the analysis. We calculated several vegetation indices (Table 3.2) using the OLI imagery to explore relationships between each VI and the field data. We then applied the VI that best explained variation in the short-term field data (see Section 3.4.3) to the Landsat time series.

In order to extend the time series beyond 2011, it was necessary to use several Landsat ETM+ images with gaps due to the scan-line corrector problem that occurred in 2003 (Chander et al., 2009). Landsat TM data is not available after the growing season of 2011 and we chose not to incorporate Landsat OLI data (available beginning in June 2013) given the wavelengths of several key bands are different from earlier Landsat satellites, and a reliable calibration process has not yet been documented. We obtained six ETM+ scenes from 2012, 2013 and 2014. We sought to connect pixels through time (z) and not space (x, y), and therefore a traditional image normalization technique would not be appropriate. We conducted a sensitivity analysis between annual images using our field plot locations (n=52) and several vegetation indices to evaluate the annual phenological stability between dates. The Pearson's correlation coefficient for each index in each of the three years was >=0.85. However, we only retained the data from 2012 as the available images were consecutive (Aug 03 and Aug 19) and the field points were highly related (Pearson's correlation coefficient NDMI= 0.95, NDVI=0.94). A composite 2012 image was created using the earlier image as the primary value and the later image was used to overwrite pixels with no data. We also obtained a Landsat OLI scene to evaluate the relationship between

field data and spectral vegetation indices. The OLI image was acquired several days before our field collection effort in 2014.

3.3.4 Field Measurements

We used a sampling approach to allow rapid collection of data to describe a range of conditions across the study area (Meigs et al., 2011). We conducted a preliminary investigation to identify areas of change and stability over time using NDVI from several years (mid-90s, early 2000s, and 2010). We identified 52 plots distributed in coniferous and deciduous dominated forests on each of the major forested ridges in the study area. We avoided areas with substantial anthropogenic activity (e.g. logging, recreational sites, roads, trails, stock tanks, etc.) or fire occurrence since 1984 (Eidenshink et al., 2007).

In 2013, we collected plot level measurements to assess tree density, species composition and structure, and tree mortality (Meigs et al., 2011). We consider these measurements long-term data as we presume they reflect conditions for a number of years prior to measurement since there were no major disturbances in each plot. Each plot was located at the center of a Landsat pixel (30 x 30 m) using a sub-meter GPS unit (Trimble GeoXT). Three, 15 m belt transects were established from the plot center at 0° (true north), 120°, and 240° with a variable width of two or four meters. In each transect we quantified live and dead tree basal area for all standing tree species greater than 2 meters in height. We noted canopy dieback, bark damage, and presence of cankers or insect damage. We also counted dead, down trees that were likely rooted within each transect (Meigs et al., 2011) and assigned a bark decay class (1-5) according to USFS Forest Inventory and Analysis standards. In this analysis, we retain the lowest decay classes (1-3) as they were most likely alive in recent decades.

In 2014 we revisited the field plots to measure canopy condition via in situ plant area index (PAI) and canopy gap fraction (CGF). We consider this short-term data as it likely reflects recent conditions at each plot. We used a hand-held CID-110 Plant Canopy Imager instrument (CID Bio-Science, Inc.) to collect hemispherical (fish-eye) plant canopy images to estimate PAI and CGF. The process relies on the gap-fraction inversion procedure (Campbell and Norman, 1989) to measure radiation transmission through the canopy (Martens et al., 1993). The instrument contains a self-leveling PENTAX lens that enabled images to be collected looking vertically upward beneath the canopy at approximately one meter above the ground. Measurements were performed under a range of sky conditions, as the study area rarely experiences prolonged overcast conditions (Pfeifer et al., 2012). Exposure, color, and contrast settings were manually adjusted to maximize the contrast between the sky and canopy. A sampling grid was established within each 30 x 30 m plot and nine photo points were collected (Figure 3.2) for 43 of the 52 plots (due to equipment issues). The images were classified into sky and plant components using CID software and PAI and CGF were averaged for each plot. We use the term plant area index instead of leaf area index because this measurement includes stems and branches (Pfeifer et al., 2012). We opted not to subtract an estimated stem-area index because preliminary results indicated the PAI was sensitive to mortality levels between plots.

3.3.5 Statistical Analysis of Vegetation Indices

We used a generalized linear model (GLM, Gaussian distribution, Identity link function) to evaluate the relationship between field and satellite data. Our goal was to identify the vegetation index with the strongest relationship to field data, not create a spatially explicit model of forest characteristics (e.g. PAI). We found the short-term data had the strongest relationship with that year's satellite data (e.g. 2014 field data with 2014 satellite data). This was expected as

the Landsat OLI scene was acquired just days before the 2014 field campaign. The Canopy Gap Fraction data was log-transformed prior to the analysis to meet the assumptions of linear regression.

3.3.6 Temporal Trend Analysis

Trend analysis was implemented on a per-pixel basis using least-squares regression between the vegetation index (dependent variable) and time (explanatory variable) (McManus et al., 2012; Vogelmann et al., 2009). We evaluated trends for several time periods of *n* images and allowed one missing observation (*n*-1) in each pixel stack. This allowed the use of several additional years of imagery with some cloud and cloud shadows present, while minimizing the potential for illegitimate trend detection (McManus et al., 2012). The slope and statistical significance of the linear regression in the selected VI values (see Section 3.4.3) were evaluated using a Student's *t*-test at 95% confidence level for each geographic pixel (McManus et al., 2012). Significant temporal trends in NDMI may be interpreted as changes in vegetation condition, given the relationship between field and satellite data. Pixels identified with significant monotonic temporal trends ($p = < 0.05$) were mapped as positive or negative change (Czerwinski et al., 2014). Trend analysis was conducted on all eligible (no more than one missing year due to clouds, cloud shadows, no fire) forested pixels in the study area over a range of time periods with at least ten observations.

3.3.7 Spatial Analysis of NDMI Trends

Positive and negative trends in NDMI between 1985 and 2012 were evaluated by dominant forest type. We obtained a 10 m raster map of forest cover and dominant type (e.g. deciduous vs. coniferous) (Assal et al., 2015) and resampled the data to 30 m using a nearest neighbor algorithm. The map was developed from 2010 SPOT imagery so we added obvious

omissions of small aspen stands documented in the field that were missing from the map due to recent mortality. Next, we evaluated trends in NDMI by elevation, slope and aspect to understand how trends were distributed with respect to landscape position. Topographic variables were derived from a 10 m National Elevation Dataset including slope, and aspect. The relationship between elevation, slope and aspect was analyzed with respect to negative NDMI trend occurrence using a binomial generalized linear model. We selected a random sample of negative and no-trend observations for 10% of total observations of each class (McManus et al., 2012).

3.4 RESULTS

3.4.1 Drought Index

The SPI for the study area (Figure 3.3) indicates high variability of precipitation over the last three and a half decades with several distinct wet and dry periods. The majority of the 1980s were wet along with the mid to late 1990s. There was a multi-year drought in the late 1980s and early 1990s. The late 1990s had two extremely wet years (1995 and 1997), while 2002 and 2012 were classified as extreme drought years. With the exception of 2005 and 2011 (severely wet years), the area has been in a dry period since 2000.

3.4.2 Field Data Analysis

The field data results indicate that our sampling effort captured a wide range of plot-level mortality. We categorized the plots into deciduous or coniferous based on the majority of the total basal area. There were very few mixed plots, and the vast majority of plots contained 70% or more of the dominant forest type. Deciduous plots ranged from low (11%) to total (100%) mortality. Coniferous forest plots exhibited a similar range from 5% to 95% mortality. Mortality

was not consistent for small, medium and large trees (stem DBH <10 cm, 10 to 20 cm, and >20 cm, respectively). We encountered fewer small and medium dead conifer trees compared to the same size classes of deciduous trees (Figure 3.4). Large conifer trees exhibited similar mortality levels compared to large deciduous trees. Within each forest type, the group means of the small and medium classes were significantly different than the mean of the large trees. Small and medium coniferous trees had significantly lower mean mortality per plot than large trees (Figure 3.4a). Conversely, small and medium deciduous trees had significantly higher mean mortality per plot than large trees (Figure 3.4b).

3.4.3 Relationship between Field and Satellite Data

Field variables with the highest correlation with 2014 vegetation indices were PAI and CGF. NDMI had the strongest correlations with field measures, and was therefore selected as the appropriate metric and thus only those results are reported here. A significant positive linear relationship ($R^2 = 0.64$, $p < 0.0001$, n=43) was found between field measured PAI and NDMI (Figure 3.5a). A significant negative linear relationship ($R^2 = 0.65$, $p < 0.0001$, n=43) was found between field measured CGF and NDMI (Figure 3.5b). This result was expected as dense, canopies have greater moisture content than sparse, open canopies or canopies with high levels of mortality. The residuals of the linear regression models were spatially independent (PAI model, Moran's I = -0.0428, $p = 0.7$; CGF model, Moran's I = -0.024, $p = 0.9$). The 2013 long-term data (collected in 2013) did not exhibit as strong of a relationship with the satellite data. The highest correlation was live tree density with NDMI ($R^2 = 0.46$, $p < 0.0001$, n=52). We also found a significant linear relationship between the short-term (2014) and long-term (2013) field data with the live tree density (strongest predictor) of PAI ($R^2 = 0.56$, $p < 0.0001$, n=43) and CGF ($R^2 = 0.54$, $p < 0.0001$, n=43).

3.4.4 Trend Analysis

The results highlight the area of significant positive and negative trend for each time period with at least ten observations. The first time period, T_{1998} (1985-1998) highlights 1705 ha (27% of the forested area) with positive, increasing trends, and only 1.6% of the forested area (98 ha) experiencing negative trends (Table 3.3). These trends began to change starting with T_{2000} (1985-2000) as the amount of forested area with a positive trend decreased and the area of forest exhibiting negative trends began to increase. From T_{2000} to T_{2012} (1985-2012) the amount of forest in a significant negative trend increased every period from 160 ha (T_{2000}) to 1606 ha (T_{2012}). The negative trend was significant in over 25% of the forested area by 2012 (Table 3.3). The decrease in the area under the positive trend was not cumulative as with the negative trend. The positive trend decreased from T_{1998} to a low of only 2.7% of the area in a significant positive trend during the drought year of 2002 (172 ha). The amount of forest in a positive trend slowly increased to a similar area at the start of the dry period (2000), with just under 10% by 2012.

The trends were not consistent across forest functional types over the full time period T_{2012} (1985-2012). A higher percentage of coniferous forest experienced significant positive trends (11.9%) compared to deciduous forest (7.1%) (Table 3.4), and both groups had substantially more area in negative trends. Deciduous forest had over twice as much area (474 ha) in a negative trend compared to positive, and coniferous forest had nearly three times as much area (1132 ha.). The disparity between positive and negative trends for each group was not consistent as coniferous forest had a much greater percentage in negative trends (32.8%) compared to deciduous (16.5%). The trends over time were not consistent by forest functional type either, as coniferous forest experienced a greater percentage in significant positive and negative trends for every time period since 2000 (Figure 3.6).

3.4.5 Spatial Analysis of Trends

Significant positive and negative trends were present across all of the forest ridges (Figure 3.7). At the landscape scale, significant trends appear somewhat clustered in large patches. Our analysis confirmed that negative trends were not randomly distributed across the landscape with respect to topography. Forested areas at higher elevations were positively correlated with the frequency of detecting negative trends (Table 3.5). Southern aspects (south, southeast and southwest) were least likely to exhibit a negative trend and north aspects were most prevalent. All aspects classes were significant, except for northeast aspects. We included forest type (deciduous or coniferous) in the GLM model, but it was not a significant explanatory variable and subsequently dropped. Positive trends with respect to topography were also analyzed, but very few variables were significant.

3.4.6 Ground Based Evidence of Trends

Field plots were identified a priori and therefore not evenly distributed with respect to trend significance or direction. A rigorous accuracy assessment or validation test could not be conducted; however, our data provides ground-based evidence that trends in NDMI reflect changing conditions in the forest. Nearly half of our field plots had a significant negative trend between 1985 and 2012. Of those plots, the magnitude of the slope provides a means to distinguish between mortality classes. An ANOVA with multi-comparison post-hoc Tukey's HSD test revealed significant differences between group means of the low and high mortality classes and the moderate and high mortality classes (Figure 3.8a). Plots with a significant negative trend had a lower mean percentage of live trees compared to plots with no trend (*p-value* significant at the 0.1 level) (Figure 3.8b). Plots with a negative trend had a significantly higher amount of standing dead trees compared to plots with no trend ($p\text{-}value < 0.05$) (Figure

3.8c). Finally, plots with a negative trend also had a significantly higher amount of total dead trees (standing dead trees + down trees) compared to plots with no trend (*p-value* < 0.05) (Figure 3.8d). Figures 3.8c and 3.8d indicate that the long-term data is particularly useful to capture the legacy of a drought period in this system.

The NDMI trajectories were extracted for each plot and analyzed to explore plot level trends over time. Figures 3.9 and 3.10 are examples of field plots that exhibited negative NDMI trends from 1985 to 2012. Figure 3.9 is a coniferous plot (dominated by Douglas-fir) with low plant area index (1.22), high canopy gap fraction (0.39), low live basal area (8.39 m^2/ha) and high plot mortality (68%). Pitch tubes were evident on many of the dead trees and it was likely that Douglas-fir beetle was responsible for the mortality at the site as exhibited with a sharp decline in NDMI beginning in 2005 (Figure 3.9). Figure 3.10 is an aspen stand with low plant area index (0.43), a very open canopy (gap fraction = 0.64), low live basal area (12.8 m^2/ha), and very high mortality (81.5%). The NDMI trend (Figure 3.10) provides a clear indication that the mortality was first instigated by drought in the early 2000s, and the stand never recovered. This is confirmed with the long-term field data as the plot had a much higher amount of total standing (live and dead) basal area (49.2 m^2/ha). Both of these plots began to decline around 2005, after a five year dry period centered on the 2002 drought (Figure 3.3). Figure 3.11 is an example of a plot that had a statistically significant positive trend over the study period. It was one of only two plots with a positive trend. The conifer dominated plot had relatively high plant area index (1.78), low canopy gap fraction (0.28), and high live basal area (34.2 m^2/ha) (Figure 3.11). Figure 3.12 is an example of a plot that did not have a statistically significant trend during the period of study. The deciduous plot is characterized by high plant area index (2.02), a low canopy gap fraction (0.2), and a high amount of live basal area (37.3 m^2/ha). The NDMI values

are fairly high and stable throughout the period of study (Figure 3.12) and track precipitation during two extremely wet years (1995 and 1997) (Figure 3.3).

3.5 DISCUSSION

3.5.1 Causes of Decline and Mortality

Physiological drivers of tree mortality are complex (McDowell et al., 2008) and are often coupled with multiple, interacting factors (Allen et al., 2010). McDowell et al. (2008) proposed a framework related to the intensity and duration of water stress that identified three mechanisms of drought-related mortality. Carbon starvation can occur when drought induces stomatal closure, in turn reducing photosynthesis and carbon uptake until the plant exhausts carbon reserves needed for maintenance of metabolism. Hydraulic failure occurs when the soil water supply is reduced, along with increased evaporative demand, leading to xylem cavitation and subsequent desiccation of plant tissues. Drought can influence the demographics of insects and pathogens which can amplify plant physiological stress and in-turn sustain greater populations of such biotic agents. Carbon starvation, hydraulic failure and biotic agents may operate either inclusively or exclusively (Allen et al., 2010; McDowell et al., 2008). Lag effects of drought are also known to operate in subalpine forests of the Rocky Mountains for as long as five to 10 years after the event (Bigler et al., 2007).

Deciduous and coniferous forests are affected by different mechanisms of mortality. It is difficult to assign absolute causes of mortality without in-depth analysis (Vogelmann et al., 2009), however, we found evidence of causal agents on several field visits. Visible documentation of pine beetle (*Dendroctonus spp.*) activity was documented on dead trees in conifer stands in the form of pitch tubes (resin). Beetle caused mortality in lodgepole pine trees was likely caused by mountain pine beetle (*Dendroctonus ponderosae*), whereas Douglas-fir

mortality was likely caused by the Douglas-fir beetle (*Dendroctonus pseudotsugae*). The Douglas-fir tussock moth (*Orgyia pseudotsugata*) and western spruce budworm (*Choristoneura occidentalis*) are defoliator species and may have also contributed to mortality in small Douglas-fir stands. However, we suspect the dominant cause of Douglas-fir mortality was a result of beetle activity due to the sharp decline in NDMI, evident of rapid mortality (Figure 3.9), as opposed to more gradual spectral changes associated with defoliator species (Vogelmann et al., 2009). Whereas fire, blowdown or defoliation events have been documented as initiating Douglas-fir beetle outbreaks (Negrón et al., 2014), this is the first time that a landscape-scale outbreak has been associated with extreme drought.

Subalpine fir decline has been attributed to mortality in fir forests in Colorado (Ciesla, 2010). Tree mortality is due to a combination of western balsam bark beetle (*Dryocoetes confuses*) (Meddens et al., 2012) and at least two species of fungi, *Armillaria spp.* and *Heterobasidium annosum* known to cause root decay (Bigler et al., 2007; Ciesla, 2010). However, subalpine fir decline does not occur in large distinct patches common with other agents of conifer mortality, but rather heightened levels of background mortality. This particular type of mortality is more challenging to detect because it is not as conspicuous to human observers or readily detected with short time periods of satellite data (< 5 years). Subalpine fir is the dominant conifer species on Little and Pine Mountains and significant negative trends were identified in these stands (Figure 3.7). Mortality in subalpine fir forests has not been studied as extensively as other coniferous species and is a future research need. Spruce beetle (*Dendroctonus rufipennis*) is an important disturbance agent in Spruce-Fir forests, however the primary host, Englemann Spruce (*Picea englemanni*), is not commonly found in the study area. Western spruce budworm is also known to cause damage and mortality to subalpine fir by

defoliation (Ciesla, 2010). We found a significantly higher percentage of mortality in large trees, which also suggests insect agents are a primary cause of mortality in the study area (Figure 3.4a).

Worrall et al. (2013) provide a thorough review of causes of damage and mortality to aspen, the primary deciduous tree in the study area. In addition to drought, there are a number of factors that can amplify or prolong the impact of moisture stress and lead to reduction in growth, partial dieback and mortality. Factors include multi-year defoliation by tent caterpillars (*Malacosoma spp.*) and stem damage by fungi and insects which can kill the cambium and interrupt phloem, which leads to crown dieback (Worrall et al., 2013). We know of no documented defoliation events in our study area, but evidence of fungi (cankers) and insects (borers on standing dead and down trees) along with crown dieback were documented at over half of the sites in our study area. Furthermore, many trees had evidence of mechanical stem damage caused by elk. Late spring frost and freeze/thaw cycles during winter dormancy can also damage leaves and previous year's growth (Worrall et al., 2013). We found a significantly higher percentage of mortality in small and medium aspen trees, compared to large trees (Figure 3.4b). A mechanistic study is needed to investigate why there has been an increase in mortality in small and medium sized aspen trees as related to drought.

3.5.2 Interpretation of Spatial Trends

We documented substantial levels of plot level mortality across forest type (Figure 3.4) and identified negative trends throughout the study area (Figure 3.7) using long-term satellite data. Although the physiology of drought-induced tree mortality is complex (McDowell et al., 2008), an understanding of the spatial pattern of tree decline is an important consideration for managers. Mechanistic studies of drought impacts on tree physiology is an emerging research

trend and out of the scope of our study. However, our results serve as a coarse filter to highlight areas of mortality where mechanistic studies could be initiated (Huang and Anderegg, 2012).

The aspect of a slope has direct influence on incident solar radiation and surface temperature (McCune and Keon, 2002) and indirectly influences evaporation and available soil moisture (Huang and Anderegg, 2012). Studies that evaluated acute drought-induced mortality in other Rocky mountain aspen forests found higher mortality rates on drier southern and western aspects (Huang and Anderegg, 2012; Worrall et al., 2008). However, our results contrast with these studies as we found higher than expected rates of deciduous and coniferous trees on north aspects (Table 3.5). This might indicate that our study area, located on the margins of the arid Wyoming Basin ecoregion, is very different than aspen forests in other parts of the intermountain west. Genetic research suggests that aspen clones exhibit wide-ranging phenotypic variation in physiology and growth traits under drought conditions (St. Clair et al., 2010). Localized mortality of aspen could be due to genotype (clonal) effects (Huang and Anderegg, 2012), and adaptation could also explain regional differences in spatial patterns of decline.

We do not know when the aspen genets (clones) were established in our study area, but conditions were presumably wetter for some period conducive to establishment. Our study area has likely always been drier than other Rocky Mountain forests for some time and as a result, these genets might be more adapted to arid conditions. We found higher elevations and northern aspects most likely to exhibit significant negative trends. These areas are cooler and wetter than other aspects, and trees would be most vulnerable in these areas in years when winter precipitation is below average. The density of trees on northern slopes could have increased during the wet decade of the 1990s (Figure 3.3), setting up those same slopes for an increase in mortality when water was limited during drought years. Although we documented substantial

mortality and areas of negative trends, we did not observe large scale mortality documented by others (Huang and Anderegg, 2012; Worrall et al., 2008). This highlights the value of spatially explicit analysis and the importance of landscape position in arid landscapes.

3.5.3 Management Implications

Regional climate exerts top-down control on ecosystems (Stephenson, 1990) and is an important consideration for managers when considering the future outlook of an ecosystem or treatment options. The current climate profiles for many of the tree species analyzed in this study are predicted to no longer be present in the isolated forests of the study area as we approach the next century (Crookston et al., 2010; Rehfeldt et al., 2009). However, many global and regional climate models do not currently take terrain into account (Crookston et al., 2010). Our study provides spatially explicit evidence that bottom-up controls, including fine-scale topography, remain important in climatically driven drought (Prichard and Kennedy, 2014). Adaptive management can benefit from spatially explicit analysis and data because aspen forests do not function the same across locations (Rogers et al., 2014) or within the confines of coarse scale data used in climate models. The results of our analysis can frame hypotheses to be tested with regard to resistance, persistence and vulnerability of forests to drought. Resistance is the capacity of an ecosystem to remain largely unchanged, with regard to structure, processes and functioning, despite stresses and disturbance (Folke et al., 2004). We suggest areas with a significant positive trend are resistant to drought episodes of these magnitudes. These areas had a statistically significant increase in canopy moisture despite several recent extreme droughts (e.g. 2002, 2012) and an extended dry period (e.g. 2000-2004). These forests likely increased in structural, functional, and physiological capacity during this time period which resulted in increased productivity. Forests that did not have a statistically significant trend in either direction

can be considered persistent during periods punctuated by drought. Finally, areas with a significant negative trend are vulnerable to drought as the structural, functional and physiological properties of these stands markedly declined after these events. We believe the results of our study can benefit managers in utilizing limited budgets to ensure the long-term persistence of aspen in this area.

3.5.4 Ecological and Technical Considerations

Several spatial and temporal characteristics of the forest-shrubland ecotone should be taken into consideration with our approach as quantifying tree canopy dynamics through remote sensing in these areas remains a challenge (Yang et al., 2012). Coniferous forests have a closed architecture which enables robust modeling using remotely sensed data (Assal et al.; in review). However, semi-arid aspen systems found at lower elevations in our study area present challenges to evaluate gradual dynamics over time. These systems tend to have low tree cover and density, a very open canopy and low values of plant area index. Furthermore, the combination of trees, shrubs and grasses may confound the spectral signal as pixel values are a mixture of ground elements (Lefsky and Cohen, 2003). Given the high heterogeneity between forest and non-forest present in our study area, mortality might be underestimated, particularly at the margins of forest patches. The time series would be more robust if we were able to obtain one image per year, but clouds, sensor issues, etc. limited availabld data. Numerious studies have utilized the rich temporal archive of MODIS data with daily to bi-weekly collections of imagery that can track both long term and interannual phenology differences. However, the fine-scale hetergeneity of the study area and our interest to extend the study prior to 2000 prevented the use of MODIS data.

There are no long-term plots in the study area so we have no information on mortality rates. However, the results of our study indicate forest change (Figure 3.6) is linked with long-term trends in precipitation (Figure 3.3) and long-term analysis is required to understand the cumulative effects of drought years in this ecosystem. Given the suggested mechanisms of mortality (section 3.5.1), we suspect there has been a continuum of mortality triggered by severe drought and our long-term field data confirm this suspicion as some plots had trees at different stages of decomposition (e.g. standing dead trees with fine branches still present, down trees in early stages of decomposition, etc.). Stands with a high level of mortality over a short time period will have a relatively quick change in NDMI. These areas will likely have a heightened chance of detection due to rapid change in NDMI. However, areas that exhibit lower amounts of mortality over longer time periods will have a smaller change in NDMI over a longer time period. The advantage of the time series approach should capture both hypothetical examples that might be otherwise missed by just two or a small number of time periods.

3.6 CONCLUSION

Coniferious and decidous forests in the southern portion of the Wyoming Basin ecoregion have experienced high levels of direct and indirect drought related mortaltiy over the last decade. This mortality has an effect on size-class distributions and thus implications for the future of these forests. In this work we identified an appropriate vegetation index (NDMI) that best represented short-term forest conditions of the study area. Through trend analysis, we identified the location, direction and magnitude of forest change by forest cover type. Our collection of long-term field data allowed us to relate plot-level changes to long term spectral trends. The results enabled us to quantify the amount of change and further assess the influence of landscape position on those trends. Our analysis provides managers with a long-term perspective of the

forest dynamics of this ecosystem with respect to variability in precipitation. Our field data provides evidence and demonstrates application of assessing long-term trends with Landsat imagery at fine spatial scales in a forest-shrubland matrix.

Previous trend analysis studies have used a variety of lines of evidence to support direction of change. Vogelmann et al. (2009) related areas of significant change to annual health aerial detection survey (ASD) polygons and qualitative field sampling. Only a small portion of our study area was surveyed by aerial detection, and only during one year. Czerwinksi et al. (2014) sampled a number of areas in the field with significant trends and qualitatively categorized each plot. McManus et al. (2012) correlated significant positive trends in NDVI to an increase in LAI based on a relationship with MODIS data across a regional scale. Our research establishes an empirical link between spatial differences in spectral reflectance and short-term field measured vegetation parameters such as plant area index and canopy gap fraction. The statistically significant (95% confidence level) spectral trajectories (Czerwinski et al., 2014; McManus et al., 2012) provide a distinct level of certainty over the duration of the study period. Furthermore, our long-term field data provides a line of ground based evidence to interpret the spectral changes over time. The framework we presented is suitable to retrospecitively characterize the effects of drought in forest ecosystems over the last 30 years. The use of Landsat data is beneficial as the time series can be extended in the future with the recently launched Landsat 8 satellite (OLI sensor).

We believe the methodology and results of this assessment provide a valuable perspective to resource managers and highlights potential opportunities to work across jurisdictional lines. This work highlights areas of forest that are resistant, persistent or vulnerable to severe drought.

The framework relies heavily on open access satellite data and could be applied to long-term monitoring of similar ecosystems.

Any use of trade, firm, or product names is for descriptive purposes only and does not imply endorsement by the U.S. Government.

3.8 TABLES

Table 3.1. Acquisition dates of Landsat scenes used in the analysis (path 36, row 32).Note, the OLI image was used to establish the relationship between field measured data and vegetation indices and was not used in the trend analysis. TM = Thematic Mapper, ETM+ = Enhanced Thematic Mapper Plus, and OLI = Operational Land Imager.

Acquisition Date (year-month-day)	**Sensor**
19850811	TM
19880724	TM
19910903	TM
19920828	TM
19930823	TM
19940709	TM
19950728	TM
19960831	TM
19970701	TM
19980805	TM
20000725	TM
20010829	TM
20020731	TM
20030819	TM
20040906	TM
20050905	TM
20070830	TM
20080731	TM
20090819	TM
20100705	TM
20110809	TM
20120803	ETM+
20120819	ETM+
20140902	OLI

Table 3.2. Spectral indices calculated from the Landsat OLI reflectance data; NDVI (Normalized Difference Vegetation Index), NDMI (Normalized Difference Moisture Index; also known as Normalized Difference Water Index), EVI (Enhanced Vegetation Index), and SAVI (Soil Adjusted Vegetation Index). EVI constants: G (gain factor) = 2.5, L (canopy background adjustment factor) = 1, C1 (atmospheric constant) = 6, C2 (atmospheric constant) = 7.5. SAVI constants: L (soil adjustment factor) = 0.5 (intermediate vegetation density).

Spectral Index	**Equation**	**Source**
NDVI	NDVI = (B5 – B4)/(B5 + B4)	(Rousse et al., 1974)
NDMI	NDMI = (B5 – B6)/(B5 + B6)	(Gao, 1996)
EVI	EVI = G * (B5 – B4)/(B5 + C1 * B4 – C2 * B2 + L)	(Huete et al., 2002)
SAVI	SAVI = (B5 – B4)/(B5 + B4) * (1 + L)	(Huete, 1988)

Table 3.3. Area of significant positive and negative trends for time series with greater than 10 observations. Trends reported have *p-values* that are significant at 0.05 or lower.

Time period	**Observations (*n*)**	**Significant positive change**		**Significant negative change**	
		Area (ha)	**% of forest cover**	**Area (ha)**	**% of forest cover**
1985 to 1998	10	1705	27	98	1.6
1985 to 2000	11	660	10.4	160	2.5
1985 to 2001	12	338	5.3	255	4.0
1985 to 2002	13	172	2.7	445	7.0
1985 to 2003	14	226	3.6	565	8.9
1985 to 2004	15	345	5.5	588	9.3
1985 to 2005	16	545	8.6	577	9.1
1985 to 2007	17	486	7.7	946	15.0
1985 to 2008	18	491	7.8	1127	17.8
1985 to 2009	19	567	9.0	1233	19.5
1985 to 2010	20	598	9.5	1291	20.4
1985 to 2011	21	720	11.4	1347	21.3
1985 to 2012	22	615	9.7	1606	25.4

Table 3.4. Summary of trends between 1985 and 2012. The area and proportion of change for each group is compared to the total amount of that forest group.

Direction of Change	Total Change Area (ha)	Functional Group			
		Deciduous		Coniferous	
		Area (ha)	% of class	Area (ha)	% of class
Increase	615	205	7.1	410	11.9
Decrease	1606	474	16.5	1132	32.8

Table 3.5. Topographic coefficients from the generalized linear model (GLM) fit of significant negative trends between 1985 and 2012. The variable *Aspect* is an indicator variable (N is the reference class). **P-value* is significant at 0.05 or lower.

Predictor Variable	Coefficient
(Intercept)	-8.22381*
Elevation	0.00286*
Slope	0.00234
Aspect	
N	NA
NE	-0.04581
E	-0.20159*
SE	-0.96975*
S	-1.27459*
SW	-0.91533*
W	-0.51793*
NW	-0.25089*

3.9 FIGURES

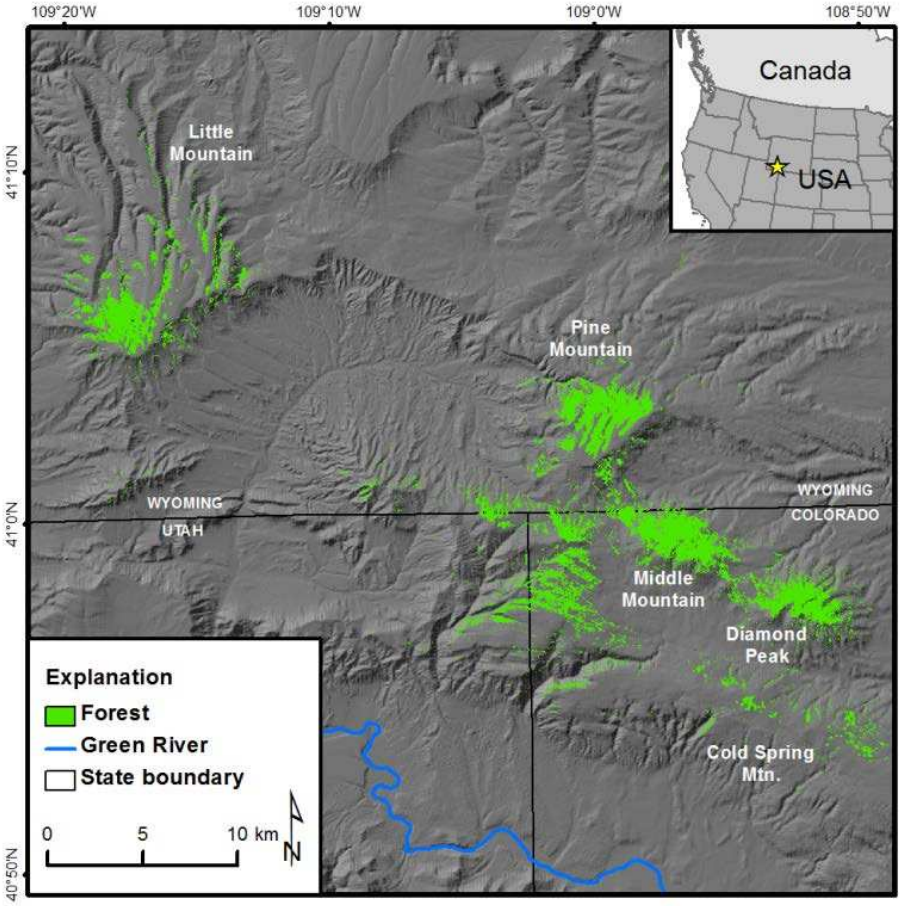

Figure 3.1. Location and extent of the forest in the study area.

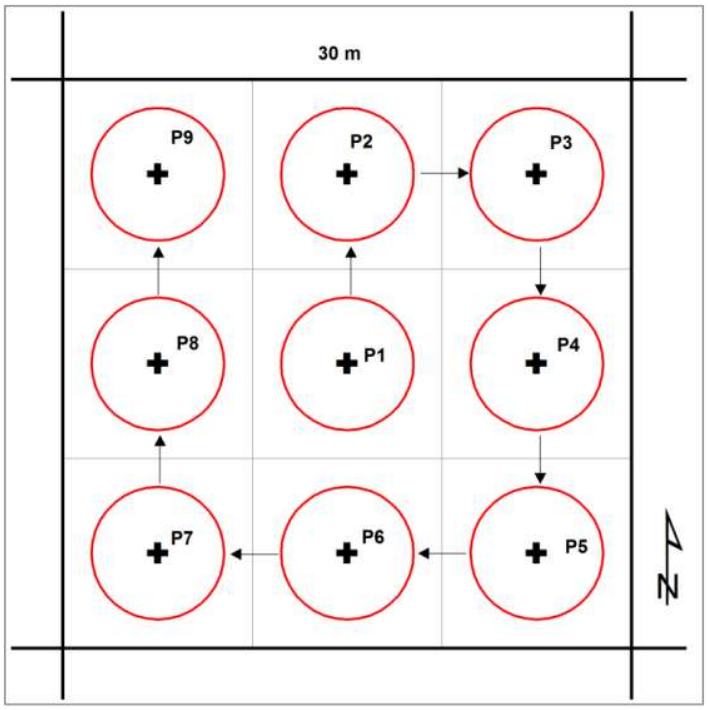

Figure 3.2. Plot based sampling design for derivation of vegetation structure traits. Each hemispheric photo location is spaced approximately 10 m from the nearest photo point. The field of view of each hemispheric photo is shown (red circle) with an approximate radius of 3.5 m.

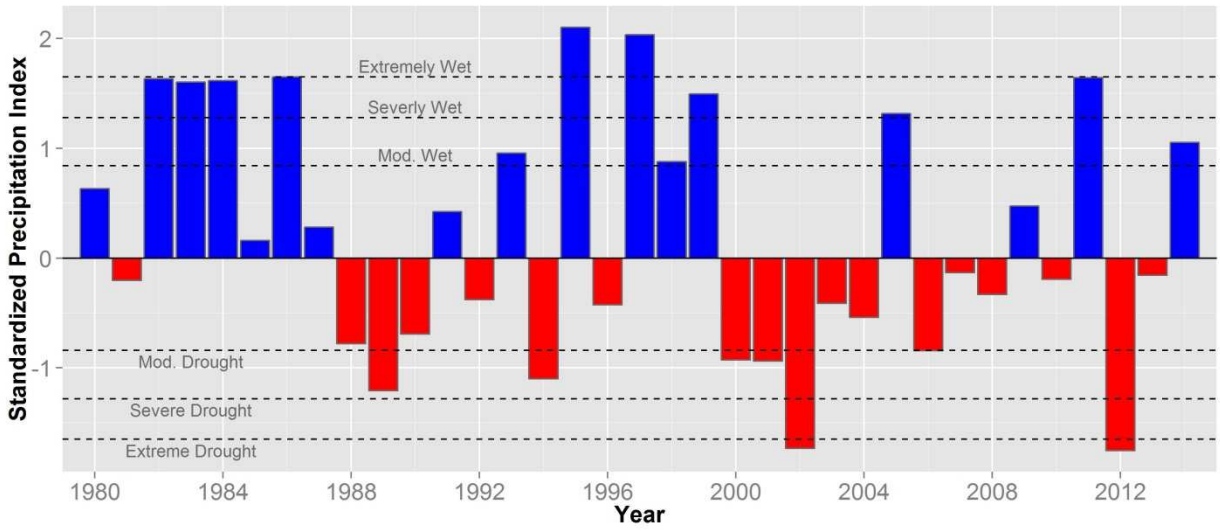

Figure 3.3. Standardized precipitation index (SPI) for the study area between 1980 and 2014. The index was calculated over a 12-month period, equivalent to the water year (October of previous year through September of current year). The SPI is classified according to Agnew (2000); values between moderate drought and moderately wet indicate the range of normal conditions.

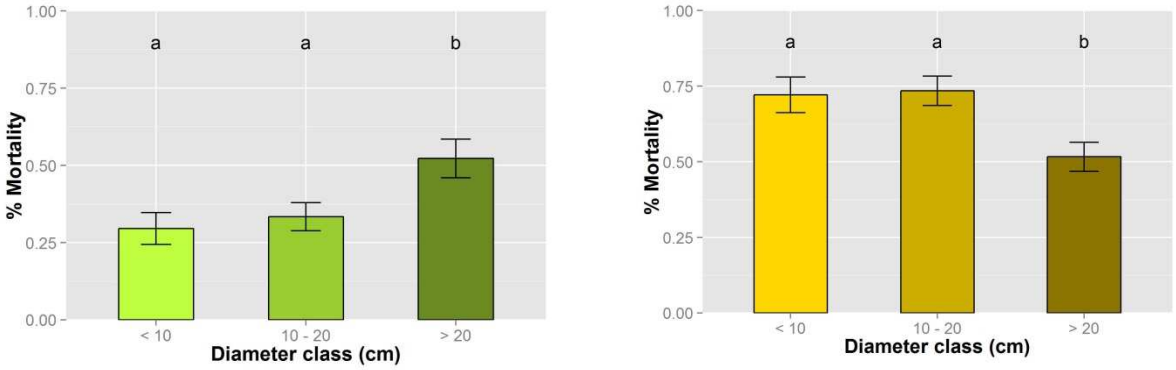

Figure 3.4. Relative mortality by tree size class in coniferous (*n*=877) (left – Fig 3.4a) and deciduous (*n*=1162) (right – Fig 3.4b) trees. Relative mortality was estimated as the percent of dead and down trees by class per plot. Different letters in each figure denote significant differences at the 95% confidence level using a Tukey HSD test.

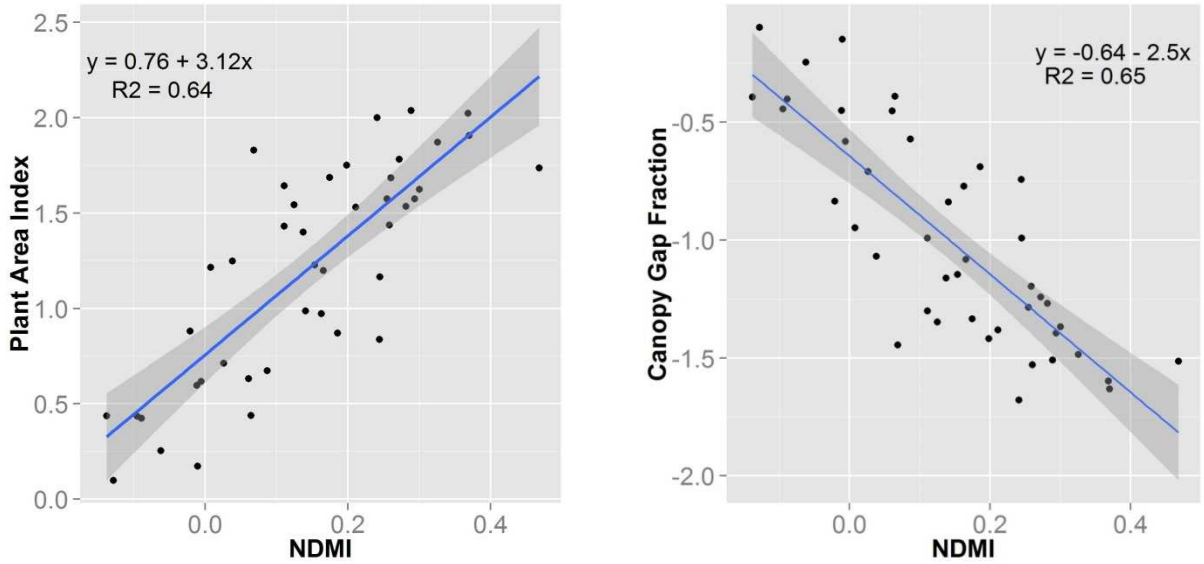

Figure 3.5. Relationships between field measured characteristics and NDMI.
(Left – Fig 3.5a) The relationship between field measured LAI/PAI and NDMI (*n*=43). (Right – Fig 3.5b) The relationship between field measured Canopy Gap Fraction and NDMI (*n*=43). Note that the y-axis is a log scale.

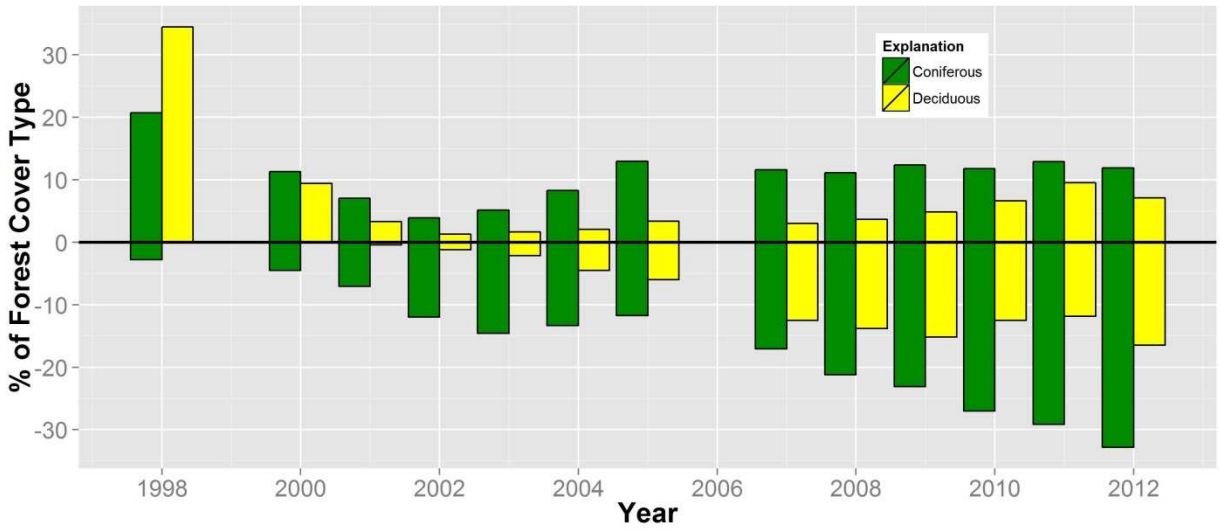

Figure 3.6. The results of the forest change analysis for trends with 10 or more observations. Compare with Table 3. There was no imagery available for 1999 and 2006.

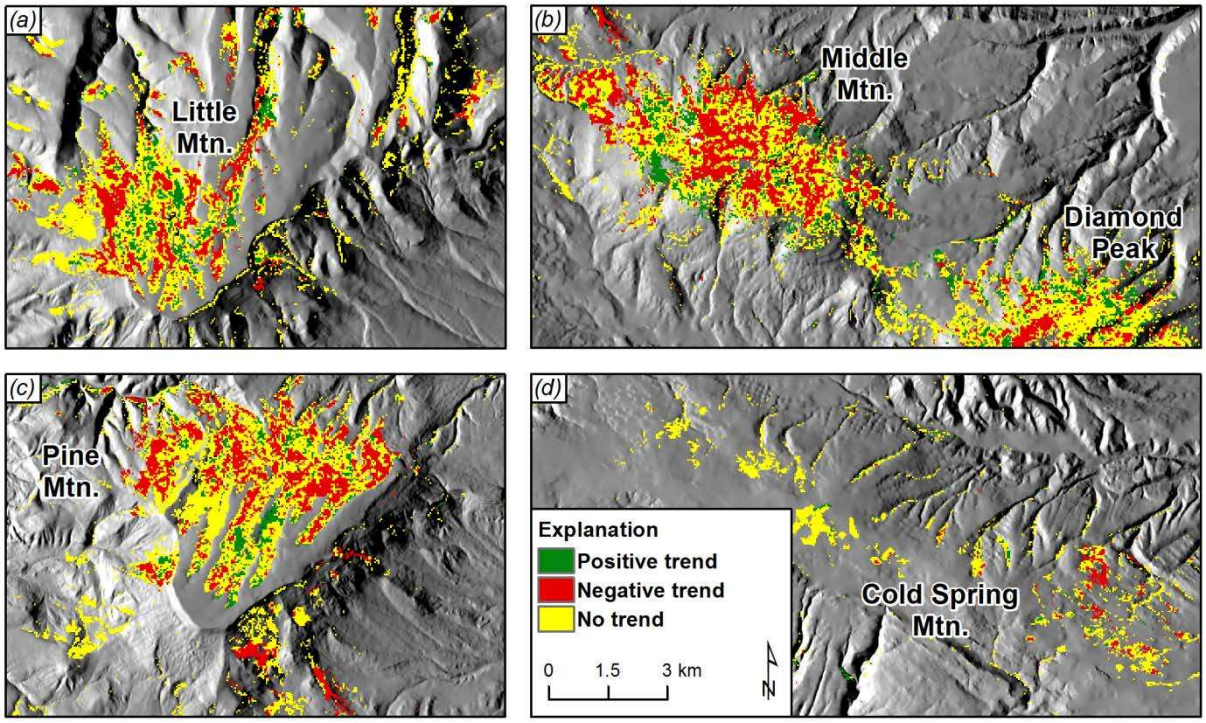

Figure 3.7. Locations of forest with positive, negative and no NDMI trend over the full time period of study (1985-2012). Positive and negative trends are significant that the 95% confidence level.

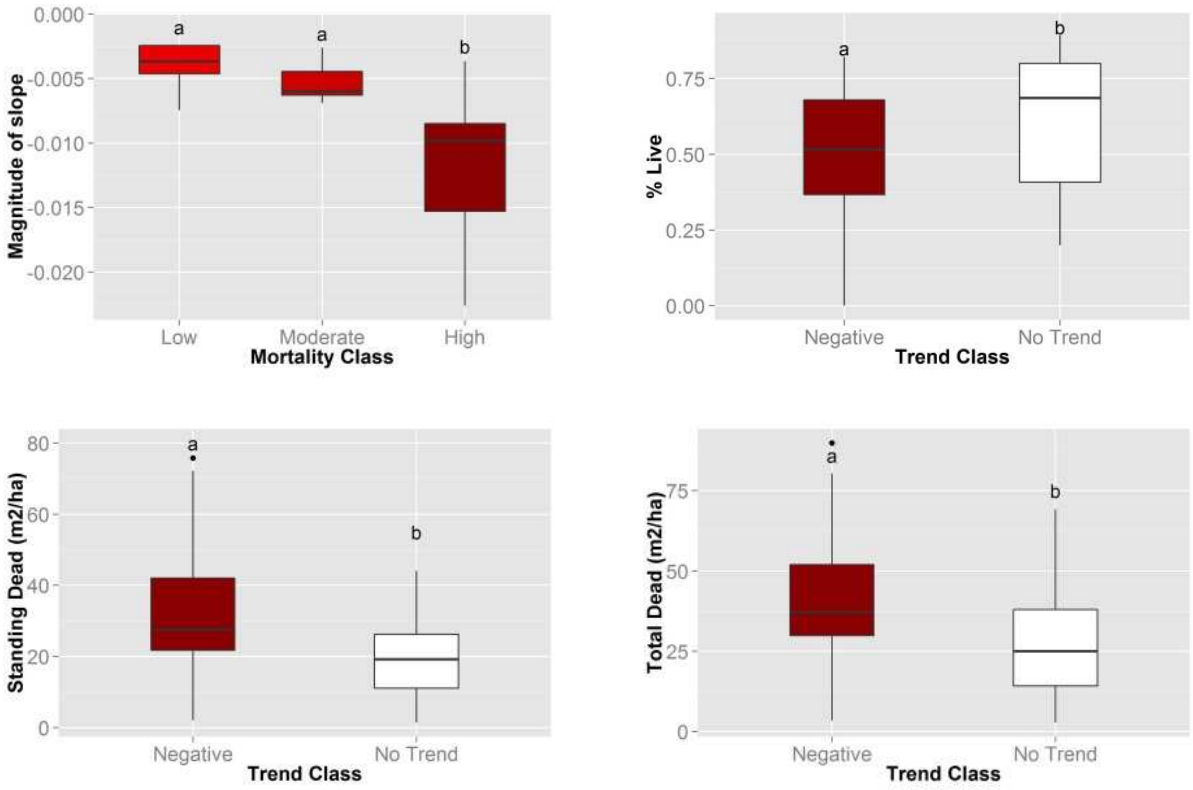

Figure 3.8. Results of boxplot analysis across trend class. Boxplots of the variation in magnitude of slope for significant negative trends categorized by relative mortality of field plots (*p-value* < 0.05) (top left). Boxplots of the variation of percent live trees between negative and no trend plots (*p-value* < 0.1) (top right). Boxplot of the variation in basal area of standing dead trees for plots with negative and no trend (*p-value* < 0.05) (bottom left). Boxplot of the variation in basal area of total dead trees (standing dead + down trees) for plots with negative and no trend (*p-value* < 0.05) (bottom right).

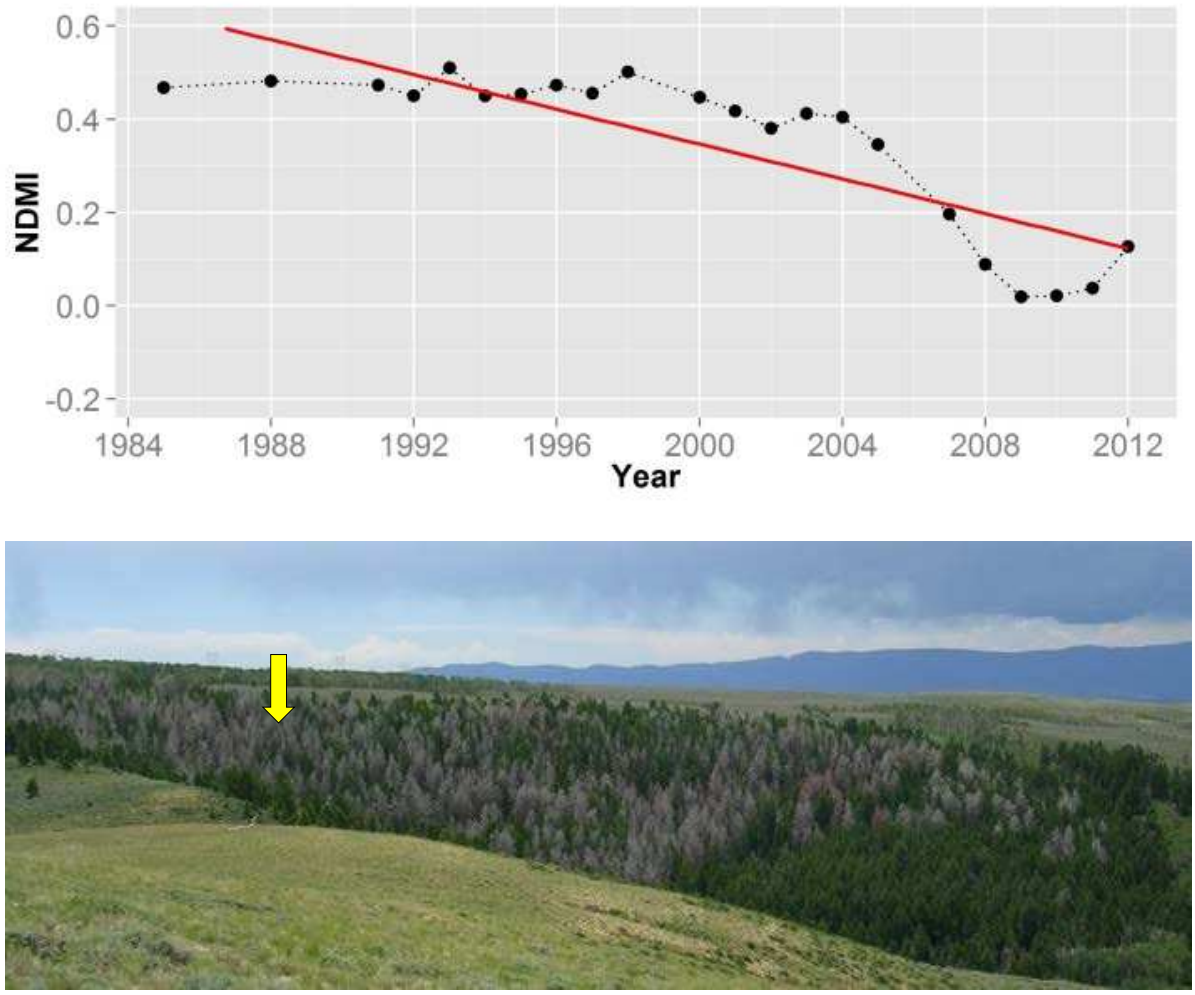

Figure 3.9. Negative trend of a high mortality coniferous forest plot. Negative NDMI trend (*p-value* < 0.05) (top) of a field plot located in coniferous forest with high levels of mortality (bottom).

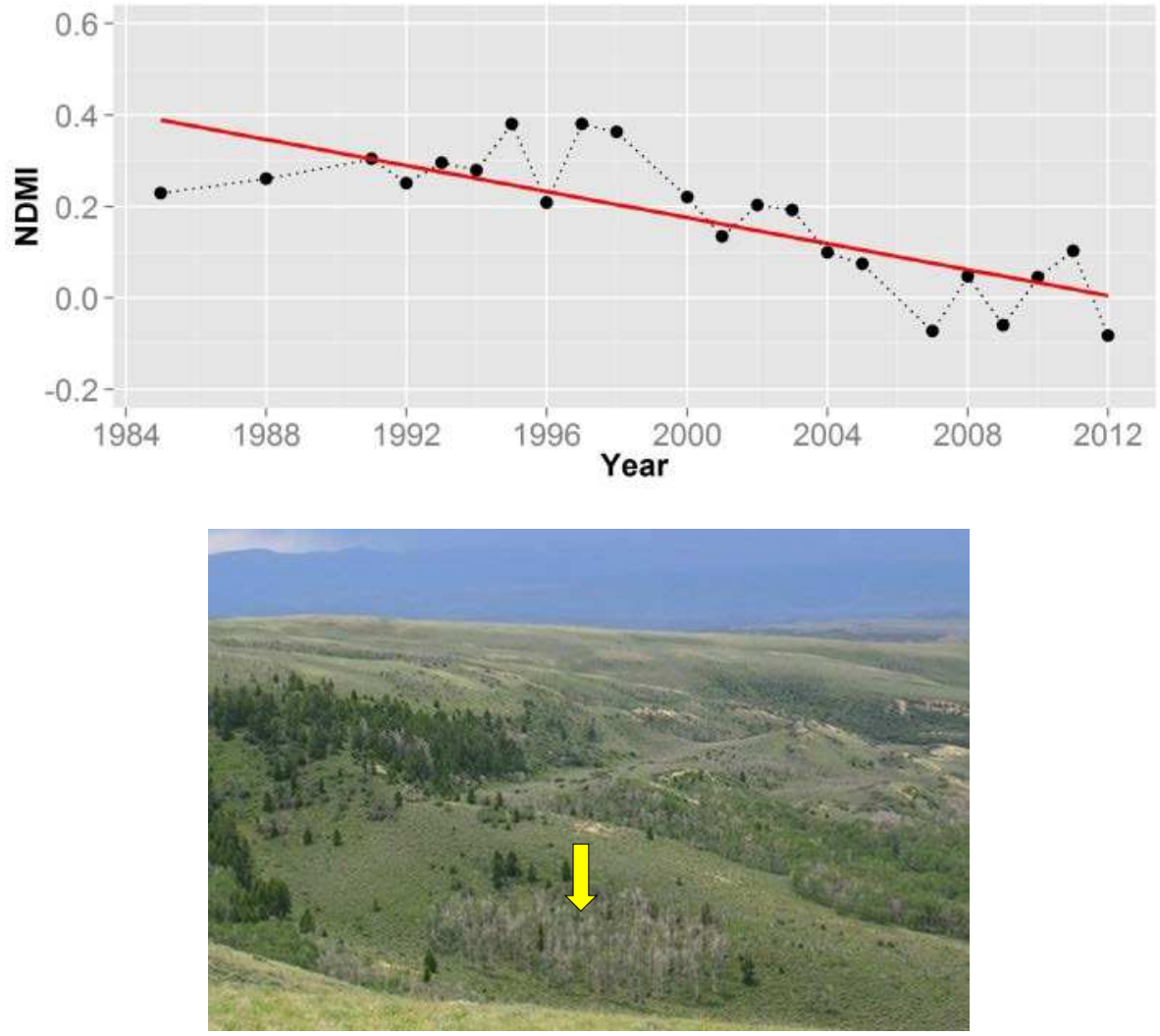

Figure 3.10. Negative trend of a high mortality deciduous forest plot. Negative NDMI trend (*p-value* < 0.05) (top) of a field plot located in an isolated aspen stand with high levels of mortality (bottom).

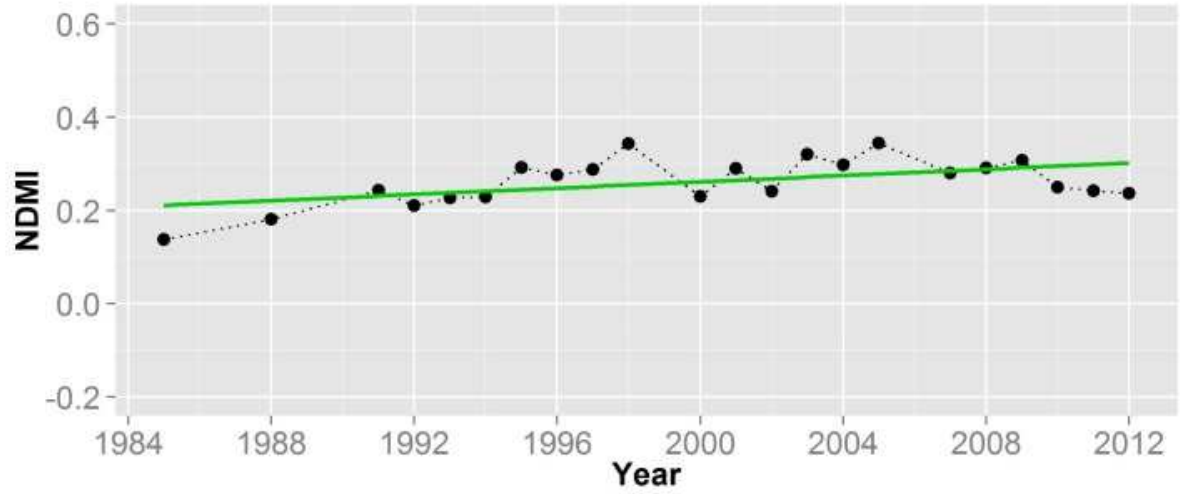

Figure 3.11. Positive trend of a low mortality coniferous forest plot. Positive NDMI trend (*p-value* < 0.05) (top) of a field plot located in a coniferous forest with low levels of mortality (bottom).

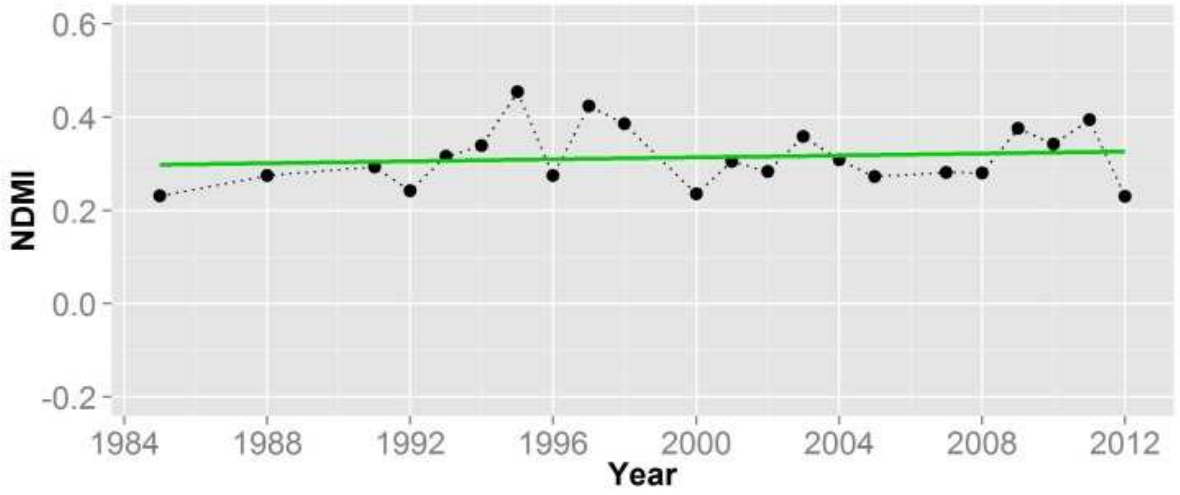

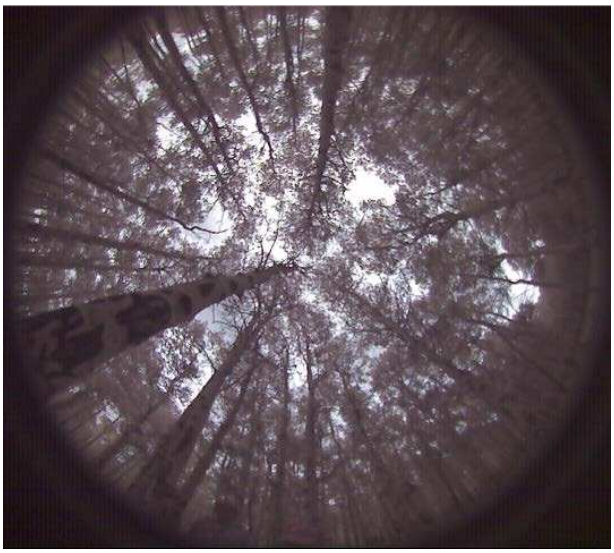

Figure 3.12. Stable trend of a low mortality deciduous forest plot. Stable NDMI trend (*p-value* not significant) (top) of a field plot located in aspen forest with low levels of mortality (bottom right). A digital hemispheric photo from the site indicates high plant area index and low canopy gap fractions (bottom left).

LITERATURE CITED

Abbas, S., Nichol, J.E., Qamer, F.M., Xu, J., 2014. Characterization of Drought Development through Remote Sensing: A Case Study in Central Yunnan, China. Remote Sens. 6, 4998–5018.

Agnew, C.T., 2000. Using the SPI to Identify Drought. Drought Netw. News 12, 6–12.

Allen, C.D., 2009. Climate-induced forest dieback: an escalating global phenomenon? Unasylva 60, 43–49.

Allen, C.D., Breshears, D.D., 1998. Drought-induced shift of a forest-woodland ecotone: rapid landscape response to climate variation. Proc. Natl. Acad. Sci. 95, 14839–42.

Allen, C.D., Macalady, A.K., Chenchouni, H., Bachelet, D., McDowell, N., Vennetier, M., Kitzberger, T., Rigling, A., Breshears, D.D., Hogg, E.H. (Ted), Gonzalez, P., Fensham, R., Zhang, Z., Castro, J., Demidova, N., Lim, J.-H., Allard, G., Running, S.W., Semerci, A., Cobb, N., 2010. A global overview of drought and heat-induced tree mortality reveals emerging climate change risks for forests. For. Ecol. Manage. 259, 660–684. doi:10.1016/j.foreco.2009.09.001

Assal, T.J., Anderson, P., Sibold, J., 2015. Mapping Forest Functional Type in a Forest-Shrubland Ecotone using SPOT Imagery and Predictive Habitat Distribution Modelling. Remote Sens. Lett. doi:10.1080/2150704X.2015.1072289

Assal, T.J., Sibold, J., Reich, R., 2014. Modeling a Historical Mountain Pine Beetle Outbreak Using Landsat MSS and Multiple Lines of Evidence. Remote Sens. Environ. 155, 275–288. doi:10.1016/j.rse.2014.09.002

Bastos, A., Gouveia, C.M., Trigo, R.M., Running, S.W., 2014. Analysing the spatio-temporal impacts of the 2003 and 2010 extreme heatwaves on plant productivity in Europe. Biogeosciences 11, 3421–3435. doi:10.5194/bg-11-3421-2014

Bentz, B.J., Régnière, J., Fettig, C.J., Hansen, E.M., Hayes, J.L., Hicke, J.A., Kelsey, R.G., Negrón, J.F., Seybold, S.J., 2010. Climate Change and Bark Beetles of the Western United States and Canada: Direct and Indirect Effects. Bioscience 60, 602–613. doi:10.1525/bio.2010.60.8.6

Bigler, C., Gavin, D.G., Gunning, C., Veblen, T.T., 2007. Drought induces lagged tree mortality in a subalpine forest in the Rocky Mountains. Oikos 116, 1983–1994. doi:10.1111/j.2007.0030-1299.16034.x

Breshears, D.D., Cobb, N.., Rich, P.M., Price, K.P., Allen, C.D., Balice, R.G., Romme, W.H., Kastens, J.H., Floyd, M.L., Belnap, J., Anderson, J.J., Myers, O.B., Meyer, C.W., 2005. Regional vegetation die-off in response to global-change-type drought. Proc. Natl. Acad. Sci. U. S. A. 102, 15144–8. doi:10.1073/pnas.0505734102

Campbell, G.S., Norman, J.M., 1989. The description and measurement of plant canopy structure, in: Russell, G., Marshall, B., Jarvis, P.G. (Eds.), Plant Canopies: Their Growth, Form, and Function. Society for Experimental Biology: 31. Cambridge University Press, Cambridge, United Kingdon, pp. 1–19.

Carreiras, J.M.B., Pereira, J.M.C., Pereira, J.S., 2006. Estimation of tree canopy cover in evergreen oak woodlands using remote sensing. For. Ecol. Manage. 223, 45–53. doi:10.1016/j.foreco.2005.10.056

Chander, G., Markham, B.L., Helder, D.L., 2009. Remote Sensing of Environment Summary of current radiometric calibration coefficients for Landsat MSS , TM , ETM + , and EO-1 ALI sensors. Remote Sens. Environ. 113, 893–903. doi:10.1016/j.rse.2009.01.007

Ciesla, W.M., 2010. 2010 Report on the Health of Colorado's Forests. Fort Collins, CO.

Cook, E.R., Woodhouse, C.A., Eakin, C.M., Meko, D.M., Stahle, D.W., 2004. Long-term aridity changes in the western United States. Science 306, 1015–8. doi:10.1126/science.1102586

Crookston, N.L., Rehfeldt, G.E., Dixon, G.E., Weiskittel, A.R., 2010. Addressing climate change in the forest vegetation simulator to assess impacts on landscape forest dynamics. For. Ecol. Manage. 260, 1198–1211. doi:10.1016/j.foreco.2010.07.013

Czerwinski, C.J., King, D.J., Mitchell, S.W., 2014. Mapping forest growth and decline in a temperate mixed forest using temporal trend analysis of Landsat imagery, 1987-2010. Remote Sens. Environ. 141, 188–200. doi:10.1016/j.rse.2013.11.006

DeRose, R.J., Long, J.N., Ramsey, R.D., 2011. Combining dendrochronological data and the disturbance index to assess Engelmann spruce mortality caused by a spruce beetle outbreak in southern Utah, USA. Remote Sens. Environ. 115, 2342–2349. doi:10.1016/j.rse.2011.04.034

Deshayes, M., Guyon, D., Jeanjean, H., Stach, N., Jolly, A., Hagolle, O., 2006. The contribution of remote sensing to the assessment of drought effects in forest ecosystems. Ann. For. Sci. 63, 579–595. doi:10.1051/forest

Dobrowski, S.Z., 2011. A climatic basis for microrefugia: the influence of terrain on climate. Glob. Chang. Biol. 17, 1022–1035. doi:10.1111/j.1365-2486.2010.02263.x

Dorman, M., Svoray, T., Perevolotsky, A., Sarris, D., 2013. Forest performance during two consecutive drought periods: Diverging long-term trends and short-term responses along a climatic gradient. For. Ecol. Manage. 310, 1–9.

Eidenshink, J., Schwind, B., Brewer, K., Zhu, Z.-L., Quayle, B., Howard, S., 2007. A Project for Monitoring Trends in Burn Severity. Fire Ecol. 3, 3–21.

Folke, C., Carpenter, S., Walker, B., Scheffer, M., Elmqvist, T., Gunderson, L., Holling, C.S., 2004. Regime Shifts, Resilience, and Biodiversity in Ecosystem Management. Annu. Rev. Ecol. Evol. Syst. 35, 557–581. doi:10.1146/annurev.ecolsys.35.021103.105711

Foster, D.R., Knight, D.H., Franklin, J.F., 1998. Landscape Patterns and Legacies Resulting from Large, Infrequent Forest Disturbances. Ecosystems 1, 497–510. doi:10.1007/s100219900046

Gao, B.C., 1996. NDWI - A normalized difference water index for remote sensing of vegetation liquid water from space. Remote Sens. Environ. 58, 257–266. doi:10.1016/S0034-4257(96)00067-3

Gitlin, A.R., Sthultz, C.M., Bowker, M.A., Stumpf, S., Paxton, K.L., Kennedy, K., Muñoz, A., Bailey, J.K., Whitham, T.G., 2006. Mortality gradients within and among dominant plant populations as barometers of ecosystem change during extreme drought. Conserv. Biol. 20, 1477–86. doi:10.1111/j.1523-1739.2006.00424.x

Goodwin, N.R., Coops, N.C., Wulder, M.A., Gillanders, S., Schroeder, T.A., Nelson, T., 2008. Estimation of insect infestation dynamics using a temporal sequence of Landsat data. Remote Sens. Environ. 112, 3680–3689. doi:10.1016/j.rse.2008.05.005

Gosz, J.R., 1992. Gradient analysis of ecological change in time and space: implications for forest management. Ecol. Appl. 2, 248–261.

Hessl, A.E., Graumlich, L.J., 2002. Interactive effects of human activities, herbivory and fire on quaking aspen (Populus tremuloides) age structures in western Wyoming. J. Biogeogr. 29, 889–902. doi:10.1046/j.1365-2699.2002.00703.x

Hogg, E.H., Brandt, J.P., Kochtubajda, B., 2005. Factors affecting interannual variation in growth of western Canadian aspen forests during 1951 – 2000. Can. J. For. Res. 622, 610–622. doi:10.1139/X04-211

Hogg, E.H., Brandt, J.P., Michaelian, M., 2008. Impacts of a regional drought on the productivity, dieback, and biomass of western Canadian aspen forests. Can. J. For. Res. 38, 1373–1384. doi:10.1139/X08-001

Hogg, E.H., Saugier, B., Pontailler, J.Y., Black, T.A., Chen, W., Hurdle, P.A., Wu, A., 2000. Responses of trembling aspen and hazelnut to vapor pressure deficit in a boreal deciduous forest. Tree Physiol. 20, 725–734.

Hope, A., Fouad, G., Granovskaya, Y., 2014. Evaluating drought response of Southern Cape Indigenous Forests, South Africa, using MODIS data. Int. J. Remote Sens. 35, 4852–4864. doi:10.1080/01431161.2014.930205

Huang, C.Y., Anderegg, W.R.L., 2012. Large drought-induced aboveground live biomass losses in southern Rocky Mountain aspen forests. Glob. Chang. Biol. 18, 1016–1027. doi:10.1111/j.1365-2486.2011.02592.x

Huete, A., Didan, K., Miura, T., Rodriguez, E.P., Gao, X., Ferreira, L.G., 2002. Overview of the radiometric and biophysical performance of the MODIS vegetation indices. Remote Sens. Environ. 83, 195–213. doi:10.1016/S0034-4257(02)00096-2

Huete, A.R., 1988. A Soil-Adjusted Vegetation Index (SAVI). Remote Sens. Environ. 25, 295–309.

Jones, H.G., Vaughan, R.H., 2010. Remote Sensing of Vegetation: Principles, Techniques, and Applications. Oxford University Press, Oxford, UK.

Kennedy, R.E., Yang, Z., Cohen, W.B., 2010. Detecting trends in forest disturbance and recovery using yearly Landsat time series: 1. LandTrendr — Temporal segmentation algorithms. Remote Sens. Environ. 114, 2897–2910. doi:10.1016/j.rse.2010.07.008

Knight, D.H., 1994. Mountains and Plains: The Ecology of Wyoming Landscapes. Yale University, New Haven, CT.

Kulakowski, D., Kaye, M.W., Kashian, D.M., 2013. Long-term aspen cover change in the western US. For. Ecol. Manage. 299, 52–59. doi:10.1016/j.foreco.2013.01.004

Lefsky, M., Cohen, W., 2003. Selection of remotely sensed data, in: Wulder, M.A., Franklin, S. (Eds.), Remote Sensing of Forest Environments: Concepts and Case Studies. Kluwer Academic Publishers, Boston, pp. 13–47.

Littell, J.S., McKenzie, D., Peterson, D.L., Westerling, A.L., 2009. Climate and wildfire area burned in western U.S. ecoprovinces, 1916-2003. Ecol. Appl. 19, 1003–1021.

Lloret, F., Lobo, a, Estevan, H., Maisongrande, P., Vayreda, J., Terradas, J., 2007. Woody plant richness and NDVI response to drought events in Catalonian (northeastern Spain) forests. Ecology 88, 2270–9.

Martens, S.N., Ustin, S.L., Rousseau, R.A., 1993. Estimation of tree canopy leaf area index by gap fraction analysis. For. Ecol. Manage. 61, 91–108.

Masek, J., Vermote, E.F., Saleous, N.E., Wolfe, R., Hall, F.G., Huemmrich, K.F., Gao, F., Kutler, J., Lim, T., 2006. A Landsat Surface Reflectance Dataset. IEEE Geosci. Remote Sens. Lett. 3, 68–72. doi:10.1109/LGRS.2005.857030

Maselli, F., 2004. Monitoring forest conditions in a protected Mediterranean coastal area by the analysis of multiyear NDVI data. Remote Sens. Environ. 89, 423–433. doi:10.1016/j.rse.2003.10.020

McCune, B., Keon, D., 2002. Equations for potential annual direct incident radiation and heat load. J. Veg. Sci. 13, 603–606.

McDowell, N., Pockman, W.T., Allen, C.D., Breshears, D.D., Cobb, N., Kolb, T., Plaut, J., Sperry, J., West, A., Williams, D.G., Yepez, E. a., 2008. Mechanisms of plant survival and mortality during drought: Why do some plants survive while others succumb to drought? New Phytol. 178, 719–739. doi:10.1111/j.1469-8137.2008.02436.x

McManus, K.M., Morton, D.C., Masek, J.G., Wang, D., Sexton, J.O., Nagol, J.R., Ropars, P., Boudreau, S., 2012. Satellite-based evidence for shrub and graminoid tundra expansion in northern Quebec from 1986 to 2010. Glob. Chang. Biol. 18, 2313–2323. doi:10.1111/j.1365-2486.2012.02708.x

Meddens, A.J.H., Hicke, J.A., Ferguson, C.A., 2012. Spatiotemporal patterns of observed bark beetle-caused tree mortality in British Columbia and the western United States. Ecol. Appl. 22, 1876–1891.

Meddens, A.J.H., Hicke, J.A., Vierling, L.A., Hudak, A.T., 2013. Evaluating methods to detect bark beetle-caused tree mortality using single-date and multi-date Landsat imagery. Remote Sens. Environ. 132, 49–58. doi:10.1016/j.rse.2013.01.002

Meigs, G.W., Kennedy, R.E., Cohen, W.B., 2011. A Landsat time series approach to characterize bark beetle and defoliator impacts on tree mortality and surface fuels in conifer forests. Remote Sens. Environ. 115, 3707–3718. doi:10.1016/j.rse.2011.09.009

Michaelian, M., Hogg, E.H., Hall, R.J., Arsenault, E., 2011. Massive mortality of aspen following severe drought along the southern edge of the Canadian boreal forest. Glob. Chang. Biol. 17, 2084–2094. doi:10.1111/j.1365-2486.2010.02357.x

Negrón, J., Lynch, A., Schaupp, W., Mercado, J., 2014. Douglas-Fir Tussock Moth- and Douglas-Fir Beetle-Caused Mortality in a Ponderosa Pine/Douglas-Fir Forest in the Colorado Front Range, USA. Forests 5, 3131–3146. doi:10.3390/f5123131

NEON, 2000. Report on first Workshop on the National Ecological Observatory Network (NEON). Lake Placid, Florida.

NOAA, 2012. NOAA National Climatic Data Center, State of the Climate: Drought for September 2012 [WWW Document]. State Clim. URL http://www.ncdc.noaa.gov/sotc/drought/201209 (accessed 5.25.15).

Pfeifer, M., Gonsamo, A., Disney, M., Pellikka, P., Marchant, R., 2012. Leaf area index for biomes of the Eastern Arc Mountains: Landsat and SPOT observations along precipitation and altitude gradients. Remote Sens. Environ. 118, 103–115. doi:10.1016/j.rse.2011.11.009

Prichard, S.J., Kennedy, M.C., 2014. Fuel treatments and landform modify landscape patterns of burn severity in an extreme fire event. Ecol. Appl. 24, 571–590.

Rehfeldt, G.E., Ferguson, D.E., Crookston, N.L., 2009. Aspen, climate, and sudden decline in western USA. For. Ecol. Manage. 258, 2353–2364. doi:10.1016/j.foreco.2009.06.005

Rogers, P.C., Landhausser, S.M., Pinno, B.D., Ryel, R.J., 2014. A Functional Framework for Improved Management of Western North American Aspen (Populus tremuloides Michx.). For. Manag. 60, 345–359.

Rousse, J.W., Hass, R.H., Schell, J.A., Deering, D.W., Harlan, J.C., 1974. Monitoring the vernal advancement of retrogradation of natural vegetation, Type III, Final Report. Greenbelt, Maryland.

Sousa, W.P., 1984. The Role of Disturbance in Natural Communities. Annu. Rev. Ecol. Syst. 15, 353–391.

St. Clair, S.B., Mock, K.E., LaMalfa, E.M., Campbell, R.B., Ryel, R.J., 2010. Genetic contributions to phenotypic variation in physiology, growth, and vigor of western aspen (Populus tremuloides) clones. For. Sci. 56, 222–230. doi:none

Stephenson, N.L., 1990. Climatic Control of Vegetation Distribution : The Role of the Water Balance. Am. Nat. 135, 649–670.

Thornthwaite, C., 1953. A charter for climatology. World Meteorol. Organ. Bull. 2, 40–46.

Turner, M.G., Baker, W.L., Peterson, C.J., Peet, R.K., 1998. Factors Influencing Succession: Lessons from Large, Infrequent Natural Disturbances. Ecosystems 511–523.

Turner, M.G., Dale, V.H., 1998. Comparing Large, Infrequent Disturbances: What Have We Learned? Ecosystems 1, 493–496.

Tüshaus, J., Dubovyk, O., Khamzina, A., Menz, G., 2014. Comparison of Medium Spatial Resolution ENVISAT-MERIS and Terra-MODIS Time Series for Vegetation Decline Analysis: A Case Study in Central Asia. Remote Sens. 6, 5238–5256. doi:10.3390/rs6065238

USGS, 2014. EarthExplorer archive [WWW Document]. URL http://edcsns17.cr.usgs.gov/NewEarthExplorer/

Van Mantgem, P.J., Stephenson, N.L., Byrne, J.C., Daniels, L.D., Franklin, J.F., Fulé, P.Z., Harmon, M.E., Larson, A.J., Smith, J.M., Taylor, A.H., Veblen, T.T., 2009. Widespread increase of tree mortality rates in the western United States. Science (80-.). 323, 521–524. doi:10.1126/science.1165000

Vicente-Serrano, S.M., 2007. Evaluating the impact of drought using remote sensing in a Mediterranean, Semi-arid Region. Nat. Hazards 40, 173–208. doi:10.1007/s11069-006-0009-7

Vogelmann, J.E., Tolk, B., Zhu, Z., 2009. Monitoring forest changes in the southwestern United States using multitemporal Landsat data. Remote Sens. Environ. 113, 1739–1748. doi:10.1016/j.rse.2009.04.014

Volcani, A., Karnieli, A., Svoray, T., 2005. The use of remote sensing and GIS for spatio-temporal analysis of the physiological state of a semi-arid forest with respect to drought years. For. Ecol. Manage. 215, 239–250. doi:10.1016/j.foreco.2005.05.063

Weiss, J.L., Gutzler, D.S., Allred, J.E., Dahm, C.N., 2004. Long-term vegetation monitoring with NDVI in a diverse semi-arid setting, central New Mexico, USA. J. Arid Environ. 58, 249–272. doi:10.1016/j.jaridenv.2003.07.001

Westerling, A.L., Hidalgo, H.G., Cayan, D.R., Swetnam, T.W., 2006. Warming and earlier spring increase western U.S. forest wildfire activity. Science (80-.). 313, 94094–3. doi:10.1126/science.1128834

Worrall, J.J., Egeland, L., Eager, T., Mask, R.A., Johnson, E.W., Kemp, P.A., Shepperd, W.D., 2008. Rapid mortality of Populus tremuloides in southwestern Colorado, USA. For. Ecol. Manage. 255, 686–696. doi:10.1016/j.foreco.2007.09.071

Worrall, J.J., Rehfeldt, G.E., Hamann, A., Hogg, E.H., Marchetti, S.B., Michaelian, M., Gray, L.K., 2013. Recent declines of Populus tremuloides in North America linked to climate. For. Ecol. Manage. 299, 35–51. doi:10.1016/j.foreco.2012.12.033

Yang, J., Weisberg, P.J., Bristow, N.A., 2012. Landsat remote sensing approaches for monitoring long-term tree cover dynamics in semi-arid woodlands: Comparison of vegetation indices and spectral mixture analysis. Remote Sens. Environ. 119, 62–71. doi:10.1016/j.rse.2011.12.004

CHAPTER 4: Modeling a Historical Mountain Pine Beetle Outbreak Using Landsat MSS and Multiple Lines of Evidence[3]

4.1 SUMMARY

Mountain pine beetles are significant forest disturbance agents, capable of inducing widespread mortality in coniferous forests in western North America. Various remote sensing approaches have assessed the impacts of beetle outbreaks over the last two decades. However, few studies have addressed the impacts of historical mountain pine beetle outbreaks, including the 1970s event that impacted Glacier National Park. The lack of spatially explicit data on this disturbance represents both a major data gap and a critical research challenge in that wildfire has removed some of the evidence from the landscape. We utilized multiple lines of evidence to model forest canopy mortality as a proxy for outbreak severity. We incorporate historical aerial and landscape photos, aerial detection survey data, a nine-year collection of satellite imagery and abiotic data. This study presents a remote sensing based framework to (1) relate measurements of canopy mortality from fine-scale aerial photography to coarse-scale multispectral imagery and (2) classify the severity of mountain pine beetle affected areas using a temporal sequence of Landsat data and other landscape variables. We sampled canopy mortality in 261 plots from aerial photos and found that insect effects on mortality were evident in changes to the Normalized Difference Vegetation Index (NDVI) over time. We tested multiple spectral indices and found that a combination of NDVI and the green band resulted in the strongest model. We report a two-step

[3] A version of this chapter was published in *Remote Sensing of Environment* on 23 Sept. 2014, available online: http://www.sciencedirect.com/science/article/pii/S0034425714003435. Assal, T.J., Sibold, J., Reich, R., 2014. Modeling a Historical Mountain Pine Beetle Outbreak Using Landsat MSS and Multiple Lines of Evidence. Remote Sens. Environ. 155, 275–288. doi:10.1016/j.rse.2014.09.002

process where we utilize a generalized least squares model to account for the large-scale variability in the data and a binary regression tree to describe the small-scale variability. The final model had a root mean square error estimate of 9.8% canopy mortality, a mean absolute error of 7.6% and an R^2 of 0.82. The results demonstrate that a model of percent canopy mortality as a continuous variable can be developed to identify a gradient of mountain pine beetle severity on the landscape.

4.2 INTRODUCTION

Temperate forest ecosystems are subject to various ecological disturbances that can have profound effects on the structure of the ecosystem for many years after the event (Turner and Dale, 1998) and influence the likelihood, severity and spread of subsequent disturbances (Veblen et al., 1994). In western North America, native bark beetles are a major disturbance agent capable of regional-scale forest mortality (Raffa et al., 2008). Remotely sensed imagery has been used to characterize such widespread disturbance events over the last two decades (Wulder et al., 2006a). However, very little research has employed these techniques to study insect disturbance prior to the recent period of extended outbreak (~pre late 1990s). The northern Rocky Mountains experienced a widespread mountain pine beetle outbreak in the late 1970s to early 1980s (Logan and Powell, 2001). However, the lack of spatially explicit data on the extent and severity of this outbreak limits our understanding of the influence that this disturbance had on the landscape. To overcome this challenge, we utilized multiple lines of evidence to retrospectively characterize forest canopy mortality from the outbreak by comparing temporal changes in archived satellite imagery.

4.2.1 Mountain Pine Beetle Overview

The mountain pine beetle (*Dendroctonus ponderosae*) is a native species found in the western United States and Canada that attacks and reproduces in live trees (Bentz et al., 2010). The mechanisms with which populations switch to epidemic levels are complex (Bentz et al., 2010; Raffa et al., 2008), but include suitable host availability (amount, vigor, age and density) and condition (Fettig et al., 2007), along with beetle population survival and growth given thermal conditions (Powell and Logan, 2005). Epidemic populations are capable of landscape-scale forest mortality leading to cascading effects on forest structure, species composition and function (Raffa et al., 2008). Major host species include lodgepole pine (*Pinus contorta*), ponderosa pine (*P. ponderosa*), and whitebark pine (*P. albicaulis*) (Bentz et al., 2010). Impacted forests exhibit unique and visible characteristics at each stage of a mountain pine beetle attack (Wulder et al., 2006a). Killed trees begin to show visible changes as the foliage changes from green to yellow to red over the first year after the attack. The gray attack stage typically commences three years after the attack, as most trees will have lost all needles at that time (Wulder et al., 2006a).

4.2.2 Remote Sensing and Disturbance

Historical aerial photography is a valuable research tool providing detailed records of forest landscapes over the last half century or more. Although limited in spatial extent, these records provide a fine-scale snapshot of landscapes at one or multiple points in time. Previous studies have successfully used aerial photos collected during two or more time periods to measure changes in tree cover (Brown et al., 2006; Di Orio et al., 2005; Kadmon and Harari-Kremer, 1999; Kennedy and Spies, 2004; Manier et al., 2005; Platt and Schoennagel, 2009; Strand et al., 2006). The use of satellite multispectral imagery to map and monitor forest

condition over larger regions is also well documented (Cohen et al., 2001; Maselli, 2004; Nemani et al., 2009; Schroeder et al., 2006; Townshend et al., 2012; Volcani et al., 2005) dating back to the early 1970s with the initiation of the Landsat program (NASA, 2013). Several studies have used aerial photos as a surrogate for field data collection and then used that information to scale up to satellite imagery. This technique has been accomplished to map various attributes including land cover type (Parmenter et al., 2003), tree cover (Carreiras et al., 2006; Cohen et al., 2001; Homer et al., 2007), and surface imperviousness (Homer et al., 2007). Photos can be used to sample post-disturbance forest patterns, such as canopy mortality. The aerial photo reference data can be used to bridge the gap in scale between localized tree mortality measures and the more coarse scale of satellite imagery (Meddens et al., 2013). This hybrid approach allows for detection of fine-scale disturbance patterns captured in the aerial photos, while taking advantage of the multispectral and multitemporal components of Landsat imagery at the landscape scale. Furthermore, it provides a pathway to conduct a retrospective analysis.

Ecological disturbance alters ecosystem structure by both abrupt, conspicuous change and by gradual, slow change over some period of time. Such impacts allow remote sensing to capture the pre- and post-landscape, and in some cases, the duration of the event. Aerial photos have been utilized to investigate the impacts of fire (Bebi et al., 2003; Johnson and Fryer, 1987), insect damage (Bebi et al., 2003; White et al., 2005), extreme drought (Allen and Breshears, 1998), and blowdown (Baker et al., 2002) on forest and woodland ecosystems. At regional scales, multispectral satellite imagery has been employed to study diverse types of forest disturbance including fragmentation (Fuller, 2001), fire (Turner et al., 1994), drought (Huang et al., 2010) and insect induced mortality (DeRose et al., 2011; Vogelmann et al., 2009). Numerous studies have utilized multispectral imagery to document the extent and severity of the recent

mountain pine beetle outbreak over the last decade. Efforts range from fine-scale satellite and aerial multispectral imagery acquired from one time period (Coops et al., 2006; Dennison et al., 2010; Hicke and Logan, 2009; Meddens et al., 2011), to moderate resolution sensors incorporating multiple time periods (Goodwin et al., 2008; Meddens et al., 2013; Meigs et al., 2011; Wulder et al., 2006b).

We found few studies in the literature that used the first generation of Landsat data to detect mountain pine beetle outbreaks or other insect-driven forest disturbance. The Landsat Multispectral Scanner System (MSS) sensor was carried onboard the first five Landsat satellites and provided imagery from 1972 until 1995 (NASA, 2013). Researchers in British Columbia (Harris et al., 1978) used single date MSS imagery to detect damage caused by the Douglas-fir tussock moth and western spruce budworm with little success. Weber et al. (1975) employed single date MSS imagery to map mountain pine beetle damage in Ponderosa pine. Rencz and Nemeth (1985) tested both a single date approach and a change detection approach over a six-year period to map mountain pine beetle damage in British Columbia. Both mountain pine beetle studies concluded that MSS imagery does not have the capability to detect beetle damage given the spatial resolution of the imagery. However, the British Columbia study (Rencz and Nemeth, 1985) noted greater detection accuracy at sites with heavy, continuous damage, suggesting the spatial resolution is less limiting in areas with high-severity outbreaks.

4.2.3. Outbreak Impacts to Forest Vegetation Spectral Properties

Living vegetation absorbs blue and red light energy, while radiation in the green and near-infrared portion of the electromagnetic spectrum is reflected (Jones and Vaughan, 2010). Therefore, color-infrared photos can be used to distinguish between areas of live trees and dead trees. As the foliage of killed trees changes during the first year after the attack, the spectral

response also begins to change (Rencz and Nemeth, 1985). At the cellular level, mortality contributes to a reduction in foliar moisture and chlorophyll, as other pigments and cellular structure begin to break down (Mauseth, 1988). As a result, the spectral reflectance in the red wavelength (630-690 nm) increases, whereas the reflectance in the green wavelength (520-600 nm) decreases (Ahern, 1988).

Disturbances where large portions of forest vegetation are removed from the landscape, such as fire and clear cutting, create a drastic change in spectral reflectance. Conversely, subtle changes in foliage color over time may prove more difficult to detect. Nevertheless, the phenology associated with mortality caused by an outbreak will lead to a change in satellite-detected reflectance of the forest canopy. An analysis of multiple years of moderate spatial resolution imagery has the potential to capture reflectance patterns before, during and after landscape-scale disturbance events (Goodwin et al., 2008; Wulder et al., 2006a).

Multiple types of spectral indices have been employed to detect the impacts of mountain pine beetle disturbance over the last decade. Examples of indices include the Normalized Difference Moisture Index (Goodwin et al., 2008, 2010; Meddens et al., 2013), the Tasseled Cap (Meddens et al., 2013), the Enhanced Wetness Disturbance Index (Skakun et al., 2003; Wulder et al., 2006b), the Normalized Burn Ratio (Meigs et al., 2011), the Red-Green Index (RGI) (Coops et al., 2006; Hicke and Logan, 2009; Meddens et al., 2013), the Band 5/Band 4 Ratio (Meddens et al., 2013), and the Normalized Difference Vegetation Index (Meddens et al., 2013). Various levels of success were obtained with each index. Many of these indices are derived from Landsat TM or ETM+ imagery. However, Landsat TM imagery is not available prior to 1984 (for the study area) and Landsat ETM+ imagery is not available before 1999. Because the outbreak that is the focus of this study erupted in the mid-1970s, Landsat MSS imagery represents the only

available satellite imagery. Given the four multispectral bands of MSS (Table 4.1), we were only able to utilize a subset of these indices.

4.2.4 Aerial Detection Survey Data

The US Forest Service (USFS) has been conducting annual forest health aerial detection surveys (ADS) since the middle of the 20th century. In summary, human observers record the type and extent of abiotic and biotic disturbances and host species onto sketch maps (Meigs et al., 2011). The sketch maps are hard copy maps used by human observers in planes that are later converted to digital form. This data has successfully been integrated into remote sensing detection studies of insect disturbance (Meddens et al., 2012; Meigs et al., 2011). The Forest Health Protection Aviation Program in USFS Region 1 (including Glacier National Park (GNP)) maintains digital files of the ADS data since 2000. Staff at GNP digitized the ADS data from 1962-1998. The data include information about insect species, host tree species, damage type, and forest type. However, very few polygons contained information on the number of trees killed per acre (severity), which is commonly included in contemporary ADS data and is critical to relating outbreaks to forest processes and change. Furthermore, the disturbance polygons identified in the ADS data were very large (e.g. > 70,000 ha). Although useful for broad-scale monitoring, we suspect the ADS data do not represent the heterogeneous impacts of the disturbance. Since we are interested in both the extent and severity of the disturbance, these missing details heavily influenced the direction of this study.

4.2.5 Objectives

The goal of the study was to test an approach combining multiple lines of evidence to reconstruct the extent and severity of a mountain pine beetle outbreak in a topographically complex landscape. Furthermore, subsequent disturbance (fire) has removed evidence from large

areas of the study area. To accomplish this, we used a combination of aerial detection survey data, historical aerial and landscape photos, National Park Service reports and a temporal sequence of satellite imagery. Each data source has limitations in the spatiotemporal record. However, by combining disparate sources of data across spatial and temporal scales, we aimed to reduce the uncertainty associated with reconstructing outbreak parameters. Employing multiple lines of evidence from independent data sources has the potential to extend the information associated with each piece of data and create a robust composite picture of the outbreak (Swetnam et al., 1999). Reference data was collected from aerial photos and scaled up to satellite imagery measurements over time. We hypothesized that the impacts of the disturbance to the forest canopy (i.e. mortality) would be captured in spatiotemporal changes in reflectance. Finally we sought to demonstrate a novel approach in the use of existing data to assess a historic disturbance.

The objectives of this study are to:

1. Relate measurements of canopy mortality from fine-scale aerial photography to coarse-scale multispectral imagery;
2. Classify the severity of mountain pine beetle affected areas using a temporal sequence of Landsat data and other landscape variables.

4.3 METHODS

4.3.1 Study Area

The study was located in Glacier National Park in northwestern Montana, USA (Figure 4.1) and chosen because of the extensive mountain pine beetle epidemic that occurred there in the 1970s (Hamel et al., 1977; McGregor et al., 1975). The park encompasses 4,080 km^2 (408,000 ha) of diverse terrain on either side of the Continental Divide. Mean average annual

precipitation is 73.1 cm, and average annual maximum and minimum temperatures are 11.9 ºC and -0.2 ºC, respectively (1971-2000) (Western Regional Climate Center, West Glacier station, elevation: 970 m, http://www.wrcc.dri.edu; accessed 17 December 2012). The climate averages from this station are consistent with stations on the east side of the park. Elevation ranges from ~ 950 m to 3184 m above sea level and major cover types include grasslands, conifer and deciduous forests, lakes, wide glacial valleys and steep alpine zones. Forests are dominated by lodgepole pine (*Pinus contorta*), western larch (*Larix occidentalis*), Engelmann spruce (*Picea engelmannii*) and Douglas-fir (*Pseudotsuga menziesii*).

Given the size and diverse landscape of the park, we limited the study area based on several assumptions. First, vegetation cover types not susceptible to mountain pine beetle attack were identified using ReGAP (Davidson et al., 2009) and omitted. Second, we calculated the cumulative extent of mountain pine beetle damage identified by the ADS data between 1971 and 1987. The area not impacted by the mountain pine beetle outbreak during the buffered time period was omitted from further analysis. The area of interest was also confined by the extent of available satellite imagery used in the analysis. The confined area of interest is 1195 km^2 (119,552 ha) and ranges in elevation from ~ 950 m to 2960 m above sea level (Figure 4.1).

4.3.2 Aerial and Landscape Photograph Processing

Six color infrared aerial photographs were obtained in digital format from the US Geological Survey's Earth Resources Observation and Science Center (Figure 4.1). Four of the photos were acquired in 1982 (west of the Continental Divide), two in 1984 (east of the divide). All photos have a scale of 1:58,000 and were scanned at a resolution of 1800 dots per inch. The photos were orthorectified to a 2009 NAIP photo (National Agriculture Imagery Program) using ground control points (GCPs) and a 30 m digital elevation model (DEM) (Leica Photogrammetry

Suite, Erdas, Inc., Norcross, GA, USA). The average root mean square error (RMSE) for each photo was less than two meters. We independently assessed the average displacement between each of the orthorectified images and the 2009 NAIP image at multiple locations within each image pair. The average displacement between both sets of images was less than two meters and deemed acceptable.

We searched two landscape photographic archives (the US Geological Survey Photographic Library and Glacier National Park Research Library) to locate additional sources with evidence of the disturbance. We obtained several color photos taken in the late 1970s or 1980 that contained evidence of the outbreak. In several cases the extent of the aerial color infrared photo and the color landscape photo were congruent. We were able to match the two photos and identify unique patterns and patches of mortality in each photo. Although this was a qualitative analysis, the additional information provided us with concrete evidence of the disturbance in the aerial photos (Figure 4.2).

4.3.3 Aerial Detection Survey Data

We obtained the digital version of the ADS data (1962-1998) from GNP and subset annual shapefiles to correspond with the start of the outbreak (1971) and the last year before extensive fires in the park (1987). We queried polygons associated with mountain pine beetle using the *Damage Causal Agent* attribute code and clipped the shapefile to the extent of the park for each year. Each annual shapefile was converted to an annual grid (30 m), snapped to the master Landsat image, and aggregated to form a cumulative mountain pine beetle extent and used to constrain the study area. We did examine the ADS data for other disturbance agents within the park to ensure there were no unaccounted disturbances. However, we found very few disturbance polygons, accounting for a very small area, within the analysis mask.

4.3.4 Satellite Data

Terrain corrected Level 1T MSS imagery were obtained from the USGS EarthExplorer Archive (USGS, 2012) of the study area before, during and after the peak of the outbreak. The imagery had been resampled by the USGS to a spatial resolution of 60 m in four spectral bands (Table 4.1). We utilized nine scenes in the analysis (Table 4.2). Late summer data were used (late August-September) due to availability of cloud-free imagery and the presumed relative phenological stability of the forests during this time period (Vogelmann et al., 2009). Geometric correction, calibration, atmospheric correction and image normalization procedures were applied to the imagery and are fully described in Appendix B.

Given the four multispectral bands of MSS, we were only able to utilize three spectral indices in the model evaluation process (Table 4.3). The GNDVI is sensitive to the presence of chlorophyll since the green spectral region is used instead of the red region (Carreiras et al., 2006). We did not use Band 3 as a covariate as it is often highly correlated with band 4 of MSS data. A preliminary investigation identified that NDVI performed the best among spectral indices. In an effort to limit redundancy in the data, we transformed the NDVI time series using principal component analysis. The principal components were used as predictor variables in one of the five models tested.

4.3.5 Sampling

We estimated beetle induced forest mortality using data collected from the aerial photos and compared these measurements with changes in spectral values over time. We segregated the landscape into 12 facets based on slope and aspect. These two variables influence forest composition, tree vigor and subsequent susceptibility to mountain pine beetle (Raffa et al., 2008). Furthermore, dividing the landscape into sub-regions of similar biophysical characteristics

can isolate spectral gradients (Homer et al., 2004). Both variables were derived from the elevation dataset. Aspect was classified into four categories (north, east, south or west) while slope was classified into three quantiles: low (<12%), moderate (12-29%) and high (>29%). Initially 350 random points were proportionally allocated in each landscape class, and square plots of 180 m x 180 m were delineated around the center of each point. The plot size was chosen considering the spatial resolution of the satellite imagery, i.e. 3 x 3 Landsat MSS pixels. A negative buffer was used to insure each plot was located completely within one landscape facet, and deleted (10%) if it fell within multiple facets. In addition, limitations due to topographic shadow or image blur from the orthorectification process warranted the omission of some plots (13%). As a result, each landscape facet did not contain the same number of sampling plots.

An unsupervised classification in Erdas Imagine was conducted on each air photo resulting in 20 classes. We used an iterative approach to determine the number of unsupervised classes that maximized spectral separation without generating an unwieldy number of classes. For each plot, we manually interpreted the 20 classes and assigned each class to live forest, dead forest, or shadow (Figure 4.3). We then calculated the ratio of dead canopy cover to total canopy cover in each plot. We omitted shadow pixels as they represent unknown cover types.

4.3.6 Statistical Analysis

Regression analysis can be used to explain large-scale variability, while model residuals can be used to describe small-scale variability in the data (Cressie, 1993). We used a generalized linear model (GLM, Gaussian distribution, Identity link function) to identify a set of explanatory variables to estimate canopy cover change on the sample plots over time. Predictor variables included spectral indices derived from nine years of Landsat MSS data, topography (elevation,

slope, aspect and topographic position index), and variables derived from the ADS data (first year detected, last year detected and total number of years detected). Aspect and the variables derived from the aerial survey data were treated as indicator variables in the analysis. Aspect was binned into four classes: North (0-45º; 315-365º), East (45-135º), South (135-225º), and West (225-315º). Three categorical variables were derived from the aerial survey data: first year of attack (early, mid, or late in the outbreak), last year of attack (early, mid, or late in the outbreak) and total number of years recorded during the outbreak (low, moderate, or high).

We tested five models in our analysis using different combinations of vegetation indices as the primary biotic variables. For each model, a stepwise selection by Akaike's Information Criterion (AIC) was used to identify the best subset of independent variables to include in the regression models (R Development Core Team, 2013). The aspect variable was allowed to interact with the primary vegetation index in each model. We evaluated the models through consideration of AIC, the mean absolute error of prediction (MAE) and the root mean square error of prediction (RMSE). Furthermore, a ten-fold cross validation procedure (DAAG package in R) was employed to calculate the prediction error of each model.

Residual error from the regression model can be utilized to describe the small-scale variability in the data (Manier et al., 2005; Reich et al., 2011). Model residuals may still contain useful information that can be utilized to gain precision in estimation (Pongpattananurak et al., 2012). We modeled the residual error from the selected regression model using a binary regression tree. We tested the residuals of the selected GLM model and the regression tree model for spatial autocorrelation using the Moran's I statistic (Legendre and Fortin, 1989). The sampled plots were clustered on the landscape into three distinct groups based on the availability of the aerial photos. We assumed points between each cluster were spatially independent and employed

a block diagonal spatial weights matrix (Upton and Fingleton, 1985) to account for the clustered nature of the plots. We used inverse distance to define the neighborhood structure of the three spatial weights matrices (one for each cluster).

The residuals of the GLM-CART model exhibited spatial autocorrelation. We addressed the issue by running the regression analysis using a Generalized Least Squares (GLS) model. A variogram was fit using the residuals of the GLM model to describe the degree of spatial dependence in the residuals. A Gaussian variogram model was fit to the sample variogram using least squares to estimate the nugget, sill and range. The GLS regression was used to estimate the parameters of the trend surface model in the presence of spatial autocorrelation. We allowed plot location (east or west of the Continental Divide) to enter the model to test if the outbreak impacts were different on either side of the divide. We used the residuals of the GLS to model the small-scale variation in the data using binary regression trees as described above.

After parameterizing and validating the models, forest canopy change was projected to the landscape area of interest in three steps. First a trend surface was created from the parameters of the GLS model using the raster calculator in ArcGIS. Next, a surface of the residuals generated from the regression tree model was created using a series of conditional statements in the raster calculator. Finally, the trend and residual surfaces were added together to create a continuous surface of forest canopy change scaled between 0 and 1. Areas of cloud cover, cloud shadow and topographic shadows represent uncertainty and were omitted from the analysis. Only two years of data (1978 and 1983) contained sparse clouds, but topographic shadows were present in all years. We applied a NDVI threshold (< 0.2) to remove clouds and topographic shadows (Hicke and Logan, 2009) and cloud shadows were manually delineated and removed.

4.4 RESULTS

4.4.1 Aerial Detection Survey Data

Our analysis of the aerial survey data indicates the outbreak was first identified in 1971 in the north-west portion of the park in very small isolated patches. The outbreak continued to spread from these centers until the mid-1970s when it was reported widely across the western portion of the park (Figure 4.4). There was no data available for 1975, and the following year the area affected by beetles significantly expanded on the western side of the park. The aerial survey continued to report large areas impacted from 1977 through 1980. The outbreak was first identified east of the Continental Divide in the north central and north east portion of the park in 1979. In the early 1980s, the area affected by beetles quickly decreased (Figure 4.5).

4.4.2 Determination of Tree Canopy Cover

A total of 261 plots were used to estimate tree canopy mortality from the air photo analysis (Table 4.4). Initially, 282 plots were analyzed, but several were removed from the dataset because the photo plots fell within topographic shadows, cloud cover or cloud shadows in the satellite imagery. The study area is dominated by west facing slopes, followed by south, east and north. Each aspect class did not contain the same number of plots (see Section 4.3.5). However, the number of plots in each aspect class is an adequate reflection of the percentage of the study area in each aspect class. Plots ranged from very little mortality (4.4%) to nearly complete mortality (99.8%). West-facing plots had the highest mean mortality (68.3%), while plots in the east aspect class had the lowest mean mortality (49.4%) (Table 4.4). The majority of the data is concentrated in mortality classes ranging from 40-90% (Figure 4.6). Given the severity and extent of the outbreak, this is not an unexpected finding.

4.4.3 Model Adjustment and Validation

The model that employed NDVI and the Green Band (NDVI+G) (Table 4.5) provided the best estimation of canopy change over time. This model had the lowest AIC (-237.55), MAE (10.8%), and RMSE (13.6%) values while accounting for the greatest amount of explained variability (65.4%) (Table 4.5). Furthermore this model had the lowest prediction error (15.4%) of any model from the cross validation procedure. The incorporation of a green band resulted in a stronger model than using NDVI alone (Table 4.5). The NDVI and PCA models had identical coefficients of determination, and similar MAE and RMSE. However, the PCA model had substantially higher prediction error. The GNDVI model did not perform as well as the three NDVI based models and the red-green index proved to be a poor indicator of mortality.

The NDVI+G model was selected to describe the large-scale variability of canopy change over time. However, the residuals of the GLM model exhibited spatial autocorrelation (Moran's *I* test; $p < 0.0001$) indicating that the null hypothesis of spatial independence in the residuals be rejected. The variables included in the NDVI+G model were then analyzed using a GLS model that explained 62% of the variability with higher MAE (18%) and RMSE (21.1%) than the GLM model (Table 4.6, Figure 4.7). However, the residuals of the GLS model did not exhibit spatial autocorrelation (Moran's *I* test; $p = 0.64$). The green band from 1978 was the most important predictor west of the Continental Divide, with a relative contribution to the model of 10.7%. The green band from 1987 was the most important predictor east of the divide, with a relative contribution to the model of 11.8%. Decreased values of green band reflectance indicated a substantial increase in canopy mortality. NDVI from 1977 and 1981 were highly significant in the model on the west side of the park ($p<0.001$) and also exhibited a negative relationship with canopy mortality. NDVI from 1977 was also significant on the east side of the park.

The residuals were used to model the small-scale variation in the data using binary regression trees. The initial regression tree identified 27 nodes and location (east or west of divide) did not enter the analysis, so one tree was used to fit both sides of the Continental Divide. Given that regression trees are prone to overfitting, we conducted a 10-fold cross validation on the data and subsequently pruned the tree to 22 nodes. This simplified the model while still accounting for spatial autocorrelation. The combined model (GLS + CART), which captures both the large- and small-scale variability, had a lower rate of MAE (7.6%) and RMSE (9.8%) than the GLS model. The combined model increased the amount of explained variability in the data by nearly 20% ($R^2 = 0.819$) (Figure 4.8). The residuals of the combined model are spatially independent (Lagrange multiplier test; p=0.27) and the standardized mean square error (SMSE) of the combined model is 0.996. An SMSE value of one indicates consistency between the estimation error variance and the observed error variance in the model (Hevesi et al., 1992).

The combined model was then applied spatially to the study area as a continuous surface with modeled canopy cover change scaled between 0 and 1. We binned the modeled data into three categories based on natural breaks in the data (Figure 4.9). This classification resulted in 20% of the project area in the low category (< 0.37 canopy change), 46% in the moderate and 34% in the severe category (>0.62 canopy change). Pockets of high severity are found throughout the park across the elevation gradient present. The three classes are generally represented across the study area. However, it should be noted that pockets of low and severe impacts are clustered, with the moderate severity often forming a transition between the classes.

To provide perspective on the classification, a color-infrared photo and corresponding classification map is shown in Figure 4.10. Based on these visual comparisons, our model appears to capture high levels of mortality associated with beetle attack areas as well as areas not

as heavily impacted. Furthermore, the gradient of impact on the landscape appears to be well represented in the model. Example spectral trajectories of the three classes show clear delineation during extent of the outbreak (Figure 4.11).

4.5 DISCUSSION

A primary objective of our analysis was to develop a methodology to reconstruct the extent and severity of the outbreak. We were able to identify a gradient of mortality on the landscape using changes in NDVI and the green band reflectance over time. Our findings confirm the outbreak was not homogenous across the landscape (Figure 4.9). The reported error metrics are reasonable given limitations in the data and comparable to related studies of insect impacts on the forest canopy (Townsend et al., 2012). Error associated with the ADS data was not quantified. Furthermore, this information was collected by observers presumably working under difficult conditions. Therefore we suggest our model represents an unbiased view of the disturbance. In addition, the modeling framework we applied in this study should be transferable to other areas with similar forest disturbance characteristics.

This study builds on the ideology of many of the aforementioned studies which used remotely sensed data to document various stages of the late 1990s-mid 2000s mountain pine beetle outbreak. The common theme is the development of a time series imagery stack to assess spectral changes over time (Goodwin et al., 2008; Meddens et al., 2013; Meigs et al., 2011). Our normalization process gave us high confidence in the time series stack, given the consistent reflectance values of the pseudo-invariant features over time (Figure 4.11). However, we were unable to utilize many of the vegetation indices (e.g. Normalized Difference Moisture Index) used in these studies. Given that our study objectives hinged around a historic disturbance that occurred in the mid-1970s and early 1980s, we were unable to use imagery with the spectral

resolution needed for many of those indices. The major difference in our study and those described in section 4.2.3, is that the disturbance we are interested in occurred in the 1970s and early 1980s. This predates the advent of Landsat TM/ETM+ imagery and other finer scale imagery employed in those studies.

There were two main differences between our study and those that used MSS data (Harris et al., 1978; Rencz and Nemeth, 1985; Weber et al., 1975). First, we attempted to capture the gradient of the disturbance on a continuous scale between 0 and 1. Second, we employed multiple time periods of imagery to assess spectral changes at sites over time. Although Rencz and Nemeth (1985) used a change detection procedure, there was a gap of six years between images. The use of just two images was likely insufficient to capture the full range of phenology associated with the disturbance from pre-attack through the green, red and gray stages, followed by the likely expansion of understory growth following canopy mortality. Conducting a retrospective analysis afforded us several advantages over the prior MSS studies. The Landsat archive is now readily available at no cost, removing the financial burden that inhibited prior investigators from developing a time series imagery stack (Woodcock et al., 2008). Furthermore, advances in radiometric calibration provide a basis for standardized comparison between images acquired on different dates and by different sensors (Chander et al., 2009).

There are several strengths associated with our study that allowed us to overcome numerous limitations. Overall, we provide an objective framework that can be applied to other areas, at other time periods, involving other types of forest disturbance. The major limitation of quantifying a disturbance over a large, topographically complex landscape where subsequent fire has erased some of the evidence was overcome using existing data. The remote sensing archive allowed us to extract information about the condition of the forest canopy across spatiotemporal

scales. By employing multiple lines of evidence, each independent data source contributed to a composite picture of the disturbance (Swetnam et al., 1999). Several key factors led to a successful analysis. The first was employing a mask to restrict the area of analysis (Garrity et al., 2013) to forest types where mountain pine beetle had the potential to impact. The second critical element was the development of a normalized time series of reflectance (Townsend et al., 2012; Vogelmann et al., 2012) to characterize changes over time. We obtained many more images (24) than we ultimately used (9), but this was necessary to conduct an exhaustive evaluation of available imagery. The consistent level of pre-processing performed on the imagery by the USGS and our procedure to convert data to at-surface reflectance aided in the success. Furthermore, the image acquisition dates were within a six-week window, which limited intra-year differences. The final critical element was the development of a novel approach to measure mortality in available aerial photos and scale up to multiple years of satellite imagery. This procedure was crucial given the absence of field data.

The absence of validation data in this study precluded the use of the holdout method where the data is separated into a training set and test set. We evaluated the suite of GLM models using several common measures, including a ten-fold cross validation procedure. Cross validation divides the data into *k* subsets of approximately equal size and the holdout method is repeated *k* times (Salzberg, 1997). There are strengths and weaknesses to this method that is commonly used in ecological studies. Cross validation is advantageous because it is less critical how the data are divided, every point is used in the test set once, and each point is used in the training set *k*-1 times. Disadvantages of the method include computation time and trade-offs between variance and bias, dependent on the number of iterations (Kohavi, 1995). Furthermore,

there is only one dataset involved in the cross validation, regardless of the number of subsets created (Esbensen and Geladi, 2010).

4.5.1 Ecological Considerations

In areas where mountain pine beetle disturbance induces high mortality in the forest canopy over a short time period, there will be a relatively quick change in NDVI. Therefore these areas will have a heightened chance of detection by remote sensing methods. In addition, the release of light, nutrients and moisture will occur at one time period. Therefore the flush of understory growth will likely occur over a relatively short time period. This increases the likelihood of obtaining a tight sequence of images to detect these rapid changes. Given the high severity of the impact, the model identified large negative relative contributions of the green band in the 1970s on the west side of the divide, indicative of an increase in canopy mortality. However, the 1987 green band was significant, with a large positive relative contribution to the model. This can be interpreted ecologically in that there was a sharp increase in canopy mortality during the late 1970s, but understory growth was prevalent in these high severity areas by the late 1980s. The outbreak moved from the west to east over the divide. The 1987 green band had a large negative contribution to the east side model, suggesting recent canopy mortality dominated the spectral signature, while understory regrowth was likely not widespread.

However, the impacts of mountain pine beetle disturbance on the forest canopy do not always exhibit characteristics that are easily identified by remote sensing methods. Areas that have lower amounts of mortality will be composed of a mix of live and dead trees resulting in a gradient of mortality over the duration of the disturbance. As trees die over this time period, they will likely be interspersed with live trees. Given that the spectral response of a pixel is an amalgamation of all elements present (Lefsky and Cohen, 2003), there will be a smaller change

in reflectance. Additionally, as individual trees die, the release of resources will impact a smaller area of understory regrowth. The localized understory regrowth could offset or suppress the change in reflectance associated with canopy mortality. This problem is manifested on the landscape as the cycle of canopy mortality, resource release, and understory flush could be occurring simultaneously in localized areas.

Several ecological phenomena could pose challenges to this methodology, particularly if the recent disturbance history of the study area is unknown. Other disturbances could be identified by this method, without being attributed to mountain pine beetle. We were able to incorporate ancillary data about the mountain pine beetle outbreak such as ADS data, park reports and knowledge from park staff to supplement the primary imagery method. Harvest events typically have sharp geometric boundaries (Goodwin et al., 2008) that often persist in reflectance patterns for quite some time after the event. Unknown fires that are low severity or small in area could be difficult to segregate from insect disturbance mortality, particularly if the event corresponds with a gap in satellite imagery. Other insect disturbances such as mortality or defoliation events in the study area could be detected as well (Meigs et al., 2011; Townsend et al., 2012). We analyzed the *Damage Causal Agent* attribute code of the aerial survey data and found nearly no other disturbance types recorded within the study area during the time periods 1971-87. Given that our objective was to detect landscape-scale mortality associated with a widespread, high-severity disturbance, we were not concerned with these small disturbances.

Periods of drought and fluctuations in hydrologic year (Oct.-Sept.) precipitation could impact inter-annual indices of vegetation reflectance in areas of low mortality. However, our normalization procedure should account for some of these differences between imagery years. The establishment of appropriate reference conditions of an area remains a challenge in

ecological studies (Millar et al., 2007). Finally, all of the aforementioned challenges are made more complex when attempting to conduct a retrospective analysis of historical forest disturbance.

4.5.2 Technical Considerations

The technological challenges associated with this study are centered on the spatial, temporal and spectral resolution of the aerial photographs and satellite imagery. Although we were constrained to the use of best available data for the time period, consideration of some of the shortcomings is necessary. We used aerial photographs collected in 1982 (four) and 1984 (two). The scale of each photograph (1:58,000) is relatively coarse and does not allow for the identification of an individual tree crown. However, we believe the size of the photo plots (180 m x 180 m) was adequate to characterize the level of mortality within a stand. Given that our objective was to measure canopy mortality, we were confined to using color-infrared photographs. We would have considered natural color photographs if they had been available in the archive. There were additional photographs available in the archive that were not selected due to a combination of acquisition date, coarse resolution and gray scale film. Although nominal, there are acquisition costs associated with historic aerial photos, and the orthorecticfication process can be time consuming.

Additional landscape photographs would have been extremely helpful. However, we were limited by those that were taken by park staff at the end of the outbreak and housed in the National Park Service archive. Although they were not used in a quantitative analysis, they provided valuable evidence of the impact of disturbance.

The Landsat MSS imagery employed in this study is also subject to spatial, temporal and spectral constraints. Although we resampled the MSS imagery to 30 m to aid in the

georectification process, the native resolution is significantly lower. Pixel values are a mixture of ground elements (Lefsky and Cohen, 2003), and given the coarse spatial resolution, MSS imagery is limiting to the amount of mortality that can be detected at one pixel between multiple time periods. Therefore, areas that experienced low mortality may have been underestimated by our model. The temporal limitations of the image archive are two-fold. The study may have benefited from a higher frequency of images collected every calendar year and additional image years to establish pre-outbreak conditions. However, it was not tenable to alleviate these constraints given the available imagery and the timing of the disturbance. The spectral resolution of MSS imagery is limited compared to TM/ETM+ imagery. Many of the indices that have been successfully applied to recent outbreaks are developed from a wider spectral range than that of MSS. All of these factors may limit the sensitivity of the study to detect different levels of mortality, especially low levels of mortality. However, given the scale and severity of the disturbance, coupled with the dense imagery stack that was assembled, we were still able to achieve acceptable results.

The Tasseled Cap transformation for Landsat data has been used to distill information from Landsat imagery in forest disturbance mapping (Healey et al., 2005). However, we did not use the Tasseled Cap transformation in our analysis. Unlike Landsat TM and ETM+, Tasseled Cap coefficients have not been developed for MSS imagery that has been converted to reflectance data (Schowengerdt, 2007). Our normalization process depended on normalized reflectance values and not Digital Numbers. The established Tasseled Cap transformation can only be applied to Landsat MSS imagery in Digital Numbers.

We chose to classify the continuous output into three categories based on natural breaks in the data. Although relative differences are taken into account, the threshold between each class

is somewhat subjective. Prior investigators have used lower thresholds (low <= 10%, moderate (11-29%), and severe > 30% of stands killed) (Aukema et al., 2006) or additional classes of mortality severity (e.g. trace, light, moderate, severe, and very severe) (Meddens et al., 2012). However, these two studies were considering ADS data which contained a measure of the number of trees or the percentage of stand killed. This type of classification scheme does not translate directly to our model. For example, if 15% of the trees were killed in a localized area, it could have a large impact on the reflectance of those pixels and overestimate the severity. This issue could be exacerbated by the coarse resolution of Landsat MSS pixels. Given that there is no precedent for this type of analysis we opted for a natural break classification scheme.

Our modeling framework was exhaustive in using multiple lines of evidence that represented the best available data. Our model incorporated the full extent of available spectral reflectance in MSS imagery (green, red and near infrared bands). Only band 3 was discarded given that it was highly correlated with band 4. Furthermore, the spectral information used by the model can be readily interpreted. NDVI is a commonly used index to assess ecological change (Pettorelli et al., 2005) and its behavior can be reasonably predicted from plant physiology theory (Garrity et al., 2013). Plant material containing chlorophyll reflects in the green wavelength. The reflectance in the green band would be expected to decrease as the amount of chlorophyll in a pixel is reduced from plant mortality. Therefore, the inclusion of the green band provides a measure of the amount of chlorophyll present within a pixel over time.

4.6 CONCLUSION

We have presented a framework that incorporates multiple lines of evidence to retrospectively characterize a landscape scale mountain pine beetle disturbance. Furthermore, we have demonstrated that Landsat MSS data is a valuable tool to extend the moderate resolution

imagery record back to the early 1970s. We conclude that our approach is suitable to characterize the extent and severity of the event despite initial data limitations. Key considerations of the application of our model include the size and severity of the disturbance, as well as the timing (first date, last date, and duration) of the satellite imagery. Our approach captures the characteristics of a disturbance event that significantly impacts numerous ecological processes. Given the availability of these data sources, the characterization of recent events will afford investigators additional tools to study disturbance interactions and ecological legacies at the landscape scale.

Any use of trade, firm, or product names is for descriptive purposes only and does not imply endorsement by the U.S. Government.

4.8 TABLES

Table 4.1. Spectral characteristics of Landsat MSS imagery (NASA, 2013).

Band	Wavelength	Spectral Region
1	500-600 nm	Green
2	600-700 nm	Red
3	700-800 nm	Near-infrared
4	800-1100 nm	Near-infrared

Table 4.2. Satellite imagery scene information and acquisition date used in the analysis.

Satellite	Scene Path/Row	Acquisition Date (year-month-day)
Landsat 1	44/26	19730910
Landsat 1	44/26	19740923
Landsat 2	44/26	19760921
Landsat 2	44/26	19770811
Landsat 3	44/26	19780902
Landsat 3	44/26	19790915
Landsat 2	44/26	19810913
Landsat 4	41/26	19830924
Landsat 5	41/26	19870911

Table 4.3. Spectral indices calculated with the Landsat MSS reflectance data. NDVI (Normalized Difference Vegetation Index), RGI (Red Green Index), and GNDVI (Green Normalized Difference Vegetation Index).

Spectral Index	Equation	Source
NDVI	$NDVI = MSS_{Band4} - MSS_{Band2}/MSS_{Band4} + MSS_{Band2}$	Rousse et al., 1974
RGI	$RGI = MSS_{Band2}/MSS_{Band1}$	Coops et al., 2006
GNDVI	$GNDVI = MSS_{Band4} - MSS_{Band1}/MSS_{Band4} + MSS_{Band1}$	Gitelson et al., 1996

Table 4.4. Descriptive statistics of estimated tree canopy mortality from the aerial photo plots grouped by aspect class (n=261).

Aspect	Number of Plots	Tree Canopy Mortality Statistics			
		Mean	Minimum	Maximum	S.D.
North	46	54.9	4.4	91.8	23.6
East	47	49.4	12.8	93.9	24.0
South	75	54.1	17.0	99.2	20.8
West	93	68.3	12.7	99.8	21.3

Table 4.5. Comparison of model evaluation metrics.

Model	**AIC**	**R^2**	**MAE**	**RMSE**	**10-fold Cross Validation Prediction Error**
NDVI + G	-237.55	0.65	10.8%	13.6%	15.4%
NDVI	-204.44	0.60	11.6%	14.5%	16.8%
PCA	-193.43	0.60	11.9%	14.6%	20.4%
GNDVI	-183.13	0.55	12.4%	15.6%	17.3%
RGI	-87.32	0.34	15.3%	18.8%	20.7%

Table 4.6. Predictor variables used in the NDVI+G GLS model. Estimates of the model parameters are listed for the west and east sides accordingly. The variables *Aspect* and *Total # of Years* (low was the only category retained in the stepwise model) were treated as indicator variables in the analysis. **P-value* is significant at 0.05 or lower.

Variable	**West Coefficient**	**East Coefficient**
(Intercept)	3.18413*	3.43654*
Aspect		
N	0.13478	-1.42706*
S	-0.24309	-
W	-0.58963*	-0.17668*
green.1973	-9.58080*	-
green.1974	-8.60109*	-
green.1977	-9.97942*	-
green.1978	-10.69192*	-12.20042
green.1979	-5.24848	-
green.1983	6.49274	-
green.1987	8.11468*	-11.77014*
Total # of Years - Low	0.15773*	-
ndvi.1973	-	-0.37092
ndvi.1974	-0.03773	-
ndvi.1976	0.41517*	-
ndvi.1977	-1.08326*	-1.74362*
ndvi.1978	-0.36746	-
ndvi.1979	0.40112	-
ndvi.1981	-1.42992*	-
ndvi.1983	-0.40449*	-0.50511
ndvi.1973 x N	-	2.01483
ndvi.1974 x N	-1.24923*	-
ndvi.1978 x N	1.69811*	-
ndvi.1978 x W	1.10049*	-
ndvi.1979 x N	-1.78641*	-
ndvi.1979 x S	-1.18434*	-
ndvi.1979 x W	-1.49155*	-
ndvi.1981 x S	1.52377*	-
ndvi.1981 x W	1.20919*	-
ndvi.1983 x N	0.9887*	-

4.9 FIGURES

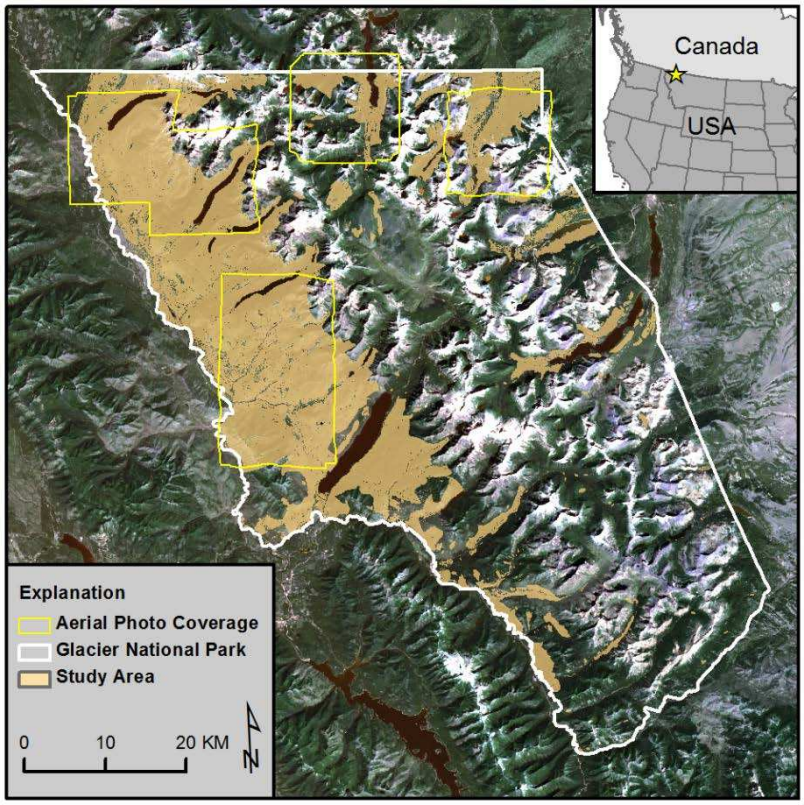

Figure 4.1. Location of study area and extent of aerial photo coverage. Background image is Landsat Thematic Mapper (TM) Imagery (bands 3, 2, 1) acquired on August 25, 2010. Yellow polygons represent the location and extent of aerial photograph coverage; tan area represents the confined study area.

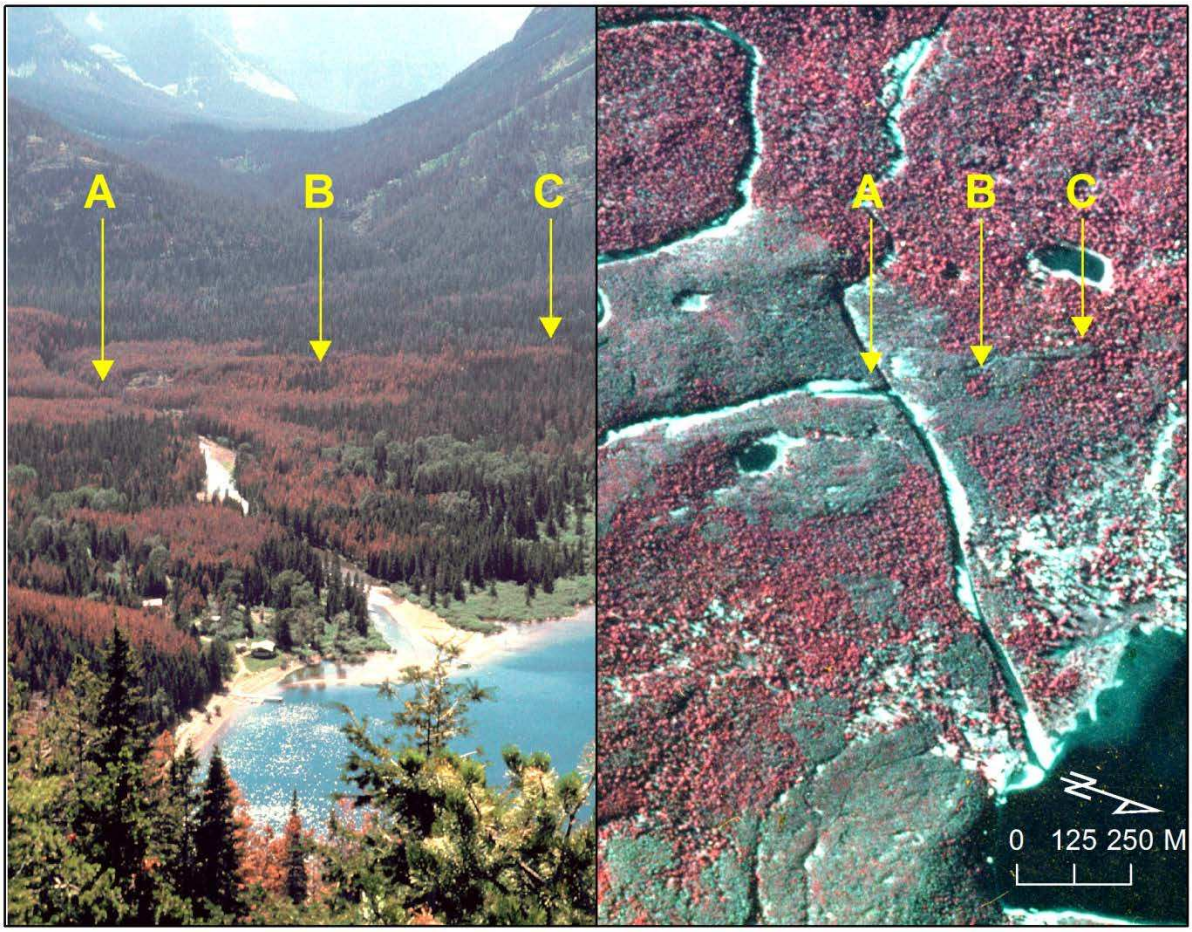

Figure 4.2. Linking landscape and aerial photos. (Left) Landscape photo taken in the Summer of 1980 showing a mixture of live and dead trees in the red attack stage in Waterton Valley (source: Glacier National Park Research Library). (Right) A color-infrared aerial photo of the same area acquired in October 1980 (source: NASA/Glacier National Park). The mosaic of live and dead forest can be identified in both images. The letters correspond to the same area in each photo (A = stream confluence, B = small patch of live trees, surrounded by dead forest, C = linear ribbon of dead forest).

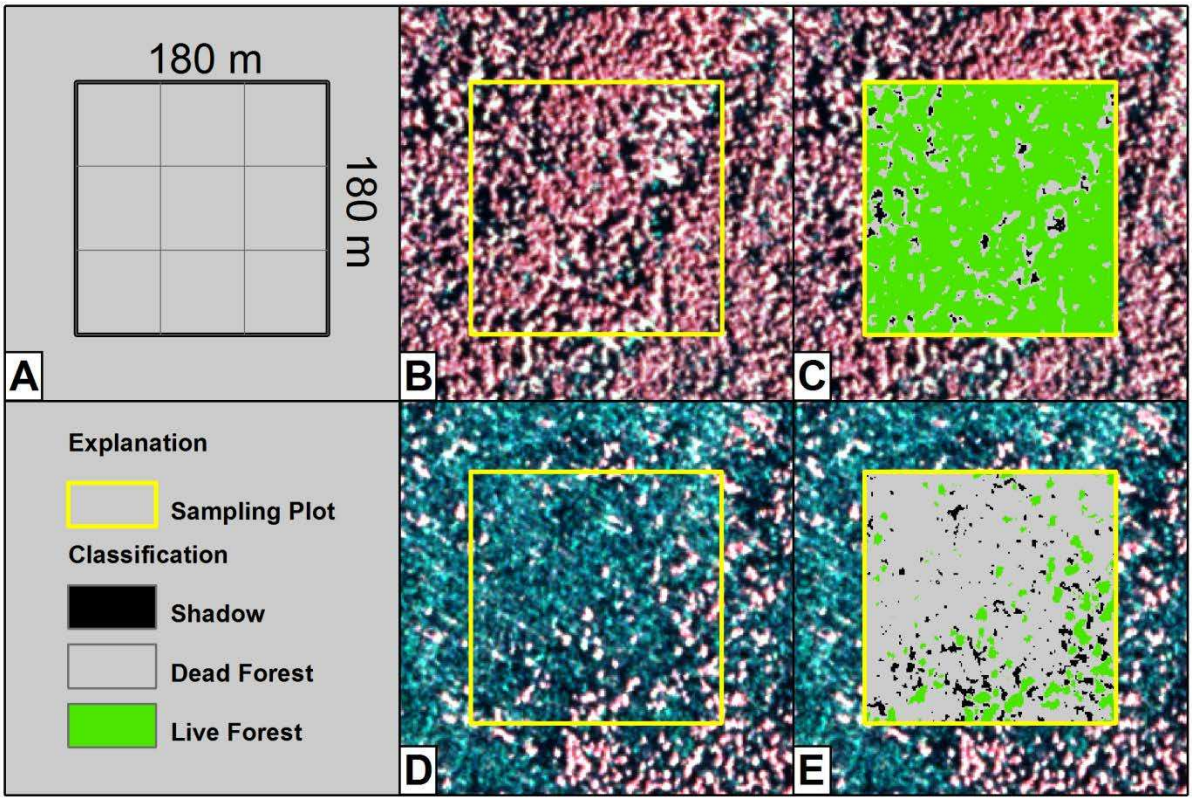

Figure 4.3. Example aerial photo sample plot.(A) Plot used to sample aerial photos. The 180 m x 180 m plot size was chosen to include a 3 x 3 block of Landsat MSS pixels. (B) Sampling plot overlaid on color infrared photo at a low mortality site. (D) Sampling plot overlaid on color infrared photo at a high mortality site. (C) Output classification from sampling plot in panel B (live canopy cover = 83%). (E) Output classification from sampling plot in panel D (live canopy cover = 10%).

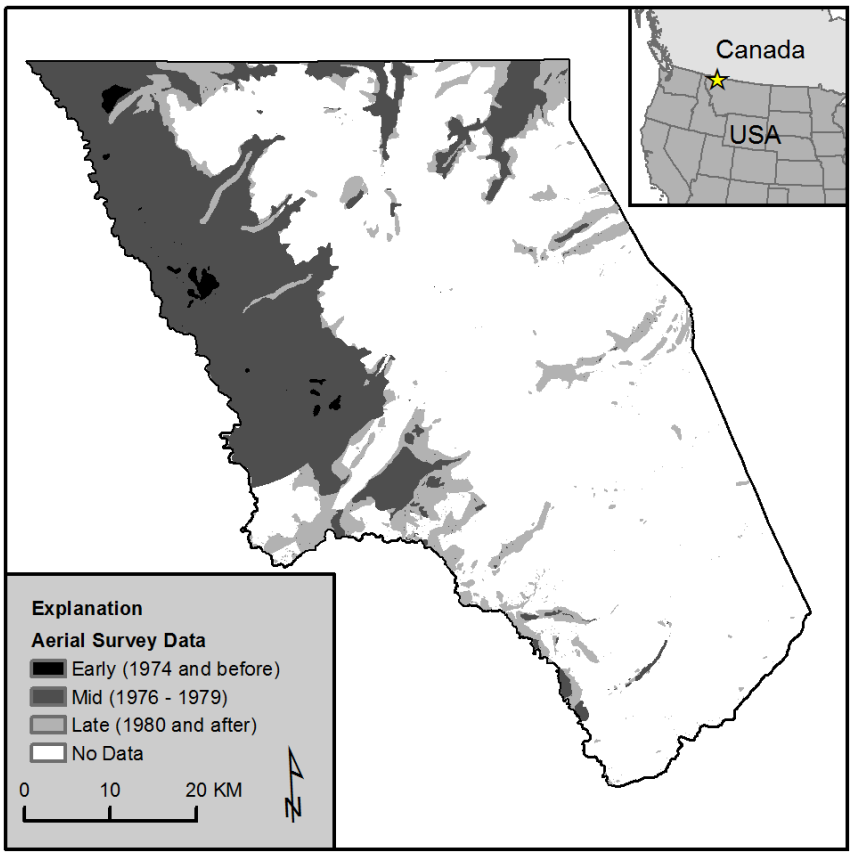

Figure 4.4. Mapped area impacted by mountain pine beetle according to the aerial detection survey data. Note: there was no data available for 1975.

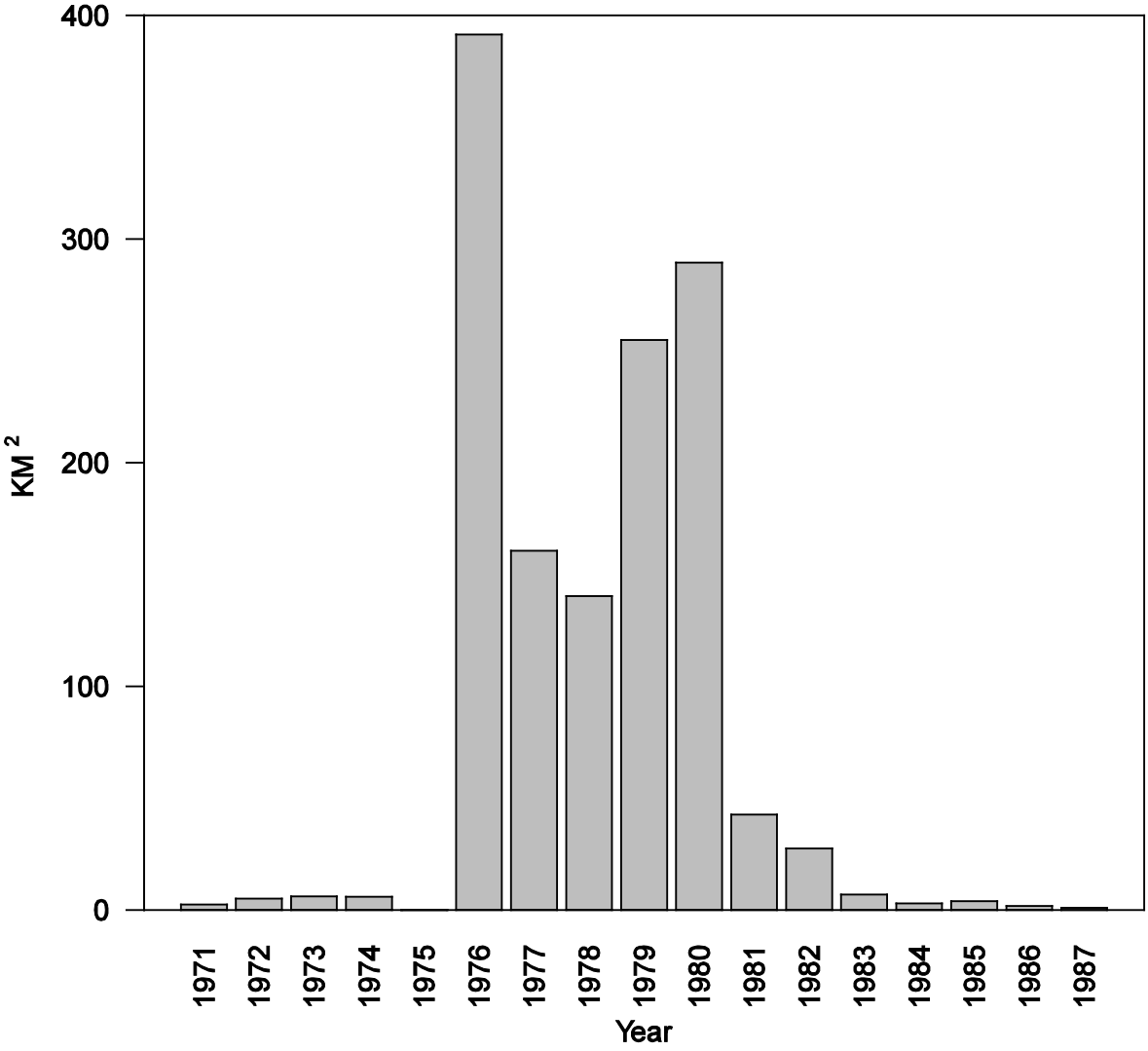

Figure 4.5. Area impacted by mountain pine beetle annually based on aerial detection survey data. Note: there was no data available for 1975.

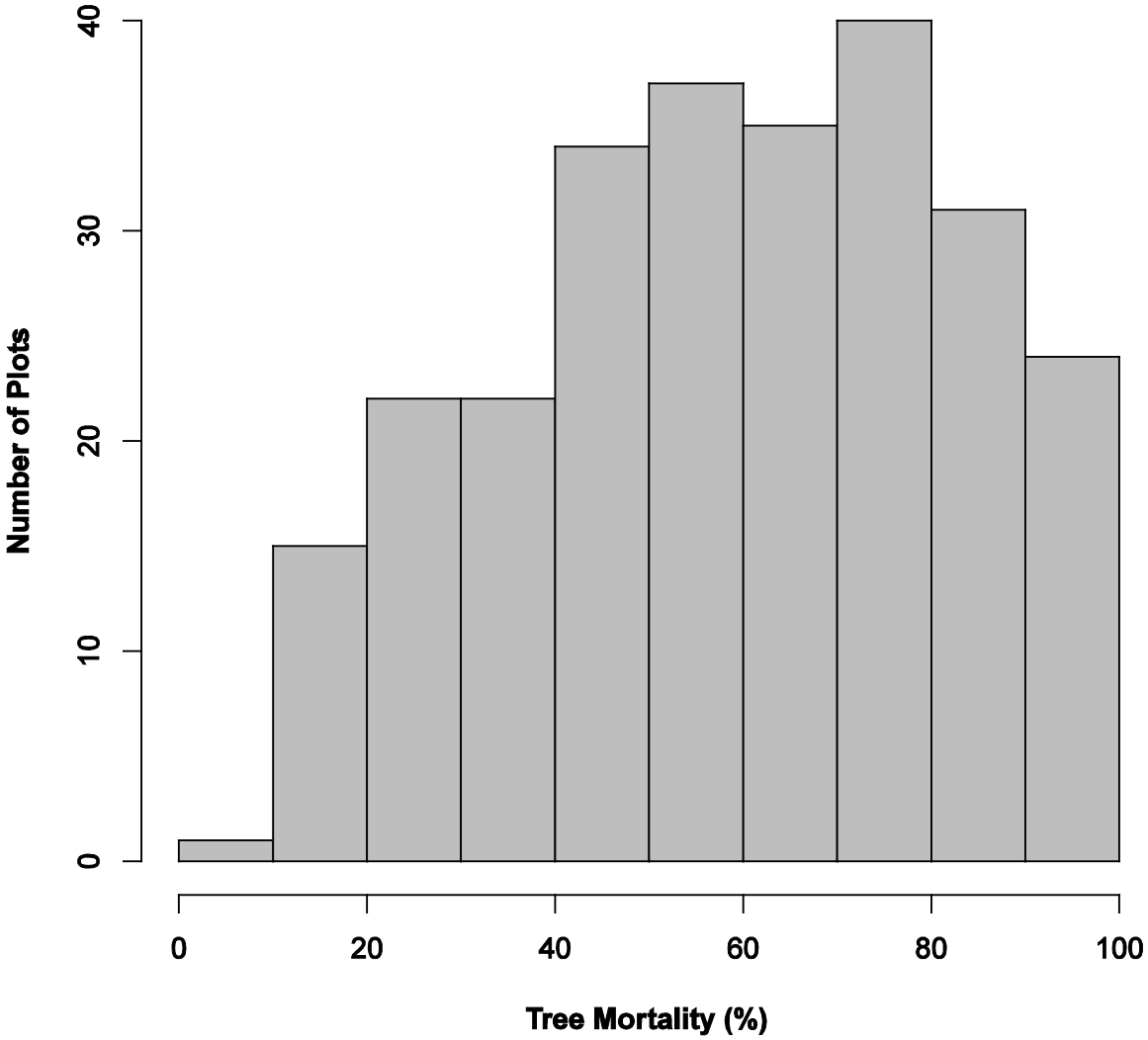

Figure 4.6. Histogram of canopy tree mortality (%) for all plots (*n*=261).

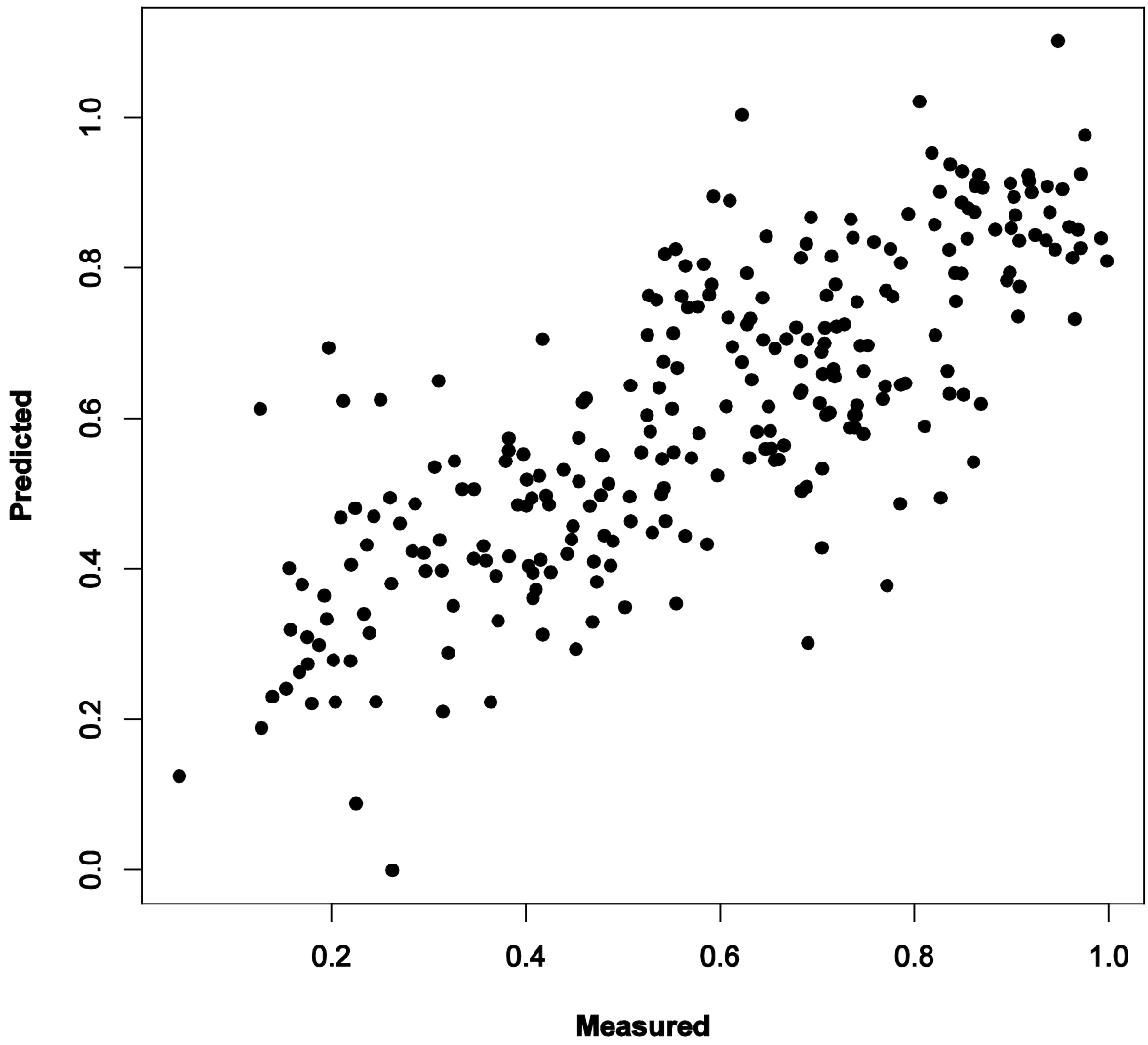

Figure 4.7. The output of the NDVI+G GLS model used to estimate canopy change over time due to mortality.

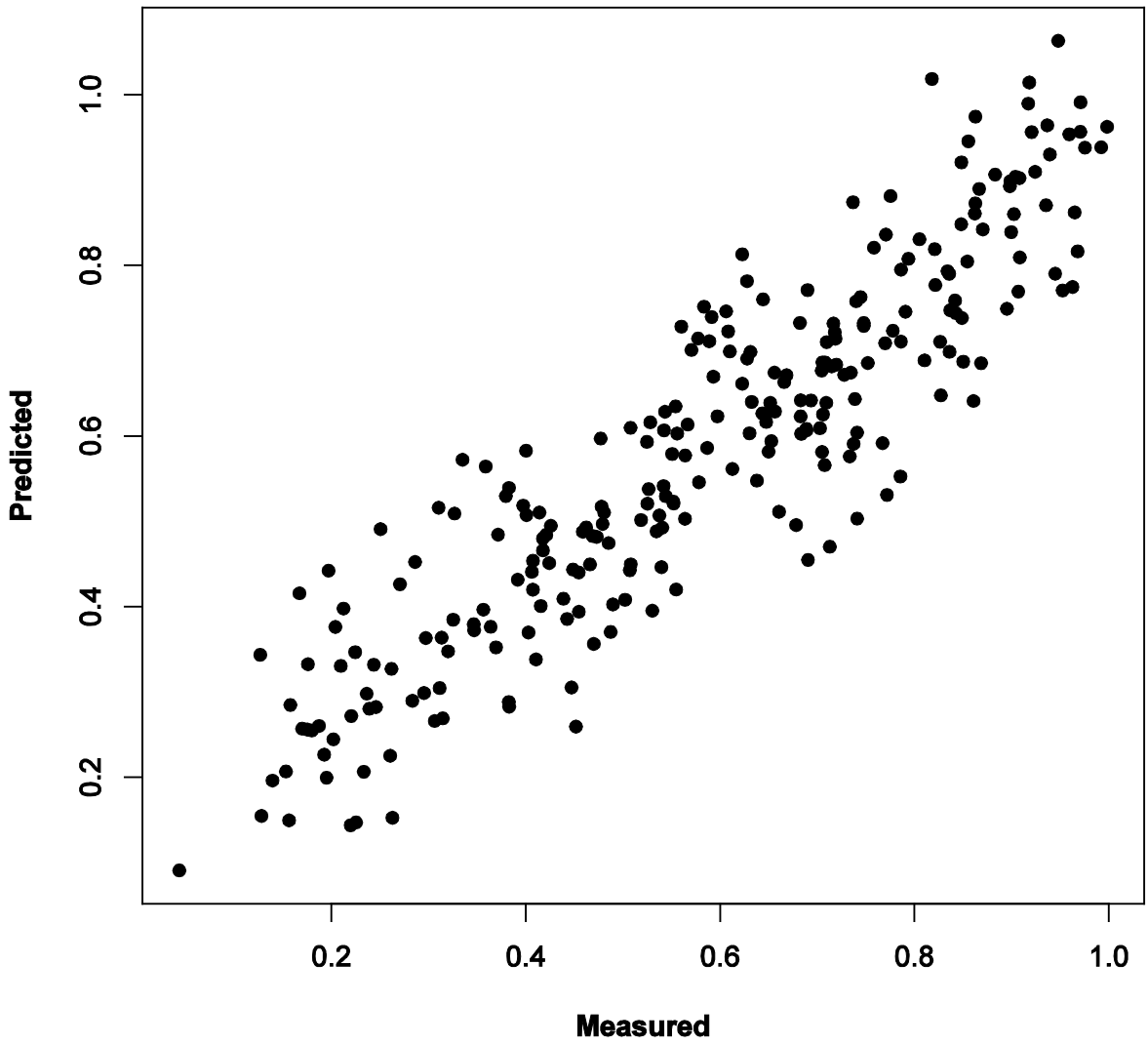

Figure 4.8. The output of the combined GLS-CART model used to estimate canopy change over time due to mortality.

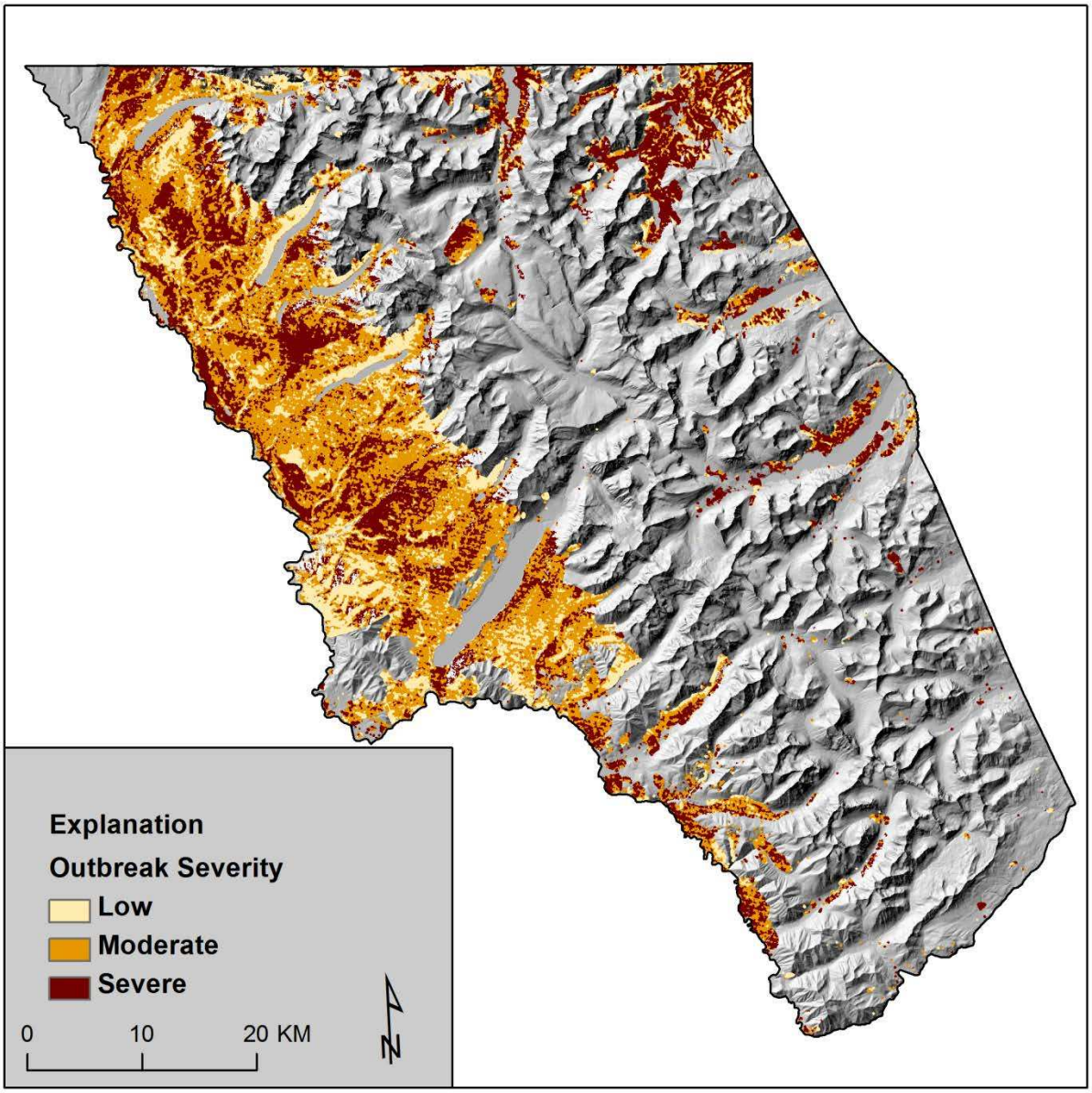

Figure 4.9. The output of the spatial model classified into three severity levels.

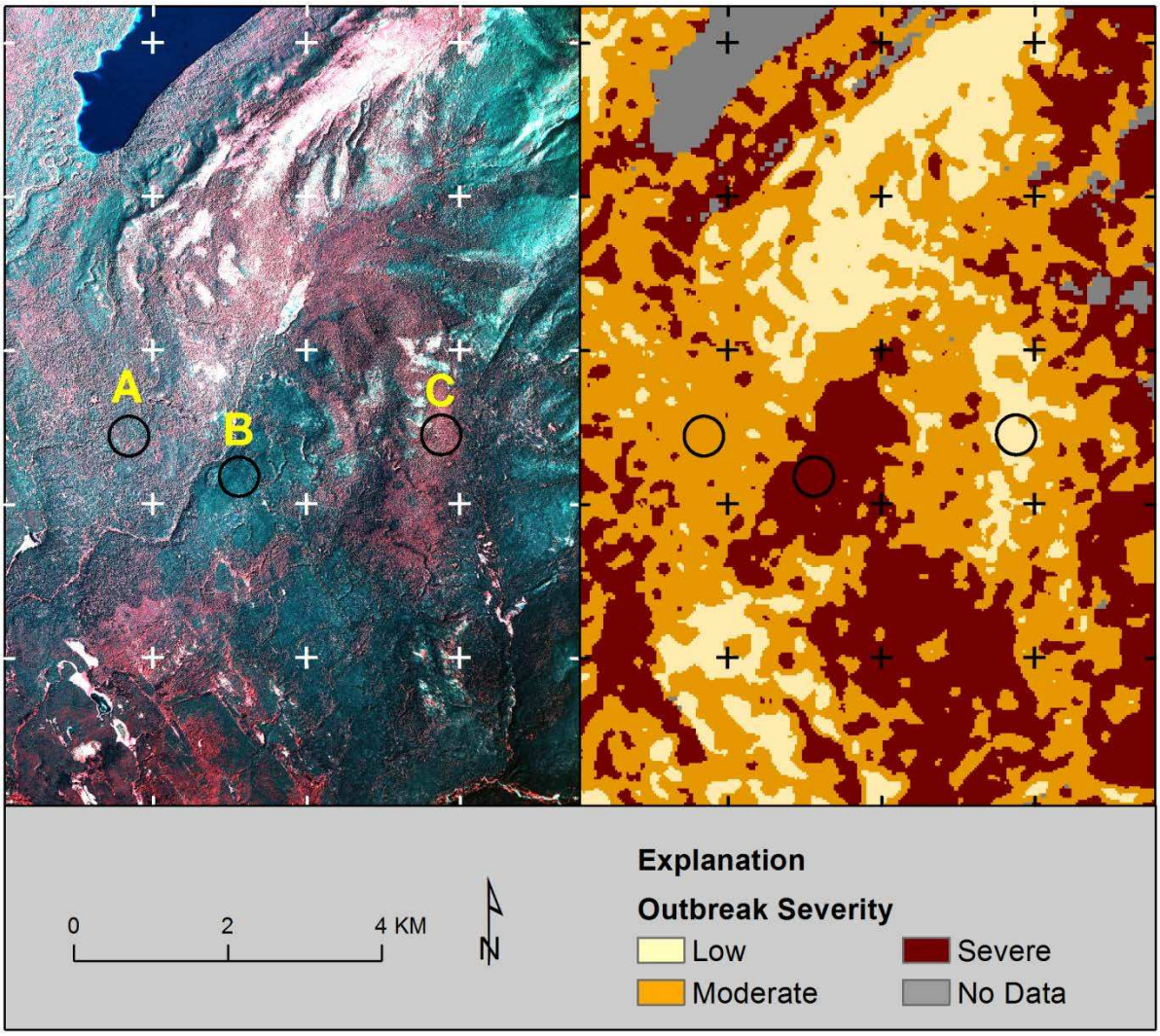

Figure 4.10. Comparison between aerial photo and model output.(Left) Color-infrared photo (year acquired = 1982). (Right) Classified map result of the same area (focal window applied). Black polygons correspond to spectral trajectories in Figure 4.11 (A=Moderate, B=Severe, C=Low). Note: tick marks are spaced on a 2 km grid; black polygons are 0.2 km^2 (20 hectares) in size.

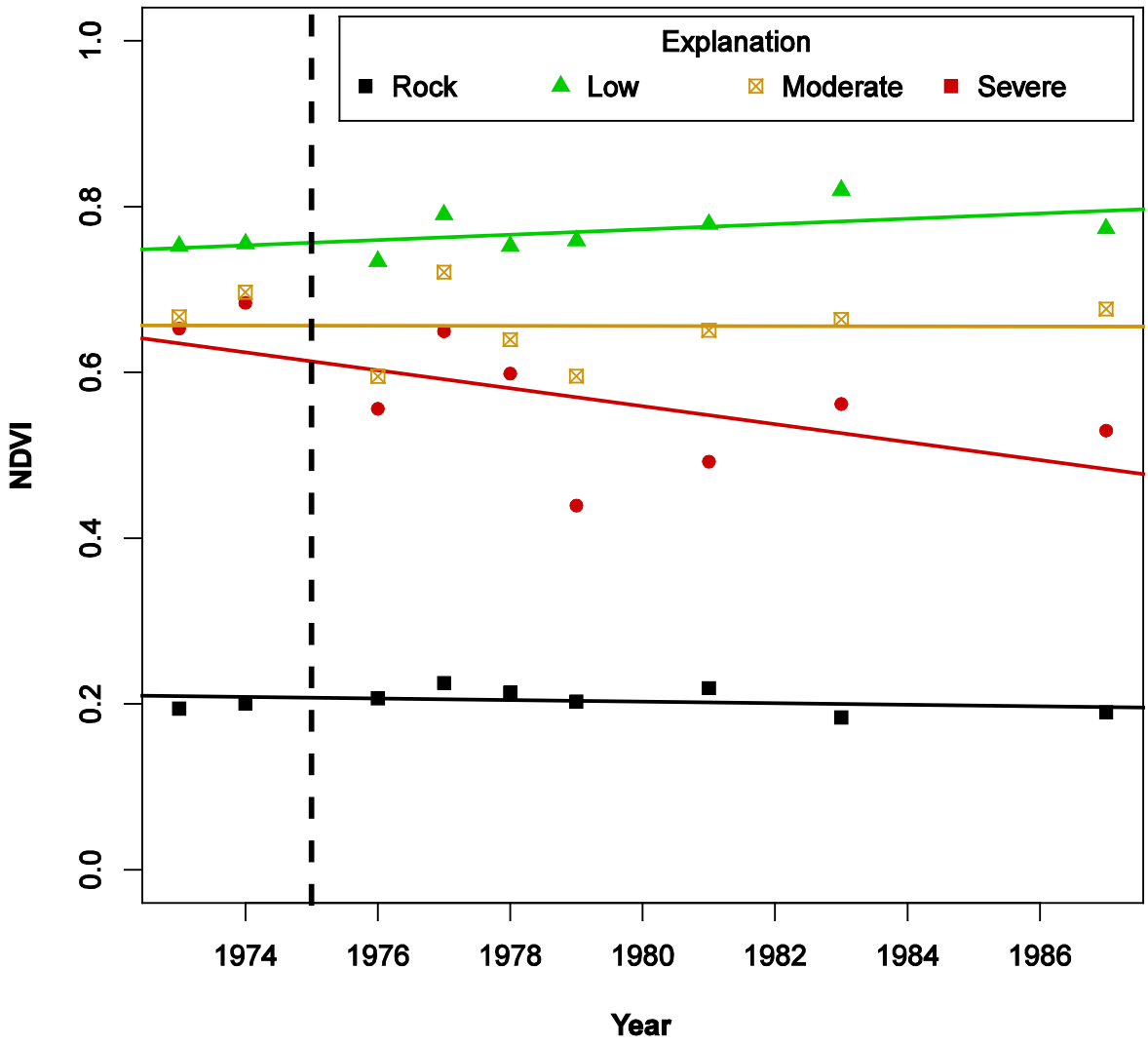

Figure 4.11. Spectral trajectories of classified outbreak severity. The three trajectories correspond to the polygons identified in Figure 4.10. Note: rock features are included to demonstrate the success of the image normalization process and the stability of pseudo-invariant features over time.

LITERATURE CITED

Ahern, F.J., 1988. The effects of bark beetle stress on the foliar spectral reflectance of lodgepole pine. Int. J. Remote Sens. 9, 1451–1468.

Allen, C.D., Breshears, D.D., 1998. Drought-induced shift of a forest-woodland ecotone: rapid landscape response to climate variation. Proc. Natl. Acad. Sci. 95, 14839–42.

Aukema, B.H., Carroll, A.L., Zhu, J., Raffa, K.F., Sickley, T.A., Taylor, S.W., 2006. Landscape level analysis of mountain pine beetle in British Columbia, Canada: spatiotemporal development and spatial synchrony within the present outbreak. Ecography (Cop.). 29, 427–441.

Baker, W.L., Flaherty, P.H., Lindemann, J.D., Veblen, T.T., Eisenhart, K., 2002. Effect of vegetation on the impact of a severe blowdown in the southern Rocky Mountains, USA. For. Ecol. Manage. 168, 63–75. doi:10.1016/S0378-1127(01)00730-7

Bebi, P., Kulakowski, D., Veblen, T.T., 2003. Interactions between Fire and Spruce Beetles in a Subalpine Rocky Mountain Forest Landscape. Ecology 84, 362–371.

Bentz, B.J., Régnière, J., Fettig, C.J., Hansen, E.M., Hayes, J.L., Hicke, J.A., Kelsey, R.G., Negrón, J.F., Seybold, S.J., 2010. Climate Change and Bark Beetles of the Western United States and Canada: Direct and Indirect Effects. Bioscience 60, 602–613. doi:10.1525/bio.2010.60.8.6

Brown, K., Hansen, A.J., Keane, R.E., Graumlich, L.J., 2006. Complex interactions shaping aspen dynamics in the Greater Yellowstone Ecosystem. Landsc. Ecol. 21, 933–951. doi:10.1007/s10980-005-6190-3

Carreiras, J.M.B., Pereira, J.M.C., Pereira, J.S., 2006. Estimation of tree canopy cover in evergreen oak woodlands using remote sensing. For. Ecol. Manage. 223, 45–53. doi:10.1016/j.foreco.2005.10.056

Chander, G., Markham, B.L., Helder, D.L., 2009. Remote Sensing of Environment Summary of current radiometric calibration coefficients for Landsat MSS , TM , ETM + , and EO-1 ALI sensors. Remote Sens. Environ. 113, 893–903. doi:10.1016/j.rse.2009.01.007

Cohen, W.B., Maiersperger, T.K., Spies, T.A., Oetter, D.R., 2001. Modelling forest cover attributes as continuous variables in a regional context with Thematic Mapper data. Int. J. Remote Sens. 22, 2279–2310. doi:10.1080/01431160121472

Coops, N.C., Johnson, M., Wulder, M.A., White, J.C., 2006. Assessment of QuickBird high spatial resolution imagery to detect red attack damage due to mountain pine beetle infestation. Remote Sens. Environ. 103, 67–80. doi:10.1016/j.rse.2006.03.012

Cressie, N.A., 1993. Statistics for Spatial Data, Revised. ed. Wiley-Interscience, New York, NY. doi:978-0471002550

Davidson, A., Aycrigg, J., Grossmann, E., Kagan, J., Lennartz, S., McDonough, S., Miewald, T., Ohmann, J., Radel, A., Sajwaj, T., Tobalske, C., 2009. Digital Land Cover Map for the Northwestern United States.

Dennison, P.E., Brunelle, A.R., Carter, V.A., 2010. Assessing canopy mortality during a mountain pine beetle outbreak using GeoEye-1 high spatial resolution satellite data. Remote Sens. Environ. 114, 2431–2435. doi:10.1016/j.rse.2010.05.018

DeRose, R.J., Long, J.N., Ramsey, R.D., 2011. Combining dendrochronological data and the disturbance index to assess Engelmann spruce mortality caused by a spruce beetle outbreak in southern Utah, USA. Remote Sens. Environ. 115, 2342–2349. doi:10.1016/j.rse.2011.04.034

Di Orio, A.P., Callas, R., Schaefer, R.J., 2005. Forty-eight year decline and fragmentation of aspen (Populus tremuloides) in the South Warner Mountains of California. For. Ecol. Manage. 206, 307–313. doi:10.1016/j.foreco.2004.11.011

Esbensen, K.H., Geladi, P., 2010. Principles of Proper Validation: use and abuse of re-sampling for validation. J. Chemom. 24, 168–187. doi:10.1002/cem.1310

Fettig, C.J., Klepzig, K.D., Billings, R.F., Munson, A.S., Nebeker, T.E., Negrón, J.F., Nowak, J.T., 2007. The effectiveness of vegetation management practices for prevention and control of bark beetle infestations in coniferous forests of the western and southern United States. For. Ecol. Manage. 238, 24–53. doi:10.1016/j.foreco.2006.10.011

Fuller, D.O., 2001. Forest fragmentation in Loudoun County , Virginia , USA evaluated with multitemporal Landsat imagery. Landsc. Ecol. 16, 627–642.

Garrity, S.R., Allen, C.D., Brumby, S.P., Gangodagamage, C., McDowell, N.G., Cai, D.M., 2013. Quantifying tree mortality in a mixed species woodland using multitemporal high spatial resolution satellite imagery. Remote Sens. Environ. 129, 54–65. doi:10.1016/j.rse.2012.10.029

Gitelson, A.A., Kaufman, Y.J., Merzlyak, M.N., 1996. Use of a Green Channel in Remote Sensing of Global Vegetation from EOS-MODIS. Remote Sens. Environ. 58, 289–298.

Goodwin, N.R., Coops, N.C., Wulder, M.A., Gillanders, S., Schroeder, T.A., Nelson, T., 2008. Estimation of insect infestation dynamics using a temporal sequence of Landsat data. Remote Sens. Environ. 112, 3680–3689. doi:10.1016/j.rse.2008.05.005

Goodwin, N.R., Magnussen, S., Coops, N.C., Wulder, M.A., 2010. Curve fitting of time-series Landsat imagery for characterizing a mountain pine beetle infestation. Int. J. Remote Sens. 31, 3263–3271. doi:10.1080/01431160903186277

Hamel, D., McGregor, M., Oakes, R., 1977. Status of Mountain Pine Beetle Infestation Glacier National Park, 1976 (No. Report No. 77-4), Forest Insect & Disease Management. Missoula, MT.

Harris, J., Dawson, A.F., Goodenough, D., 1978. Evaluation of LANDSAT Data for Forest Pest Detection and Damage Appraisal Surveys in British Columbia (No. Report BC-X-182), Report BC-X-182. Pacific Forest Research Centre, Victoria, BC.

Healey, S., Cohen, W., Zhiqiang, Y., Krankina, O., 2005. Comparison of Tasseled Cap-based Landsat data structures for use in forest disturbance detection. Remote Sens. Environ. 97, 301–310. doi:10.1016/j.rse.2005.05.009

Hevesi, J.A., Istok, J.D., Flint, A.L., 1992. Precipitation Estimation in Mountainous Terrain Using Multivariate Geostatistics. Part I: Structural Analysis. J. Appl. Meteorol. 31, 661–676.

Hicke, J., Logan, J., 2009. Mapping whitebark pine mortality caused by a mountain pine beetle outbreak with high spatial resolution satellite imagery. Int. J. Remote Sens. 30, 4427–4441. doi:10.1080/01431160802566439

Homer, C., Dewitz, J., Fry, J., Coan, M., Hossain, N., Larson, C., Herold, N., Mckerrow, A., Vandriel, J.N., Wickham, J., 2007. Completion of the 2001 National Land Cover Database for the Conterminous United States. Photogramm. Eng. Remote Sens. 337–341.

Homer, C., Huang, C., Yang, L., Wylie, B., Coan, M., 2004. Development of a 2001 National Land-Cover Database for the United States. Photogramm. Eng. Remote Sens. 70, 829–840.

Huang, C., Asner, G.P., Barger, N.N., Neff, J.C., Floyd, M.L., 2010. Regional aboveground live carbon losses due to drought-induced tree dieback in piñon–juniper ecosystems. Remote Sens. Environ. 114, 1471–1479. doi:10.1016/j.rse.2010.02.003

Johnson, E.A., Fryer, G.I., 1987. Historical vegetation change in the Kananaskis Valley, Canadian Rockies. Can. J. Bot. 65, 853–858. doi:10.1139/b87-116

Jones, H.G., Vaughan, R.H., 2010. Remote Sensing of Vegetation: Principles, Techniques, and Applications. Oxford University Press, Oxford, UK.

Kadmon, R., Harari-Kremer, R., 1999. Studying Long-Term Vegetation Dynamics Using Digital Processing of Historical Aerial Photographs. Remote Sens. Environ. 68, 164–176. doi:10.1016/S0034-4257(98)00109-6

Kennedy, R., Spies, T., 2004. Forest cover changes in the Oregon Coast Range from 1939 to 1993. For. Ecol. Manage. 200, 129–147. doi:10.1016/j.foreco.2003.12.022

Kohavi, R., 1995. A Study of Cross-Validation and Bootstrap for Accuracy Estimation and Model Selection. Int. Jt. Conf. Artif. Intell. 14, 1137–1145.

Lefsky, M., Cohen, W., 2003. Selection of remotely sensed data, in: Wulder, M.A., Franklin, S. (Eds.), Remote Sensing of Forest Environments: Concepts and Case Studies. Kluwer Academic Publishers, Boston, pp. 13–47.

Legendre, P., Fortin, M., 1989. Spatial Pattern and Ecological Analysis. Vegetatio 80, 107–138.

Logan, J.A., Powell, J.A., 2001. Ghost Forests, Global Warming, and the Mountain Pine Beetle (Coleoptera: Scolytidae). Am. Entomol. 47, 160–173.

Manier, D.J., Hobbs, N.T., Theobald, D.M., Reich, R.M., Kalkhan, M.A., Campbell, M.R., 2005. Canopy dynamics and human caused disturbance on a semi-arid landscape in the Rocky Mountains, USA. Landsc. Ecol. 20, 1–17. doi:10.1007/s10980-004-3987-4

Maselli, F., 2004. Monitoring forest conditions in a protected Mediterranean coastal area by the analysis of multiyear NDVI data. Remote Sens. Environ. 89, 423–433. doi:10.1016/j.rse.2003.10.020

Mauseth, J., 1988. Plant Anatomy, First Ed. ed. The Benjamin/Cummings Publishing Company, Menlo Park, CA.

McGregor, M., Hamel, D., Lood, R., Meyer, H., 1975. Status of Mountain Pine Beetle Infestation Glacier National Park, 1974. Missoula, MT.

Meddens, A.J.H., Hicke, J.A., Ferguson, C.A., 2012. Spatiotemporal patterns of observed bark beetle-caused tree mortality in British Columbia and the western United States. Ecol. Appl. 22, 1876–1891.

Meddens, A.J.H., Hicke, J.A., Vierling, L.A., 2011. Evaluating the potential of multispectral imagery to map multiple stages of tree mortality. Remote Sens. Environ. 115, 1632–1642. doi:10.1016/j.rse.2011.02.018

Meddens, A.J.H., Hicke, J.A., Vierling, L.A., Hudak, A.T., 2013. Evaluating methods to detect bark beetle-caused tree mortality using single-date and multi-date Landsat imagery. Remote Sens. Environ. 132, 49–58. doi:10.1016/j.rse.2013.01.002

Meigs, G.W., Kennedy, R.E., Cohen, W.B., 2011. A Landsat time series approach to characterize bark beetle and defoliator impacts on tree mortality and surface fuels in conifer forests. Remote Sens. Environ. 115, 3707–3718. doi:10.1016/j.rse.2011.09.009

Millar, C.I., Stephenson, N.L., Stephens, S.L., 2007. Climate change and forests of the future: managing in the face of uncertainty. Ecol. Appl. 17, 2145–51.

NASA, 2013. The Multispectral Scanner System [WWW Document]. URL http://landsat.gsfc.nasa.gov/about/mss.html

Nemani, R., Hashimoto, H., Votava, P., Melton, F., Wang, W., Michaelis, A., Mutch, L., Milesi, C., Hiatt, S., White, M., 2009. Monitoring and forecasting ecosystem dynamics using the Terrestrial Observation and Prediction System (TOPS). Remote Sens. Environ. 113, 1497–1509. doi:10.1016/j.rse.2008.06.017

Parmenter, A.W., Hansen, A.J., Kennedy, R.E., Cohen, W.B., Langner, U., Lawrence, R., Maxwell, B., Gallant, A., Aspinall, R., 2003. Land Use and Land Cover Change in the Greater Yellowstone Ecosystem: 1975 – 1995. Ecol. Appl. 13, 687–703.

Pettorelli, N., Vik, J.O., Mysterud, A., Gaillard, J.M., Tucker, C.J., Stenseth, N.C., 2005. Using the satellite-derived NDVI to assess ecological responses to environmental change. Trends Ecol. Evol. 20, 503–10. doi:10.1016/j.tree.2005.05.011

Platt, R.V., Schoennagel, T., 2009. An object-oriented approach to assessing changes in tree cover in the Colorado Front Range 1938–1999. For. Ecol. Manage. 258, 1342–1349. doi:10.1016/j.foreco.2009.06.039

Pongpattananurak, N., Reich, R.M., Khosla, R., Aguirre-Bravo, C., 2012. Modeling the Spatial Distribution of Soil Texture in the State of Jalisco, Mexico. Soil Sci. Soc. Am. J. 76, 199. doi:10.2136/sssaj2011.0180

Powell, J.A., Logan, J.A., 2005. Insect seasonality: circle map analysis of temperature-driven life cycles. Theor. Popul. Biol. 67, 161–79. doi:10.1016/j.tpb.2004.10.001

R Development Core Team, 2013. R: A language and environment for statistical computing.

Raffa, K.F., Aukema, B.H., Bentz, B.J., Carroll, A.L., Hicke, J.A., Turner, M.G., Romme, W.H., 2008. Cross-scale Drivers of Natural Disturbances Prone to Anthropogenic Amplification: The Dynamics of Bark Beetle Eruptions. Bioscience 58, 501. doi:10.1641/B580607

Reich, R.M., Aguirre-Bravo, C., Bravo, V.A., Briseño, M.M., 2011. Empirical evaluation of confidence and prediction intervals for spatial models of forest structure in Jalisco, Mexico. J. For. Res. 22, 159–166. doi:10.1007/s11676-011-0144-1

Rencz, A.N., Nemeth, J., 1985. Detection of Mountain Pine Beetle Infestation Using Landsat MSS and Simulated Thematic Mapper Data. Can. J. Remote Sens. 11, 50–58.

Rousse, J.W., Hass, R.H., Schell, J.A., Deering, D.W., Harlan, J.C., 1974. Monitoring the vernal advancement of retrogradation of natural vegetation, Type III, Final Report. Greenbelt, Maryland.

Salzberg, S.L., 1997. On Comparing Classifiers: Pitfalls to Avoid and a Recommended Approach. Data Min. Knowl. Discov. 1, 317–328.

Schowengerdt, R.A., 2007. Remote Sensing: Models and Methods for Image Processing, Third Ed. ed. Academic Press, San Diego, CA, San Diego.

Schroeder, T.A., Cohen, W.B., Song, C., Canty, M.J., Yang, Z., 2006. Radiometric correction of multi-temporal Landsat data for characterization of early successional forest patterns in western Oregon. Remote Sens. Environ. 103, 16 – 26. doi:10.1016/j.rse.2006.03.008

Skakun, R.S., Wulder, M.A., Franklin, S.E., 2003. Sensitivity of the thematic mapper enhanced wetness difference index to detect mountain pine beetle red-attack damage. Remote Sens. Environ. 86, 433–443. doi:10.1016/S0034-4257(03)00112-3

Strand, E., Smith, A., Bunting, S., Vierling, L., Hann, D., Gessler, P., 2006. Wavelet estimation of plant spatial patterns in multitemporal aerial photography. Int. J. Remote Sens. 27, 2049–2054. doi:10.1080/01431160500444764

Swetnam, T.W., Allen, C.D., Betancourt, J.L., 1999. Applied Historical Ecology: Using the Past To Manage for the Future. Ecol. Appl. 9, 1189–1206. doi:10.1890/1051-0761(1999)009[1189:AHEUTP]2.0.CO;2

Townsend, P.A., Singh, A., Foster, J.R., Rehberg, N.J., Kingdon, C.C., Eshleman, K.N., Seagle, S.W., 2012. A general Landsat model to predict canopy defoliation in broadleaf deciduous forests. Remote Sens. Environ. 119, 255–265. doi:10.1016/j.rse.2011.12.023

Townshend, J.R., Masek, J.G., Huang, C., Vermote, E.H., Gao, F., Channan, S., Sexton, J.O., Feng, M., Narasimhan, R., Kim, D., Song, K., Song, D., Song, X., Noojipady, P., Tan, B., Hansen, M.C., Li, M., Wolfe, R.E., 2012. Global characterization and monitoring of forest cover using Landsat data: opportunities and challenges. Int. J. Digit. Earth 5, 373–397.

Turner, M.G., Dale, V.H., 1998. Comparing Large, Infrequent Disturbances: What Have We Learned? Ecosystems 1, 493–496.

Turner, M.G., Hargrove, W.W., Gardner, R.H., Romme, W.H., 1994. Effects of Fire on Landscape Heterogeneity in Yellowstone National Park, Wyoming. J. Veg. Sci. 5, 731–742.

Upton, G.J.G., Fingleton, B., 1985. Spatial data Analysis by Example. Volume 1: Point Pattern and Quantitative Data. John Wiley & Sons, Chichester.

USGS, 2014. EarthExplorer archive [WWW Document]. URL http://edcsns17.cr.usgs.gov/NewEarthExplorer/

Veblen, T.T., Hadley, K.S., Nel, E.M., Kitzberger, T., Reid, M., Villalba, R., 1994. Disturbance regime and disturbance interactions in a Rocky Mountain subalpine forest. J. Ecol. 82, 125–135.

Vogelmann, J.E., Tolk, B., Zhu, Z., 2009. Monitoring forest changes in the southwestern United States using multitemporal Landsat data. Remote Sens. Environ. 113, 1739–1748. doi:10.1016/j.rse.2009.04.014

Vogelmann, J.E., Xian, G., Homer, C., Tolk, B., 2012. Monitoring gradual ecosystem change using Landsat time series analyses: Case studies in selected forest and rangeland ecosystems. Remote Sens. Environ. 122, 92–105. doi:10.1016/j.rse.2011.06.027

Volcani, A., Karnieli, A., Svoray, T., 2005. The use of remote sensing and GIS for spatio-temporal analysis of the physiological state of a semi-arid forest with respect to drought years. For. Ecol. Manage. 215, 239–250. doi:10.1016/j.foreco.2005.05.063

Weber, F.P., Roberts, E.H., Waite, T.H., 1975. Forest Stress Detection: Ponderosa Pine Mortality from Mountain Pine Beetle, in: Evaluation of ERTS-1 Data for Forest and Rangeland Surveys. USDA Forest Service Research Paper PSW-112, Berkeley, California, pp. 44–61.

White, J., Wulder, M.A., Brooks, D., Reich, R., Wheate, R., 2005. Detection of red attack stage mountain pine beetle infestation with high spatial resolution satellite imagery. Remote Sens. Environ. 96, 340–351. doi:10.1016/j.rse.2005.03.007

Woodcock, C., Allen, R., Anderson, M., Belward, A., Bindschadler, R., Cohen, W., Gao, F., Goward, S., Helder, D., Helmer, E., Nemani, R., Oreopoulos, L., Schott, J., Thenkabail, P., Vermote, E., Vogelmann, J., Wulder, M.A., Wynne, R., 2008. Free Access to Landsat Imagery. Science (80-.). 320, 1011.

Wulder, M.A., Dymond, C., White, J.C., Leckie, D.G., Carroll, A.L., 2006a. Surveying mountain pine beetle damage of forests: A review of remote sensing opportunities. For. Ecol. Manage. 221, 27–41.

Wulder, M.A., White, J.C., Bentz, B.J., Alvarez, M.F., Coops, N.C., 2006b. Estimating the probability of mountain pine beetle red-attack damage. Remote Sens. Environ. 101, 150–166.

CHAPTER 5: The Influence of an Historic Mountain Pine Beetle Outbreak on Burn Severity in Glacier National Park

5.1 SUMMARY

Native bark beetles are capable of causing widespread mortality during outbreak events in the forests of western North America. These disturbances can have vast effects on forest structure and there is concern that such changes could influence subsequent wildfire behavior and its impact on ecosystems. New research has looked at the recent mountain pine beetle outbreak (~1986-2006), but few studies have analyzed the ecological legacies of historic events. Northern Rocky Mountain forests were impacted by a widespread mountain pine beetle outbreak in the late 1970s through the early 1980s. In this study, we evaluated the effect of the historic mountain pine beetle outbreak and other biophysical variables on the burn severity of 11 different fires in Glacier National Park over an 18-year period. The extent and arrangement of these disturbances presented a unique opportunity to evaluate the influence of an earlier disturbance on ensuing wildfires. We used sequential autoregression to obtain accurate estimates of model parameters given the high level of spatial autocorrelation associated with wildfire. Models included additional explanatory variables known to influence burn severity such as topography and fuel moisture and variables were evaluated at increasing spatial scales. Historic mountain pine beetle severity was a significant predictor of burn severity in 10 of the 11 fires. The relationship between beetle severity and burn severity was positive across all models and we found no relationship between the effect size of beetle severity and time since the beetle outbreak. However, our results suggest the influence of the beetle outbreak on burn severity is scale-dependent on the pattern of beetle intensity. Fires where beetle severity was the best predictor at broad scales tended to have a larger beetle effect size compared to fires where local beetle

severity was the best predictor. A number of factors are responsible for the burn severity associated with a given fire. However, our work shows that the effects of high severity mountain pine beetle outbreak can influence the burn severity of wildfire for many years after the initial disturbance event.

5.2 INTRODUCTION

In western North America, native bark beetles are a major disturbance agent capable of regional-scale forest mortality (Raffa et al., 2008) and fire as a disturbance agent is well documented (Agee, 1993; Turner and Dale, 1998). These disturbances can have profound effects on the structure of the ecosystem for many years after the event (Turner and Dale, 1998) and influence the likelihood, severity and spread of subsequent disturbances (Veblen et al., 1994). There is concern that the disturbance regime associated with each of these events is changing and fire-beetle linkages need more research (Lynch et al., 2007). Recent bark beetle outbreaks have become more frequent and widespread in the forests of western North American (Raffa et al., 2008). The frequency of large fires in the western United States has increased due to warming temperatures, earlier snowmelt, and longer fire seasons (Littell et al., 2009; Westerling et al., 2006). Future predictions indicate that fires may become more frequent and severe, leading to novel fire-climate-vegetation relationships (Lutz et al., 2009; Westerling et al., 2011). Projections indicate the climate will get warmer (*IPCC Third Assessment Report,* 2001) which could lead to an increase in forest disturbance in the near future given that both fire and bark beetles are vulnerable to climactic controls (Bentz et al., 2010; Logan et al., 2003; Westerling et al., 2006). The response of bark beetles is not expected to be uniform among and within genera, but several widespread species are predicted to become more widespread as temperature warms (Bentz et al., 2010).

5.2.1 Compounded Disturbances

The interaction of fire and insect agents is an area of active research due to the increased probability of compounded disturbances and the potential for unexpected ecological outcomes (Paine et al., 1998). Empirical studies on compounded disturbances have reported a range of results. In Colorado, Kulakowski and Veblen (2007) found that fire extent was independent of prefire disturbance history, however, fire severity was influenced by stands that were severely blown down five years earlier. Bebi et al. (2003) found that spruce-fir forests in Colorado impacted by spruce beetle (10-50 years earlier) were not more likely to burn compared to unaffected stands. Kulakowski and Jarvis (2011) found no detectable increase in occurrence of high-severity fires following mountain pine beetle outbreaks and concluded climate has been the primary driver of the fire regime in northwestern Colorado and southern Wyoming. Harvey et al. (2014) concluded recent beetle outbreak severity in the northern Rocky Mountains was largely unrelated to subsequent fire severity. Turner et al. (1999) found high severity bark beetle damage increased the likelihood of crown fire in the 1988 Yellowstone National Park fires, whereas intermediate beetle severity did not. Lynch et al. (2006) found severe fire was more likely to occur in lodgepole forest that experienced mountain pine beetle 15 years prior, but not in areas that were impacted by beetles seven years earlier. These studies highlight the importance of spatially explicit research as the effects of disturbance interactions vary across ecosystems, weather patterns, and time and severity associated with each disturbance.

5.2.2 Impacts of Mountain Pine Beetle on Forest Structure

The widespread mortality associated with mountain pine beetle (*Dendroctonus ponderosae*) outbreaks has cascading effects on numerous ecological processes, including forest composition (Veblen et al., 1991), the condition and arrangement of fuels (Hicke et al., 2012)

and wildfire characteristics (Schoennagel et al., 2012; Simard et al., 2011). As beetles induce stand level tree mortality, the foliage changes from green to red in the first few years after attack (Wulder et al., 2006). The gray stage begins once needles and some small branches fall to the ground (> 3 years), but larger dead fuels remain in the canopy (Schoennagel et al., 2012). Fine surface fuels increase in the gray phase as canopy bulk density decreases (Hicke et al., 2012). Approximately a decade later, the affected stands enter the Old-MPB phase (Schoennagel et al., 2012) where coarse surface fuels increase significantly as large branches and snags fall (Hicke et al., 2012). During this phase, the release of resources allows shrubs and seedlings to establish alongside any surviving trees. The new growth results in an increase of ladder fuels (Hicke et al., 2012) which has implications on crown fire potential due to lower canopy bases and increased canopy bulk density (Schoennagel et al., 2012; Simard et al., 2011). Fuel moisture is likely to decrease as the canopy opens and wind speed increases (Schoennagel et al., 2012). Hicke et al. (2012) developed a conceptual framework of beetle induced changes to the probability of fire occurrence and burn severity based on a review of nearly 40 studies. They found an increase in crown fire probability during the red phase, but surface fire probability remained unchanged in this phase. Once a stand transitions into the gray phase, crown fire probability decreases, largely due to reduced canopy bulk density. However, the probability of surface fire increases with the redistribution of fuels from the canopy to the surface and an increase in ladder fuels. Likewise, the probability of burn severity reflects changing conditions of phases too. Foliar moisture is reduced during the red phase which could increase torching and active crown fire resulting in high mortality and subsequent burn severity in the canopy (Keeley, 2009). In the gray phase, the probability of burn severity is reduced in the canopy due to reduced canopy bulk density, but there is an increase in the probability of high burn severity along the forest floor due to higher

surface loads and greater reaction intensity. However, their framework highlights substantial knowledge gaps and a lack of consensus in the literature dependent upon the research question addressed, time since the outbreak, weather conditions, and fire behavior (Hicke et al., 2012; Simard et al., 2011).

5.2.3 Remote Sensing of Burn Severity

There has been considerable confusion within the field on the usage of fire intensity, fire severity and burn severity, with terms occasionally being used synonymously (Keeley, 2009). The Monitoring Trends in Burn Severity (MTBS) program defines fire severity as the degree to which a site has been altered or disrupted by fire; loosely, a product of fire intensity and residence time (Eidenshink et al., 2007); whereas burn severity is defined broadly as the effect of fire on an ecosystem (Agee, 1993). We follow the lead of (Lee et al., 2009) and use the term burn severity as a metric of vegetation change derived from remotely sensed imagery data that has been made available for recent, large fire events through the MTBS program (Eidenshink et al., 2007). The Normalized Burn Ratio (Key and Benson, 2006) is calculated using the near and mid-infrared portions of the electromagnetic spectrum (bands 4 and 7 in Landsat TM). The near-infrared band is sensitive to living vegetation whereas the mid-infrared band is sensitive to ash, char, and water content. Since both of these ecosystem properties are impacted by fire, the change in the Normalized Burn Ratio (dNBR) using pre and post fire imagery provides a robust measure of burn severity (Duffy et al., 2007). However, dNBR may overestimate burn severity in areas that have smaller amounts of photosynthetic active vegetation in the pre-fire image, therefore, a relative measure of dNBR (RdNBR) was developed to account for pre-fire conditions at each pixel (Miller and Thode, 2007). MTBS data (dNBR or RdNBR) has been used to test for spatial variation in wildfires in the western US (Parisien et al., 2012), examine the

relationship between snowpack and fire size in Yellowstone National Park (Lutz et al., 2009), understand patterns of burn severity by vegetation type and landscape complexity in Alaska (Duffy et al., 2007) and assess the influence of multiple factors such as topography (Holden et al., 2009), climate and weather (Dillon et al., 2011) on burn severity in the western US. Several studies have used dNBR or RdNBR to analyze the effects of a prior disturbance on burn severity. Finney et al. (2005) found that prescribed fire treatments reduced burn severity in two Arizona wildfires. Thompson et al. (2007) analyzed burn severity on a fire in southwest Oregon that burned 25 years prior and was partially salvage logged and replanted. Wimberly et al. (2009) and Prichard and Kennedy (2014) evaluated the effectiveness of fuel treatments in wildfires in California and Washington. However, to our knowledge, no study has analyzed the influence of beetle severity on burn severity of wildfire.

5.2.4 Challenges Associated with Modeling Contagious Landscape Disturbances

Analysis of forest disturbances, such as wildfire, present challenges to traditional statistical tests because wildfire is inherently spatially structured and subject to both endogenous and exogenous processes (Kissling and Carl, 2008). Spatial pattern is an artifact of the inherent property of fire (endogenous processes) in which areas in close proximity to active fire are more likely to burn (Lynch et al., 2007). Exogenous processes operate independent of wildfire, but influence fire patterns because landscapes are spatially structured via climate, geomorphology prevailing wind patterns, topography and vegetation characteristics (Kissling and Carl, 2008). Therefore, simple overlays of burn severity and an explanatory variable of interest can result in misleading conclusions (Wimberly et al., 2009). Classical statistical tests assume independently distributed errors which lead to problems with spatial autocorrelation because model coefficients could be biased, impacting hypothesis testing and model inference (Kissling and Carl, 2008).

Recent studies have addressed these issues using several different methods. Variograms can be used to determine the distance where observations are no longer spatially correlated. However, the variogram range associated with fire is often quite large, which greatly reduces the number of observations (Lee et al., 2009). Lynch et al. (2006) used Markov chain Monte Carlo technique to accurately capture the latent spatial autocorrelation and Thompson et al. (2007) used a spherical theoretical variogram model to describe correlation in the data and estimate parameters of a generalized least squares model. Wimberly et al. (2009) and Prichard and Kennedy (2014) used sequential autoregression (SAR) (Cressie, 1993) which incorporates a spatial term (i.e. spatial weights matrix) in a standard regression model, to account for spatial autocorrelation. The spatial weights matrix considers the neighborhood (user-defined distance) of each observation and weights each neighbor as a function of distance (Kissling and Carl, 2008) to model the spatial dependence using a variance-covariance matrix (Cressie, 1993). In this way, SAR models utilize inherent spatial autocorrelation in the data (e.g. values of neighboring locations) to provide a proxy for missing variables that are not accounted for by explanatory variables (e.g. local fire weather) (Kissling and Carl, 2008; Prichard and Kennedy, 2014; Wimberly et al., 2009). SARs are computationally intensive, but have become more widely used with advances in computing capacity and offer an additional advantage for contagious disturbances in that they account for the missing variables problem.

Recognition of pattern and scale are paramount in ecology (Levin, 1992), yet many ecological studies analyze processes at a single scale. Observations from remotely sensed data default to the raw pixel size associated with the image used to collect the information (Wu et al., 2014). Multi-scale analysis expands the frame of reference in a study (Falk et al., 2007) through consideration of topology (or the surrounding neighborhood) of an environmental variable

associated with an observation. Fire is a complex disturbance which is influenced by the interaction of fuels, topography and climate, each of which may vary as a function of the spatial scale of study (Falk et al., 2007). Therefore multi-scale analysis of factors that contribute to fire behavior is an important consideration in evaluation of fire-environment relationships (Falk et al., 2007; Parks et al., 2011; Wu et al., 2014). Several studies have demonstrated that information contained in the surrounding neighborhood of an observation may be more relevant to controls on fire than observations made at the individual pixel scale. For example, a study in eastern Canada demonstrated that dominant aspect was related to fire frequency, but only at broad spatial scales (Cyr et al., 2007). Parks et al. (2011) showed that burn probability in the western US was most influenced by fuels and elevation at fine scales, but fuels and aspect at broad scales (Parks et al., 2011). Cross-scale research in the boreal forest of Northeastern China identified burn severity was mainly controlled by vegetation at local scales and topography at broad scales (Wu et al., 2014).

5.2.5 Objectives

In the late 1970s and early 1980s a high-severity mountain pine beetle outbreak occurred in the northern Rocky Mountains, which covered over 30% of Glacier National Park (GNP) (Assal et al., 2014). Then additional disturbance impacted the landscape as 17 fires burned 27% of the forest within the park between 1984 and 2006. The timing, arrangement, and data availability of these events presented a unique opportunity to study the effect of multiple disturbances. In this study, we use SAR modeling to evaluate the effect of an historic mountain pine beetle outbreak and other biophysical variables on the burn severity of 11 fires in GNP. The main objective of the study was to determine if the severity of the beetle outbreak in the 1970s and 80s had an effect on the burn severity of subsequent wildfires. Numerous other factors likely

influenced the extent and severity of the wildfires such as vegetation, landform, and regional weather (Prichard and Kennedy, 2014). Therefore, it was necessary to evaluate other factors that could contribute to patterns of burn severity. If mountain pine beetle severity had a measurable influence on burn severity, we hypothesize the following: 1) the influence of beetle severity on burn severity would decline with time since the beetle outbreak (time since beetle hypothesis), 2) the influence of beetle severity on burn severity would be negated under extreme fire weather (weather hypothesis), 3) the influence of beetle severity would be contingent on the pattern of beetle severity intensity (beetle pattern hypothesis). In this study, we utilize data on beetle severity and burn severity that exploits two large disturbance processes that played out over broad spatial and temporal scales. The focus of our work is to determine if there is any measureable ecological legacy from the mountain pine beetle disturbance on the landscape with regard to fire severity. Burn severity is influenced by numerous factors but retrospective analysis is a promising approach to evaluate the influence of beetle severity on burn severity and the results hold great interest for those charged with management of forests impacted by the recent beetle outbreak (~1996-2006) that occurred in the Rocky Mountains.

5.3 METHODS

5.3.1 Study Area

The study is located in Glacier National Park in northwestern Montana (Figure 5.1), which encompasses over 400,000 ha of topographically diverse terrain, bisected by the Continental Divide. Mean average annual precipitation is 73.1 cm, and average annual maximum and minimum temperatures are 11.9 ºC and -0.2 ºC, respectively (1971-2000) (Western Regional Climate Center, West Glacier station, elevation: 970 m, http://www.wrcc.dri.edu; accessed 17 December 2012). Elevation ranges from ~ 950 m to 3184 m above sea level and major cover

types include grasslands, conifer and deciduous forests, lakes, wide glacial valleys and steep alpine zones. Forests are dominated by lodgepole pine (*Pinus contorta*), western larch (*Larix occidentalis*), Engelmann spruce (*Picea* engelmannii) and Douglas-fir (*Pseudotsuga menziesii*). The area was chosen because of the extensive mountain pine beetle epidemic that took place in the late 1970s and the number of wildfires that occurred since that time. The analysis area was limited to burned area inside the park of selected fires (Table 5.1, Figure 5.2).

5.3.2 Data

5.3.2.1 Burn Severity Data

We considered 17 wildfires that intersected GNP between 1984 and 2006 (Figure 5.1). We obtained fire progression information where available from GNP and retained 11 fires for the analysis (Table 5.1). We chose to use RdNBR in our multi-fire analysis because the relative index has been shown to provide a consistent definition of burn severity across time and space (Miller and Thode, 2007). We used the continuous RdNBR data as opposed to classified burn severity data because information is lost when using categorical data because burn severity occurs on a continuum (Miller and Thode, 2007).

5.3.2.1 Explanatory Variables

Fire behavior is contingent on topography, weather conditions, and the arrangement and amount of fuels. In our model, topography and other important abiotic landscape features for fire behavior are accounted for by elevation, heat load, and topographic position, all derived from a 30 m digital elevation model. The heat load index (HLI) is a potential measure of direct incident radiation (McCune and Keon, 2002) (Equation 3), which varies with aspect and slope; whereas a topographic position index (TPI), a measure of slope position and landform type with respect to adjacent grid cells, identifies the portion of the landscape a cell occupies (e.g. valley bottom, mid

slope, ridgetop, etc.) (Table 5.2). We used a daily fuel moisture data set which represents the fuel moisture of large fuels (e.g. 100-hr and 1000-hr fuels). The data was developed by the US Forest Service Rocky Mountain Research Station and derived from a 4 km gridded dataset of surface meteorological variables (Abatzoglou, 2013). Each burned pixel was assigned the daily fuel moisture value for fuel size that corresponded to the daily fire progression interval at that pixel.

Several studies have used recent aerial survey detection data to account for mountain pine beetle disturbance (Meddens et al., 2012; Meigs et al., 2011). However, a previous study concluded the historic aerial survey data in GNP to lack an adequate measure of severity and developed a model of mountain pine beetle severity using multiple lines of evidence (Assal et al., 2014). The dataset identifies the amount of canopy change as a measure of beetle induced mortality over a 14-year period as the disturbance progressed. We used the continuous dataset of beetle severity from the late 1970s and early 1980s to account for the previous mountain pine beetle disturbance. This data set was developed from numerous vegetation indices over the 14-year period and represents the best proxy for the amount of fuels on the landscape prior to fire activity (Table 5.2).

We evaluated the relationship of the explanatory variables (Table 5.2) on burn severity at seven spatial scales. We calculated the mean value within a circular moving window at radii of 45, 90, 180, 360, 720, 990, and 1440 m, ranging from 0.64 ha to 650 ha in size. Scales were considered based on the spatial resolution of the data, the complex and variable terrain of the study area, and a range of values covered in other fire research (Parks et al., 2011; Wu et al., 2014). We did not evaluate fuel moisture at multiple scales on account of the coarse resolution of the data (4 km). We opted to use a moving window analysis over other landscape metrics (e.g. patch size, mean shape index, etc.) to fully exploit the continuous nature of the data and avoid

arbitrary categories. Our intent was to evaluate the best set of predictor's at the most appropriate scale for each fire. Since we analyzed 11 independent fire events, we did not enforce a static scale for each explanatory variable across all fires.

5.3.3 Statistical Analysis

Variogram models of each fire indicated spatial autocorrelation in the burn severity data between 1500 m to over 3000 m. Therefore we used SAR modeling (Prichard and Kennedy, 2014), to predict continuous burn severity (RdNBR) using a suite of independent variables that characterize topography and previous mountain pine beetle severity (Table 5.2). The analyses were conducted using the extent of the data for each fire, with the sample of pixels distributed on a 60 x 60 m lattice (Wimberly et al., 2009). All statistical analyses were performed in the R statistical environment (R Development Core Team, 2013).

We used the error version of SAR (Wimberly et al., 2009):

$$\mathbf{Y = X\beta + \lambda W(Y - X\beta) + \varepsilon}$$

Where

Y dependent variable (e.g. fire severity)

X matrix of independent variables

β vector of parameter

λ autoregressive coefficient

W spatial weights matrix. Inverse distance was used to define the neighborhood structure of the 12 nearest neighbors (Wimberly et al., 2009)

ε uncorrelated error term

The model can also be viewed as:

Xβ the spatial trend of fire severity predicted by the independent variables

λW(Y-Xβ) the spatial signal, indicative of spatial autocorrelated deviations from the spatial trend, modeled as an autoregressive function of deviations in neighboring sites

ε the noise term which represents deviations from the trend that were not spatially autocorrelated

We first evaluated the univariate relationship between each explanatory variable and burn severity to identify the scale of the explanatory variable which best describes burn severity. We selected the appropriate scale using Akaike's Information Criterion (AIC) and used that scale of the variable in the full model. The full covariate model included variables to account for topography (elevation, slope, TPI, HLI), a proxy for weather (fuel moisture of 100 and 1000-hour fuels) and previous vegetation disturbance (beetle severity). We retained the full covariate model for each fire to maintain a consistent covariance structure, with minimal AIC penalty given the large number of observations in each model.

5.4 RESULTS

5.4.1 SAR Models

We produced a model of predicted burn severity for each of the 11 fires using the SAR modeling approach and variables known to influence fire severity (Table 5.2). Appendix C contains the final models used for each fire. Although the full covariate model was used in each fire, the scales of several explanatory variables differed between fire models (Table 5.3). Overall,

the models performed well and explained between 54% and 80% of the variability in the burn severity data for each fire (Table 5.3). The SAR models captured spatial patterns of high and low burn severity that are visibly similar to measured values (Figure 5.3). Furthermore, there was no spatial pattern in the error term of the SAR in each model, indicating spatial independence in the residuals. We standardized the regression coefficients (Bring, 1994) of each model in order compare the effect size of each variable within and across fires (Table 5.4).

5.4.2 Topography

Elevation was a significant predictor in most of models and typically had a large positive effect on burn severity (Table 5.4). The finest scale of elevation (e.g. one 30 m pixel) was consistently the strongest scale identified by the univariate analysis. The topographic position index (TPI) was a significant predictor of burn severity in nearly all of the fires (Table 5.4). Effects of TPI, a measure of landform with respect to adjacent grid cells, were small and nearly always positive. This indicates that locations found at mid-slope to the top of slope were more strongly correlated with higher levels of burn severity compared to valley bottoms. Scales of TPI that best fit models varied from single pixel up to 90 m neighborhoods. Heat load was a significant predictor in 10 of the 11 models and always had a positive association with burn severity. Slope was significant in the fewest fires; however, steeper slopes generally had a positive effect on burn severity.

5.4.3 Fuel Moisture

The fuel moisture of 100-hr fuels was a significant predictor of burn severity in half of the models. The results indicate that a decrease in the fuel moisture of 100-ha fuels is correlated with an increase in burn severity (Table 5.4). The moisture of 1000-hr fuels was a significant

predictor in the majority of the models, but the effect on burn severity was a mix of positive and negative influence on burn severity depending on the fire.

5.4.4 Mountain Pine Beetle

We found that historic mountain pine beetle severity had a significant effect on burn severity in 10 of the 11 fire models. Beetle severity was not significant in the Middle Fork Complex fire, where elevation and heat load had the largest effect size, suggesting burn severity was largely driven by topographic processes. The effect of beetle severity varied by fire, but there was always a positive association between beetle and burn severity. Several different scales were identified as the most appropriate for beetle severity, ranging from neighborhoods of 10 hectares (e.g. 180 m radius) or less.

5.5 DISCUSSION

Our study builds on the ideas of earlier work that assessed the effects of wildfire (Thompson et al., 2007), prescribed burning (Finney et al., 2005), and fuels reduction (Prichard and Kennedy, 2014; Wimberly et al., 2009) on burn severity. However, our study is different for several reasons. First, a continuous data set of beetle severity (Assal et al., 2014) allowed us to extend our analysis beyond outbreak presence or absence used in other studies (Lynch et al., 2007). This enabled us to shift the focus from potential events (i.e. changes in probability of fire) to the consequences of actual events (i.e. ecological consequences of burn severity). Second, the arrangement of the area impacted by the beetle outbreak and subsequent wildfire presented a unique opportunity to consider numerous wildfires as opposed to a single fire event (Bebi et al., 2003; Finney et al., 2005; Thompson et al., 2007). Observations drawn from multiple fires broaden the perspective of these compounded disturbances. Our findings support some of the prior research (Lynch et al., 2007), but are inconsistent with the conclusions of several other

recent studies. The long-term perspective of our study shows that ecological legacies of prior high-severity disturbance may continue to influence subsequent disturbance for many years after the initial event and can shed light on future disturbance interactions associated with the recent mountain pine beetle outbreak. Much of the landscape impacted by the recent outbreak is in the gray phase. Harvey et al. (2014) concluded that beetle severity from the contemporary outbreak had little effect on burn severity. However, their analysis was conducted on a post-outbreak landscape in the gray phase. As ladder fuels continue to build across post-outbreak forests as time since the outbreak increases, these areas could experience higher burn severity which has important implications for post-fire regeneration (Kulakowski and Veblen, 2007).

5.5.1 Ecological Mechanisms

There were common variables that influenced burn severity across the different models, including the primary variable in question, previous beetle disturbance. Numerous abiotic variables were relevant in the models, including elevation. Burn severity was generally found to be more severe at higher elevations and elevation had the strongest effect in the Moose, Wedge Canyon and Anaconda fires, which may be explained in part by the physiography of the study area (Figure 5.1). These fires ignited or first entered the study area on the west side of the park in the North Fork Flathead River valley. The fires spread east and upslope into drier forests at mid-elevations before encountering alpine vegetation. Our results are consistent with other studies that noted a decrease in severity as fire moved higher into vegetation with lower fuel loads (Bigler et al., 2005; Lee et al., 2009). There was typically a small, positive relationship between TPI and burn severity (Table 5.4), which indicates locations found between mid-slope and the top of the slope were more strongly correlated with higher levels of burn severity compared to valley bottoms. This is consistent with other findings which found higher severity crown fires

less likely to occur in valley bottoms (Bradstock et al., 2010). TPI at scales of 45 and 90 m radii were often the best predictors of TPI, which suggests the TPI over a broad area is a more important predictor of burn severity than at the pixel level. HLI and slope were analyzed due to their influences on fuel type, configuration and moisture levels (Bradstock et al., 2010; Parks et al., 2011). The relationship between burn severity and HLI was positive, which indicates aspects that receive a higher amount of direct incident radiation experienced higher levels of burn severity. Our results are consistent with other studies that found an increase in wildfire occurrence (Rollins et al., 2002) or burn severity (Wimberly et al., 2009) in areas that have a higher HLI such as west and southwestern slopes. In the northern Rocky Mountains, spatially continuous biomass and fuel moisture conditions are most favorable to fire in areas that have a high HLI (Parks et al., 2011). The scale of HLI was not consistent across fires, and the largest effect of HLI were at scales of 45 and 90 m radii respectively (Tables 5.3 and 5.4), which suggests fuels were likely more continuous at broad scales. The inconsistency across scales may also suggest an interaction between aspect and prevailing weather conditions at the time of the fire. The mixed results with respect to slope are consistent with other studies that reported either a positive (Collins et al., 2007) or a negative correlation with burn severity (Lee et al., 2009; Prichard and Kennedy, 2014).

We found burn severity to be higher in areas where the moisture of 100-hr fuels was lower when this variable was significant (Table 5.4). However, the effect of fuel moisture of 1000-hr fuels on burn severity is inconsistent, with both positive and negative influences on burn severity. This may be explained in part by prevailing drought conditions at the time of each fire. The Palmer Drought Severity Index from the month of each fire and one month prior to each fire indicated mild to severe drought conditions during all fires (Western Regional Climate Center,

WestWide Drought Tracker, http://www.wrcc.dri.edu/wwdt/time/; accessed 20 July 2014). Fuel moisture was low during each fire year and differences in fuel moisture were likely minimal across each burned area (Turner et al., 1999). Furthermore, the inclusion of weather variables in burn severity modeling is problematic, largely due to the scale of input data (Wimberly et al., 2009). Fire progression information is often recorded in broad polygons and weather data collected from nearby weather stations (or used to develop continuous surfaces (e.g. PRISM data)) might not accurately reflect the conditions at the fire front. Given the availability of data, we chose to incorporate fuel moisture as a proxy for recent weather conditions. However, the data set has coarse spatial resolution (4 km) which likely does not capture the variability in fuel moisture. Furthermore, the fire progression data sometimes included large time gaps between intervals which might not have adequately portrayed fire spread.

To meet our primary objective, we found that beetle severity was a statistically significant predictor of burn severity in 10 of the 11 fires, even with a wide range of other variables included in the models. We found a positive correlation between these variables which indicates areas with higher beetle severity also experienced higher burn severity. Our results do not support the time since disturbance hypothesis as there is no clear trend in the size of the beetle effect over time (Figure 5.4). However, no distinct outbreak phase gradient was present in our analysis, as all of the fires burned during the Old-MPB phase (Schoennagel et al., 2012). Likewise the results do not support the weather hypothesis as beetle severity was significant across all fires except the Middle Fork complex fire. Although the Middle Fork complex fire burned during an extreme fire year (2003), there were four other fires analyzed during that same year (Table 5.1) and beetle severity was found to be significant in those fires (Table 5.4).

Our results indicate historic beetle severity has an influence on subsequent burn severity (Table 5.4). The time scale between the beetle outbreak and the occurrence of each fire is consistent with the time required for a significant release of understory vegetation (Lynch et al., 2007), or new establishment (Sibold et al., 2007) resulting in an increase in ladder fuels (Hicke et al., 2012). Stands that were heavily impacted by beetles likely had surviving mature individuals (Sibold et al., 2007; Schoennagel et al., 2012) that along with ladder fuels, contributed to the vertical heterogeneity of these stands (Lynch et al., 2007). Several recent studies concluded the secondary effects of beetle activity (i.e. the change in stand structure and composition) have a larger effect on fire risk than the primary effect of tree mortality (Bigler et al., 2005; Lynch et al., 2007). Although our study considered the effect of beetle severity on burn severity as opposed to fire risk, our results are consistent with the aforementioned studies in that long-term changes in stand structure associated with beetle outbreaks can have an effect on subsequent disturbance well into the future. Furthermore, our results lend support to those of Lynch et al. (2007), who found that areas in the Old-MPB phase influence the probability of burning, whereas stands in the more recent gray phase did not.

These results do lend support to the beetle pattern hypothesis that the influence of beetle severity is contingent on the pattern and level of beetle severity at different scales (Figure 5.5, Table 5.4). Our results show several different scales of beetle severity were found to be the best predictors of burn severity (Table 5.3). The effect size of beetle severity, where stand structure was influenced by severity of the beetle outbreak, was not consistent across all fires. In several fires, inclusion of the beetle severity variable at larger neighborhoods (e.g. 180 m radius, 10 hectares) resulted in the best model fit. We interpret that this indicates consistent forest structure at that scale for some fires, but not others. Fires where beetle severity was the best predictor at

broad scales tended to have a larger effect size compared to fires where local beetle severity was the best predictor (Figure 5.5). We found an increasing gradient of effect size as the neighborhood size increased. The data suggests a positive relationship, although the sample size (n=10) precludes a test for statistical significance. This may be the result of consistent forest structure at broad scales resulting in spatially continuous biomass and fuel conditions compared to fires that burned in areas with high heterogeneity at local scales.

5.5.2 Considerations for Future Research

Research on interactions among disturbances has increased in recent years, yet remains a key challenge in ecology (Turner, 2010). Furthermore, there is a need for additional study on beetle-fire interactions given the mixed results on the limited research on this complex topic (Schoennagel et al., 2012; Simard et al., 2011). To move this line of research forward, Hicke et al. (2012) suggest studies improve the specificity and discussion of the question addressed, time since disturbance, fuels and fire characteristics associated with an analysis. Retrospective approaches, such as the current study, describe actual events, yet there are shortcomings with this type of analysis. Remotely sensed burn severity data do not delineate between active and passive crown fire, which has implications on fire behavior (Simard et al., 2011). Models of burn severity could benefit with the inclusion of additional weather variables in the analysis as data become more readily available at finer scales. Retrospective analyses are often unable to incorporate information on wind speed, which has implications on fire behavior and can vary across beetle outbreak phase (Schoennagel et al., 2012). Additional investigation is needed on the influence of beetle severity across multiple scales of analysis. Our analysis focused on a high severity insect disturbance in the Old-MPB phase at the time of each fire. The effect of the historic outbreak is contingent on the severity of the disturbance and the elapsed time before the

next disturbance. Finally, the influence of insect outbreaks on fire characteristics and subsequent burn severity will vary by feeding guild, including different species of bark beetle and defoliators (Lynch et al., 2007).

5.6 CONCLUSIONS

A primary objective of our analysis was to determine if mountain pine beetle severity had a measureable influence on burn severity. A continuous data set of beetle severity allowed us to focus on the ecological consequences of fire as opposed to changes in the probability of fire. The arrangement and pattern of the area impacted by the beetle outbreak and subsequent wildfire presented a unique opportunity to consider numerous wildfires as opposed to a single fire event. Using remotely sensed burn severity data, topographic and fuel moisture data, coupled with SAR analysis, we were able to determine that beetle severity was a significant predictor of burn severity in 10 out of the 11 fires we analyzed. Furthermore, we were able to determine the relative contribution of each variable to burn severity of each fire and observations drawn from multiple fires broaden the perspective of these compounded disturbances. Given the availability of geospatial data, the framework we employed is transferable to other ecosystems where there is an opportunity for retrospective assessment of coupled disturbances. The long-term perspective of our study shows that ecological legacies of prior high severity disturbance may continue to influence subsequent disturbance for many years after the initial event and can shed light on future disturbance interactions associated with the recent mountain pine beetle outbreak. Much of the landscape impacted by the recent outbreak is in the gray phase. As we move into the future, these areas could experience higher burn severity which has important implications for the structure and composition of future forests. (Kulakowski and Veblen, 2007).

Any use of trade, firm, or product names is for descriptive purposes only and does not imply endorsement by the U.S. Government.

5.8 TABLES

Table 5.1. Wildfire activity in Glacier National Park during the period 1984 to 2006.

Fire Name	Start Date (year-month-day)	Area (Ha.)	Area inside Park	Used in Analysis (Rationale)
Napi Peak	19840819	1,489	2%	No (nearly all of fire was outside of park)
Crystal	19840827	1,317	85%	No (no pre-fire NBR data available)
Red Bench	19880906	13,705	71%	Yes
Adair-Howling	19940807*	4,182	100%	Yes
Starvation	19940814	3,640	51%	No (no fire progression data available)
Kootenai	19980830	3,255	100%	No (only trace amounts of beetle activity in fire perimeter)
Anaconda	19990806	4,637	100%	Yes
Parke Peak	20000722	805	100%	Yes
Moose	20010816	29,644	38%	Yes
Wolf Gun	20030716	5,636	100%	Yes
Trapper	20030718	7,298	100%	No (no beetle activity in fire perimeter)
Wedge	20030718	21,053	55%	Yes
Robert	20030723	22,065	75%	Yes
Middle Fork	20030817	4,984	100%	Yes
Rampage	20030819	9,584	100%	Yes
Poll Haven	20031019	1,819	1%	No (nearly all of fire was outside of park)
Red Eagle	20060728	13,178	58%	Yes

*The Howling fire started on 8/7/1994 and Adair fire started on 8/12/1994, but the fires are treated as one complex.

Table 5.2. Description of the explanatory variables considered in the analysis. The fuel moisture variables have a spatial resolution of 4 km, all other variables have a spatial resolution of 30 m.

Variable	Description
Elevation (Elev)	Derived from National elevation data set
Heat load index (HLI)	Potential direct incident radiation (McCune and Keon, 2002; equation 3)
Slope	Derived from National elevation data set
Topographic position index (TPI)	A measure of slope position and landform type with respect to adjacent grid cells
Fuel Moisture 100-hour fuels (FM100)	Standard moisture content of 100-hr fuel expressed as a percentage of dry weight.
Fuel Moisture 1000-hour fuels (FM1000)	Standard moisture content of 100-hr fuel expressed as a percentage of dry weight.
Historic Mountain Pine Beetle Severity (MPB)	A measure of MPB severity (0-1) for each grid cell (Assal et al., 2014).

Table 5.3. Regression models of the Relative difference normalized burn ratio (RdNBR) for each fire.

Fire Name	**Predictor Variables**	***n***	R^2
Red Bench	Elev, TPI90, Slope90, MPB90, HLI, FM100, FM1000	25,956	0.722
Adair-Howling	Elev, TPI, Slope, MPB180, HLI90, FM100, FM1000	11,149	0.671
Anaconda	Elev, TPI45, Slope, MPB90, HLI45, FM100, FM1000	11,748	0.756
Parke Peak	Elev, TPI90, Slope, MPB180, HLI, FM100, FM1000	2,085	0.537
Moose	Elev, TPI90, Slope, MPB180, HLI, FM100, FM1000	24,146	0.802
Wolf Gun	Elev, TPI90, Slope, MPB180, HLI45, FM100, FM1000	7,869	0.583
Wedge Canyon	Elev, TPI90, Slope90, MPB90, HLI45, FM100, FM1000	30,897	0.74
Robert	Elev, TPI45, Slope45, MPB, HLI, FM100, FM1000	40,580	0.697
Middle Fork Complex	Elev, TPI90, Slope45, MPB90, HLI, FM100, FM1000	11,986	0.639
Rampage	Elev, TPI45, Slope90, MPB, HLI, FM100, FM1000	21,287	0.598
Red Eagle	Elev, TPI45, Slope90, MPB90, HLI, FM100, FM1000	16,668	0.586

Note: the numbers after the variables TPI, Slope, MPB and HLI refer to the scale (moving window size) of the variable that resulted in the best model fit.

Table 5.4. The standardized the regression coefficients for each fire model based on predictor variables used in Table 5.3.**P-value* is significant at 0.05 or lower.

Fire	**Elevation**	**TPI**	**HLI**	**Slope**	**FM100**	**FM1000**	**MPB**
Red Bench	0.1457*	0.0451*	0.0854*	0.1535*	0.2493*	0.2165*	0.1761*
Adair-Howling	0.0599	-0.0217*	0.1674*	0.0533*	0.0287	-0.0832*	0.1784*
Anaconda	0.3718*	0.06*	0.1121*	-0.0112	-0.0583*	-0.0079	0.1003*
Parke Peak	0.2522*	0.0171	0.0535	-0.0387	-0.0637	0.0116	0.2315*
Moose	0.4994*	0.0458*	0.0607*	-0.0109	-0.0206*	-0.0493*	0.2761*
Wolf Gun	0.006	0.0898*	0.1899*	0.0982*	-0.1369*	0.1386*	0.1656*
Wedge Canyon	0.4025*	0.0321*	0.0934*	0.0245	0.0228	-0.055*	0.09*
Robert	-0.0639*	0.037*	0.1111*	0.1494*	-0.0065	-0.0458*	0.0285*
Middle Fork Complex	0.246*	0.088*	0.1288*	0.1057*	0.0077	-0.0917*	-0.0199
Rampage	0.0386	0.0314*	0.0414*	-0.0796*	-0.0005	-0.0434	0.0231*
Red Eagle	0.1841*	0.0699*	0.0659*	-0.2143*	-0.1391*	0.1054*	0.1059*

5.9 FIGURES

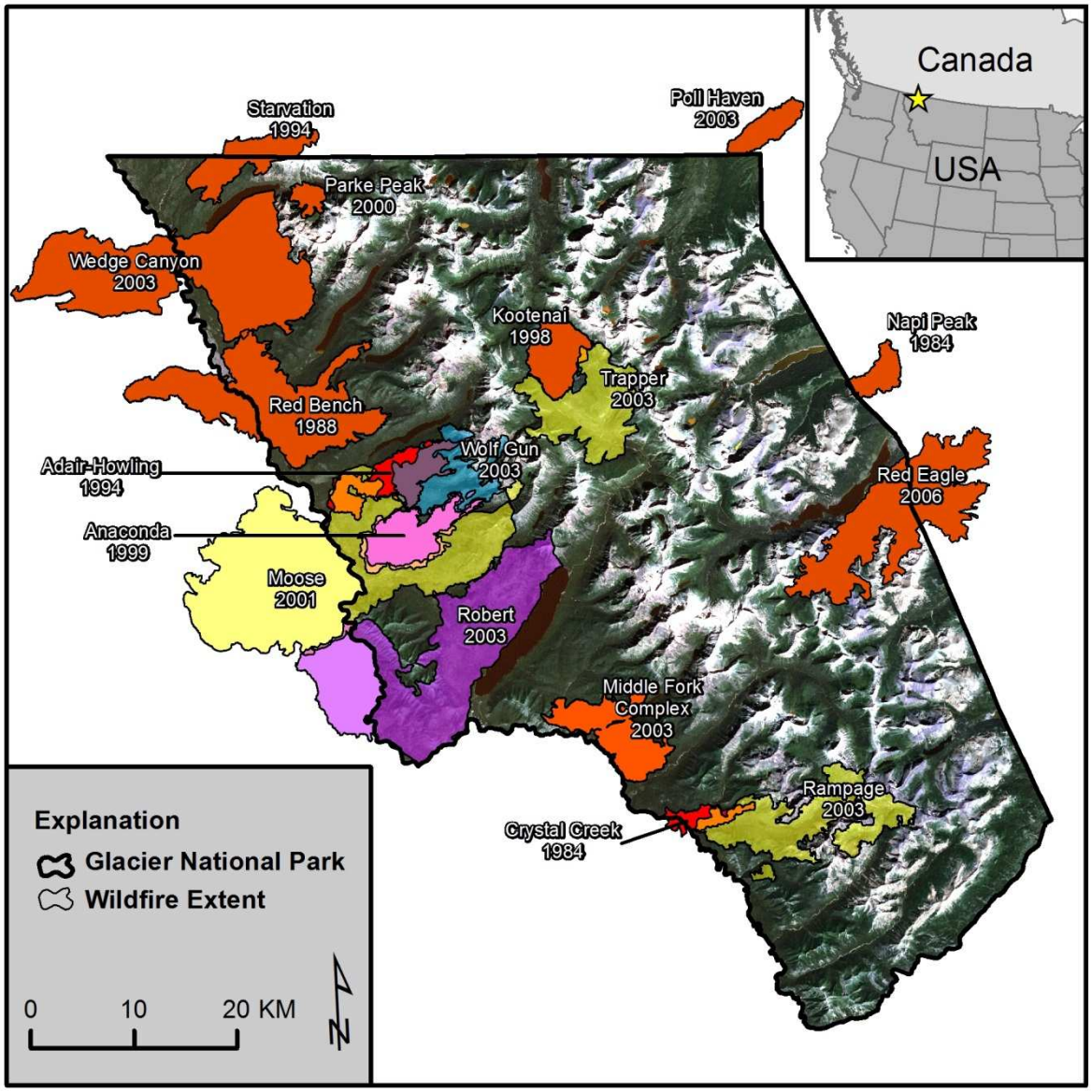
Canada
USA
Starvation 1994
Poll Haven 2003
Parke Peak 2000
Wedge Canyon 2003
Kootenai 1998
Napi Peak 1984
Trapper 2003
Red Bench 1988
Wolf Gun 2003
Adair-Howling 1994
Red Eagle 2006
Anaconda 1999
Moose 2001
Robert 2003
Middle Fork Complex 2003
Rampage 2003
Crystal Creek 1984
Explanation
Glacier National Park
Wildfire Extent
0
10
20 KM
N

Figure 5.1. Location and extent of fires in the study area.

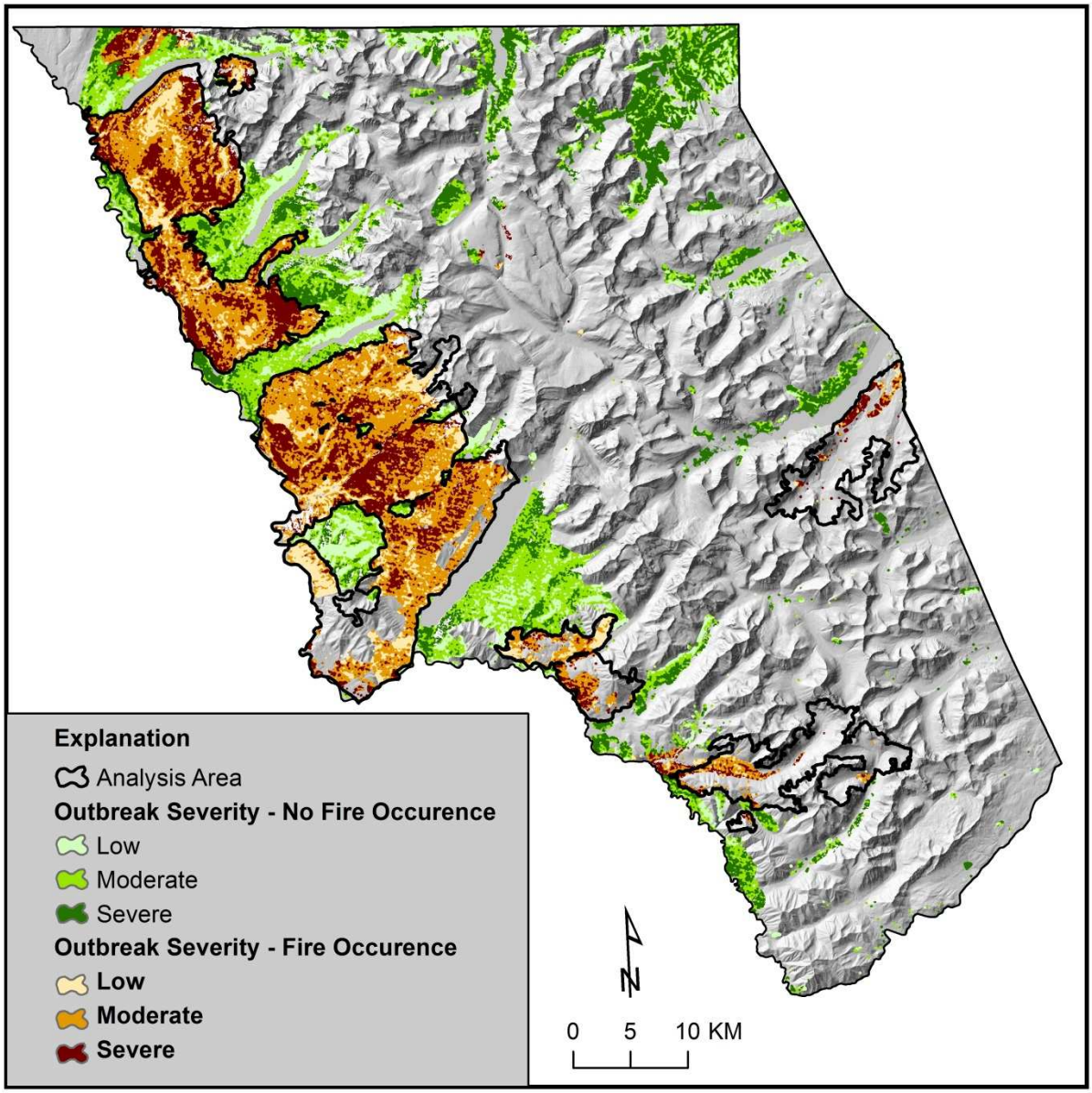

Figure 5.2. Location of project analysis area. The location and extent of the historic mountain pine beetle disturbance (Assal et al., 2014) classified into three severity levels for areas that later burned (orange color ramp) and did not burn (green color ramp) in subsequent wildfire.

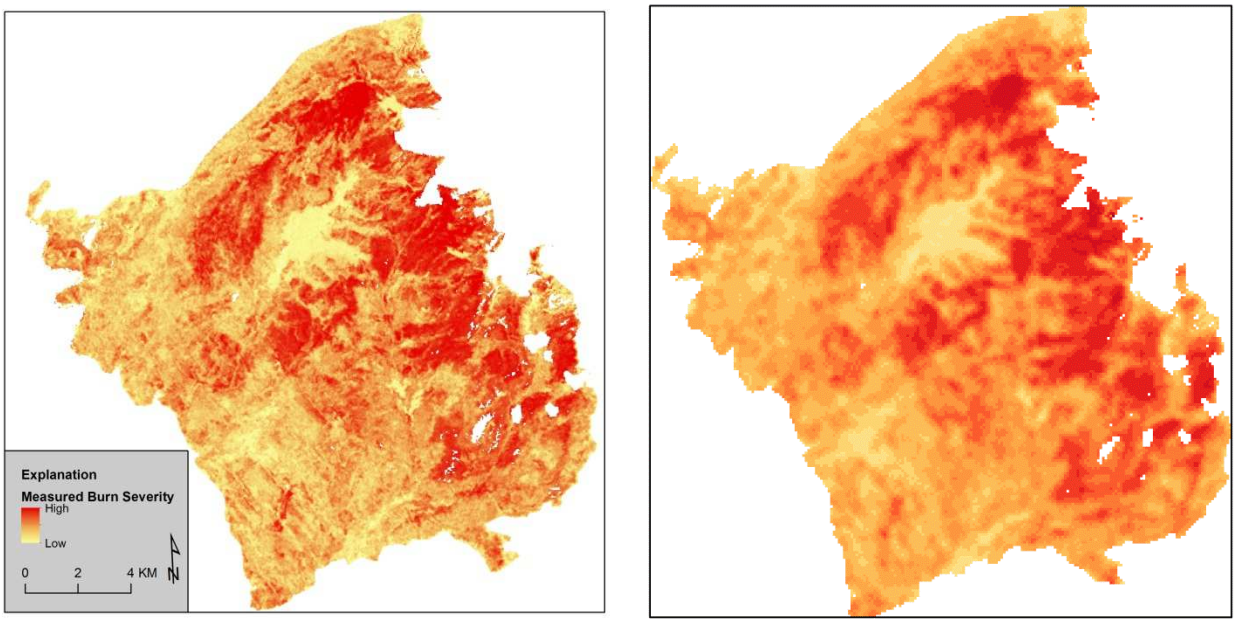

Figure 5.3. Comparison between measured and predicted burn severity. Example of measured (left) and predicted (right) burn severity in the Wedge Canyon fire. Note: measured burn severity from RdNBR (30 m resolution); predicted burn severity from the SAR model (60 m resolution).

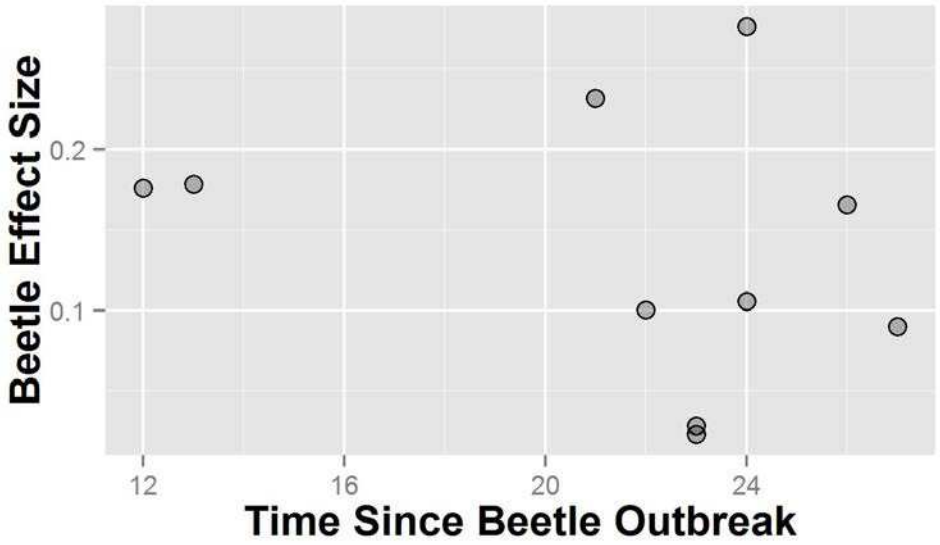

Figure 5.4. The relationship between the effect size of beetle severity and time since outbreak for each fire (*n*=10).

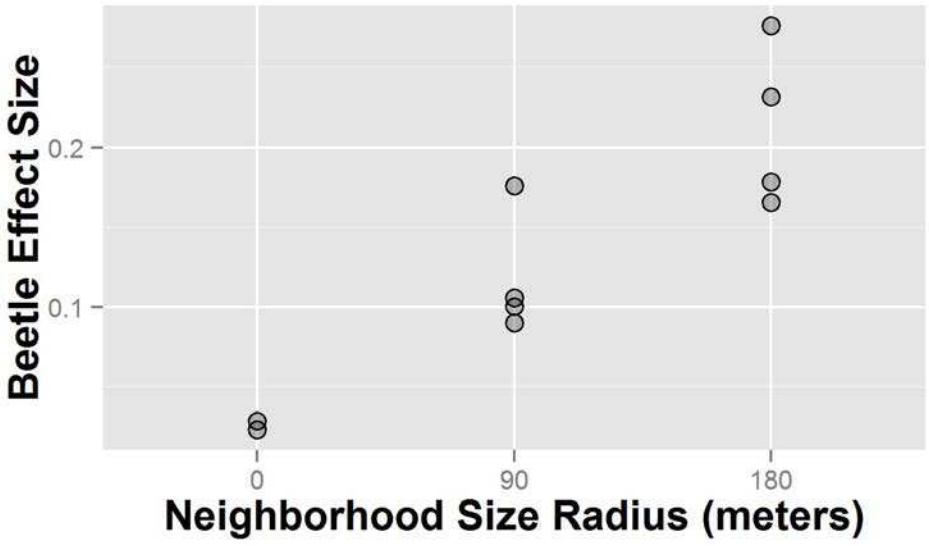

Figure 5.5. The relationship between the effect size of beetle severity and the scale of beetle severity used in each model (*n*=10).

LITERATURE CITED

Abatzoglou, J.T., 2013. Development of gridded surface meteorological data for ecological applications and modelling. Int. J. Climatol. 33, 121–131. doi:10.1002/joc.3413

Agee, J.K., 1993. Fire ecology of Pacific Northwest foersts. Island Press, Washington D.C.

Assal, T.J., Sibold, J., Reich, R., 2014. Modeling a Historical Mountain Pine Beetle Outbreak Using Landsat MSS and Multiple Lines of Evidence. Remote Sens. Environ. 155, 275–288. doi:10.1016/j.rse.2014.09.002

Bebi, P., Kulakowski, D., Veblen, T.T., 2003. Interactions between Fire and Spruce Beetles in a Subalpine Rocky Mountain Forest Landscape. Ecology 84, 362–371.

Bentz, B.J., Régnière, J., Fettig, C.J., Hansen, E.M., Hayes, J.L., Hicke, J.A., Kelsey, R.G., Negrón, J.F., Seybold, S.J., 2010. Climate Change and Bark Beetles of the Western United States and Canada: Direct and Indirect Effects. Bioscience 60, 602–613. doi:10.1525/bio.2010.60.8.6

Bigler, C., Kulakowski, D., Veblen, T.T., 2005. Multiple Disturbance Interactions and Drought Influence Fire Severity in Rocky Mountain Subalpine Forests. Ecology 86, 3018–3029. doi:10.1890/05-0011

Bradstock, R.A., Hammill, K.A., Collins, L., Price, O., 2010. Effects of weather, fuel and terrain on fire severity in topographically diverse landscapes of south-eastern Australia. Landsc. Ecol. 25, 607–619. doi:10.1007/s10980-009-9443-8

Bring, J., 1994. How to Standardize Regression Coefficients. Am. Stat. 48, 209–213.

Collins, B.M., Kelly, M., van Wagtendonk, J.W., Stephens, S.L., 2007. Spatial patterns of large natural fires in Sierra Nevada wilderness areas. Landsc. Ecol. 22, 545–557. doi:10.1007/s10980-006-9047-5

Cressie, N.A., 1993. Statistics for Spatial Data, Revised. ed. Wiley-Interscience, New York, NY. doi:978-0471002550

Cyr, D., Gauthier, S., Bergeron, Y., 2007. Scale-dependent determinants of heterogeneity in fire frequency in a coniferous boreal forest of eastern Canada. Landsc. Ecol. 22, 1325–1339. doi:10.1007/s10980-007-9109-3

Dillon, G.K., Holden, Z.A., Morgan, P., Crimmins, M.A., Heyerdahl, E.K., Luce, C.H., 2011. Both topography and climate affected forest and woodland burn severity in two regions of the western US, 1984 to 2006. Ecosphere 2, 1–33. doi:10.1890/ES11-00271.1

Duffy, P.A., Epting, J., Graham, J.M., Rupp, T.S., Mcguire, A.D., 2007. Analysis of Alaskan burn severity patterns using remotely sensed data. Int. J. Wildl. Fire 16, 277–284.

Eidenshink, J., Schwind, B., Brewer, K., Zhu, Z.-L., Quayle, B., Howard, S., 2007. A Project for Monitoring Trends in Burn Severity. Fire Ecol. 3, 3–21.

Falk, D.A., Miller, C., McKenzie, D., Black, A.E., 2007. Cross-scale analysis of fire regimes. Ecosystems 10, 809–823. doi:10.1007/s10021-007-9070-7

Finney, M.A., McHugh, C.W., Grenfell, I.C., 2005. Stand- and landscape-level effects of prescribed burning on two Arizona wildfires. Can. J. For. Res. 35, 1714–1722. doi:10.1139/x05-090

Haining, R.P., 1990. Spatial data analysis in the social and environmental sciences. Cambridge University Press, Cambridge, United Kingdon.

Harvey, B.J., Donato, D.C., Turner, M.G., 2014. Recent mountain pine beetle outbreaks, wildfire severity, and postfire tree regeneration in the US Northern Rockies. Proc. Natl. Acad. Sci. 111. doi:10.1073/pnas.1411346111

Hicke, J.A., Johnson, M.C., Hayes, J.L., Preisler, H.K., 2012. Effects of bark beetle-caused tree mortality on wildfire. For. Ecol. Manage. 271, 81–90. doi:10.1016/j.foreco.2012.02.005

Holden, Z.A., Morgan, P., Evans, J.S., 2009. A predictive model of burn severity based on 20-year satellite-inferred burn severity data in a large southwestern US wilderness area. For. Ecol. Manage. 258, 2399–2406. doi:10.1016/j.foreco.2009.08.017

IPCC Third Assessment Report, 2001.

Keeley, J.E., 2009. Fire intensity, fire severity and burn severity: a brief review and suggested usage. Int. J. Wildl. Fire 18, 116. doi:10.1071/WF07049

Key, C., Benson, N., 2006. Landscape assessment: ground measure of severity, the Composite Burn Index, and remote sensing of severity, the Normalized Burn Ratio. In “FIREMON: Fire Effects Monitoring and Inventory System”. (Eds DC Lutes, RE Keane, JF Caratti, CH Key, NC Benson, S Su. Fort Collins, CO.

Kissling, W.D., Carl, G., 2008. Spatial autocorrelation and the selection of simultaneous autoregressive models. Glob. Ecol. Biogeogr. 17, 59–71. doi:10.1111/j.1466-8238.2007.00334.x

Kulakowski, D., Jarvis, D., 2011. The influence of mountain pine beetle outbreaks and drought on severe wildfires in northwestern Colorado and southern Wyoming: A look at the past century. For. Ecol. Manage. 262, 1686–1696. doi:10.1016/j.foreco.2011.07.016

Kulakowski, D., Veblen, T.T., 2007. Effect of prior disturbances on the extent and severity of wildfire in Colorado subalpine forests. Ecology 88, 759–769.

Lee, S.W., Lee, M.B., Lee, Y.G., Won, M.S., Kim, J.J., Hong, S.K., 2009. Relationship between landscape structure and burn severity at the landscape and class levels in Samchuck, South Korea. For. Ecol. Manage. 258, 1594–1604. doi:10.1016/j.foreco.2009.07.017

Levin, S.A., 1992. The Problem of Pattern and Scale in Ecology. Ecology 73, 1943–1967.

Littell, J.S., McKenzie, D., Peterson, D.L., Westerling, A.L., 2009. Climate and wildfire area burned in western U.S. ecoprovinces, 1916-2003. Ecol. Appl. 19, 1003–1021.

Logan, J.A., Régnière, J., Powell, J.A., 2003. Assessing the impacts of global warming on forest pest dynamics. Front. Ecol. Environ. 1, 130–137.

Lutz, J.A., van Wagtendonk, J.W., Thode, A.E., Miller, J.D., Franklin, J.F., 2009. Climate, lightning ignitions, and fire severity in Yosemite National Park, California, USA. Int. J. Wildl. Fire 18, 765–774. doi:10.1071/WF08117

Lynch, H.J., Renkin, R.A., Crabtree, R.L., Moorcroft, P.R., 2007. The Influence of Previous Mountain Pine Beetle (Dendroctonus ponderosae) Activity on the 1988 Yellowstone Fires. Ecosystems 9, 1318–1327. doi:10.1007/s10021-006-0173-3

McCune, B., Keon, D., 2002. Equations for potential annual direct incident radiation and heat load. J. Veg. Sci. 13, 603–606.

Meddens, A.J.H., Hicke, J.A., Ferguson, C.A., 2012. Spatiotemporal patterns of observed bark beetle-caused tree mortality in British Columbia and the western United States. Ecol. Appl. 22, 1876–1891.

Meigs, G.W., Kennedy, R.E., Cohen, W.B., 2011. A Landsat time series approach to characterize bark beetle and defoliator impacts on tree mortality and surface fuels in conifer forests. Remote Sens. Environ. 115, 3707–3718. doi:10.1016/j.rse.2011.09.009

Miller, J.D., Thode, A.E., 2007. Quantifying burn severity in a heterogeneous landscape with a relative version of the delta Normalized Burn Ratio (dNBR). Remote Sens. Environ. 109, 66–80. doi:10.1016/j.rse.2006.12.006

Paine, R.T., Tegner, M.J., Johnson, E.A., 1998. Compounded Perturbations Yield Ecological Surprises. Ecosystems 1, 535–545. doi:10.1007/s100219900049

Parisien, M.-A., Snetsinger, S., Greenberg, J.A., Nelson, C.R., Schoennagel, T., Dobrowski, S.Z., Moritz, M.A., 2012. Spatial variability in wildfire probability across the western United States. Int. J. Wildl. Fire 21, 313. doi:10.1071/WF11044

Parks, S.A., Parisien, M.A., Miller, C., 2011. Multi-scale evaluation of the environmental controls on burn probability in a southern Sierra Nevada landscape. Int. J. Wildl. Fire 20, 815–828. doi:10.1071/WF10051

Prichard, S.J., Kennedy, M.C., 2014. Fuel treatments and landform modify landscape patterns of burn severity in an extreme fire event. Ecol. Appl. 24, 571–590.

R Development Core Team, 2013. R: A language and environment for statistical computing.

Raffa, K.F., Aukema, B.H., Bentz, B.J., Carroll, A.L., Hicke, J.A., Turner, M.G., Romme, W.H., 2008. Cross-scale Drivers of Natural Disturbances Prone to Anthropogenic Amplification: The Dynamics of Bark Beetle Eruptions. Bioscience 58, 501. doi:10.1641/B580607

Rollins, M.G., Morgan, P., Swetnam, T., 2002. Landscape-scale controls over 20th century fire occurrence in two large Rocky Mountain (USA) wilderness areas. Landsc. Ecol. 17, 539–557. doi:10.1023/A:1021584519109

Schoennagel, T., Veblen, T.T., Negron, J.F., Smith, J.M., 2012. Effects of mountain pine beetle on fuels and expected fire behavior in lodgepole pine forests, Colorado, USA. PLoS One 7, e30002. doi:10.1371/journal.pone.0030002

Sibold, J.S., Veblen, T.T., Chipko, K., Lawson, L., Mathis, E., Scott, J., 2007. Influences of Secondary Disturbances on Lodgepole Pine. Ecol. Appl. 17, 1638–1655.

Simard, M., Romme, W.H., Griffin, J.M., Turner, M.G., 2011. Do mountain pine beetle outbreaks change the probability of active crown fire in lodgepole pine forests? Ecol. Monogr. 81, 3–24.

Thompson, J.R., Spies, T. a, Ganio, L.M., 2007. Reburn severity in managed and unmanaged vegetation in a large wildfire. Proc. Natl. Acad. Sci. U. S. A. 104, 10743–10748. doi:10.1073/pnas.0700229104

Turner, M.G., 2010. Disturbance and landscape dynamics in a changing world. Ecology 91, 2833–2849. doi:10.1080/03630242.2010.516702

Turner, M.G., Dale, V.H., 1998. Comparing Large, Infrequent Disturbances: What Have We Learned? Ecosystems 1, 493–496.

Turner, M.G., Romme, W.H., Gardner, R.H., 1999. Prefire Heterogeneity, Fire Severity, and Early Postfire Plant Reestablishment in Subalpine Forests of Yellowstone National Park, Wyoming. Int. J. Wildl. Fire 9, 21–36. doi:doi:10.1071/WF99003

Veblen, T.T., Hadley, K.S., Nel, E.M., Kitzberger, T., Reid, M., Villalba, R., 1994. Disturbance regime and disturbance interactions in a Rocky Mountain subalpine forest. J. Ecol. 82, 125–135.

Veblen, T.T., Hadley, K.S., Reid, M.S., 1991. Disturbance and Stand Development of a Colorado Subalpine Forest 18, 707–716.

Westerling, A.L., Hidalgo, H.G., Cayan, D.R., Swetnam, T.W., 2006. Warming and earlier spring increase western U.S. forest wildfire activity. Science (80-.). 313, 94094–3. doi:10.1126/science.1128834

Westerling, A.L., Turner, M.G., Smithwick, E.A.H., Romme, W.H., Ryan, M.G., 2011. Continued warming could transform Greater Yellowstone fire regimes by mid-21st century. Proc. Natl. Acad. Sci. 108, 13165–13170. doi:10.1073/pnas.1110199108

Wimberly, M.C., Cochrane, M.A., Baer, A.D., Pabst, K., 2009. Assessing fuel treatment effectiveness using satellite imagery and spatial statistics. Ecol. Appl. 19, 1377–1384.

Wu, Z., He, H.S., Bobryk, C.W., Liang, Y., 2014. Scale effects of vegetation and topography on burn severity under prevailing fire weather conditions in boreal forest landscapes of Northeastern China. Scand. J. For. Res. 29, 60–70. doi:10.1080/02827581.2013.861922

Wulder, M.A., Dymond, C., White, J.C., Leckie, D.G., Carroll, A.L., 2006. Surveying mountain pine beetle damage of forests: A review of remote sensing opportunities. For. Ecol. Manage. 221, 27–41.

CHAPTER 6: Synthesis

The overall goal of this dissertation was to investigate the ecological legacies of disturbance in two different ecosystems. A secondary objective of my research, data development, was motivated by a lack of available data which precluded ecological investigation of each disturbance. The findings of this research contribute new and detailed information applicable to both ecological theory and land management. I studied the effects of drought on deciduous and coniferous forest along a forest-shrubland ecotone in the southern portion of the Wyoming Basin. This study was undertaken because little is known about the baseline condition of forest in the area and specifically how drought affects forest in this topographically complex ecosystem. The results show that forests in the region have experienced high levels of drought related mortality over the last decade. Negative spectral trends were not consistent across forest type or distributed randomly across the study area. These patterns of long-term trends highlight areas of forest that are resistant, persistent and vulnerable to severe drought. In the second thread of my dissertation, I assessed the influence of an historic mountain pine beetle outbreak on wildfire in Glacier National Park. I addressed the current debate in disturbance ecology regarding linkages between beetle outbreak and the effect on wildfire. Specifically, I determined if beetle severity had a measureable influence on burn severity in the ensuing decades after the outbreak. Although a number of factors contribute to burn severity, the results indicated that beetle severity was positively correlated to burn severity in the majority of the fires I analyzed.

In chapter two I found highly dissected forest cover in the Little Mountain Ecosystem was best predicted using a combination of fine-scale topographic and spectral variables. Independent predictive models of the two major forest functional types were highly accurate and showed little overlap between the cover derived from the two models. The models were integrated into a

synthesis map with an overall classification accuracy of 87%, that identified 61.7 km^2 of forest (56% coniferous, 44% deciduous). The results suggest my method adequately captures the functional type, size, and distribution pattern of forest cover in this spatially heterogeneous landscape. Furthermore, I considered spatial autocorrelation in our framework, which is often overlooked in species distribution modeling. Consideration of plant physiology and species traits, such as phenology, illuminates the ecological context of biophysical variables that were captured with leaf-on and leaf-off SPOT imagery. The study addresses the important management need of accurate cover maps of deciduous and coniferous forest characteristic of this region. To explore the utility of my findings, I compared my results with basic metrics of forest cover derived from several regional land cover datasets (Appendix A) and found high levels of disagreement between all datasets. The total area of forest type was generally overestimated by regional products, and my results identify the largest number of patches of each forest cover type and the smallest mean patch size. This has large implications on basic management questions regarding the extent and juxtaposition of forest cover in the study area. Ecological studies requiring highly accurate forest cover and plant functional type should consider using multi-temporal SPOT imagery to derive regionally specific land cover maps. Furthermore, this framework offers a powerful alternative to traditional image classification and utilizes open access aerial photos and satellite data. In this way, it is transferable to highly heterogeneous ecosystems to develop critical baseline tree cover data that can be updated at regular intervals to monitor the effects of disturbance and long-term ecosystem dynamics.

In my study of drought effects, I found coniferous and deciduous forests in the southern portion of the Wyoming Basin ecoregion have experienced high levels of drought related mortality over the last decade. I analyzed multiple satellite derived indices and found the

Normalized Difference Vegetation Index best reflected conditions on the ground, most notably plant area index and canopy gap fraction of a plot. I used these empirical relationships to measure trends over time in moisture content as a proxy for canopy cover. Dense canopies have greater moisture content than sparse, open canopies and the moisture content will reflect changes in forest canopy cover over time. During the study period, 25% of the forested area experienced a statistically significant negative trend in canopy moisture, compared to less than 10% in a positive trend. The cumulative negative trend began in 2000 and increased with cumulative drought years. I found negative trends were not consistent across forest functional type as a larger amount of coniferous forest was impacted by negative trends than deciduous forest. Negative trends were not randomly distributed across the landscape as southern aspects were least likely to exhibit a negative trend and north aspects most prevalent. Using field collected information I concluded plots with a negative trend had a lower live density, and higher amounts of standing dead and down trees compared to plots with no trend. My analysis identifies spatially explicit patterns of long-term trends anchored with ground based evidence to highlight areas of forest that are resistant, persistent or vulnerable to severe drought. The results provide a much needed long-term perspective to local managers and offers an avenue to assess fine-scale trends in the forest-shrubland matrix. These results can be used to test hypotheses with regard to resistance, persistence and vulnerability of forests to drought and give insight behind the mechanisms of mortality. Many global and regional climate models do not currently take terrain into account, and my results show that bottom-up topographic controls are important during climatically driven drought. I believe this research gives insight to local managers where broad climate models do not: a cost effective avenue to delineate local areas that could benefit from targeted management.

The analysis in chapter four sought to overcome a data limitation that precluded deeper investigation of disturbance linkages. The lack of spatially explicit data on this disturbance was both a major data gap and a critical research challenge in that wildfire fire had removed some of the evidence from the landscape. Using multiple lines of evidence, I developed a model of forest canopy mortality as a proxy for beetle outbreak severity. I mapped tree mortality in aerial photos and scaled-up the information to a time series of satellite images in order to track the beetle-induced changes over time. I found a generalized least squares (GLS) model that utilized a time series of the Normalized Difference Vegetation Index and Green band best described the large-scale variability of canopy change associated with mortality from outbreak. The GLS model was used to address spatial autocorrelation in the generalized linear model. I used the residuals of the GLS model to account for the small-scale variation in the data using binary regression trees. The combined model explained over 80% of the variability in the data and was used to create a continuous surface of beetle severity. The model identifies a gradient of mortality on the landscape using topographic variables and changes in spectral reflectance over time that confirms the outbreak was not homogenous across the landscape. My approach is of interest to the spatial ecology community because it demonstrates the value of Landsat MSS data to extend the moderate resolution imagery record back to the early 1970s. Given the availability of these data sources, the characterization of recent events will afford investigators a platform for future research of historical forest disturbance that would be beneficial to the field of forest ecology.

In the final analysis, I found that beetle severity was positively correlated to burn severity in 10 of the 11 fires I analyzed. I used sequential autoregression (SAR) to obtain accurate estimates of model parameters given the high level of spatial autocorrelation associated with wildfire. I produced a model of predicted burn severity for each of the 11 fires using the SAR

modeling approach and variables known to influence fire severity. The models captured spatial patterns of high and low burn severity that are visibly similar to measured values and explained between 54% and 80% of the variability in the burn severity data. I evaluated the relationship at multiple spatial scales and determined the influence of the surrounding neighborhood for a given variable was dependant on conditions associated with each fire, although broad trends emerged. Elevation at local scales was a significant predictor in most models and typically had a large positive effect on burn severity. Areas located between mid-slope and the top of slope were more strongly correlated with higher levels of burn severity compared to valley bottoms. Locations in the study area with a higher heat load experienced higher burn severity. Fuel moisture showed mixed effects which were likely due to dry conditions across the study area at the time of fire and the coarse resolution of the data. Our results suggest the change in stand structure and composition associated with beetle outbreak severity had an effect on burn severity. This was likely due to the accumulation of ladder fuels in areas with high amounts of beetle activity. I considered several additional hypotheses, and found the effect of beetle severity on burn severity might be contingent on the patterns of severity at different scales. Fires where beetle severity was best predicted at broad scales tended to have a larger effect size compared to fires where beetle severity was best predicted at local scales. This suggests spatially continuous biomass and fuel conditions compared across broad scales can contribute to higher burn severity compared to areas with high heterogeneity of fuels. This study is unique because I included a continuous data set of beetle severity (developed in chapter four) and focused on the consequences of actual, instead of potential events. These results can help managers prioritize monitoring or restoration efforts. The spatial arrangement of the beetle outbreak and subsequent wildfire presented a unique opportunity to consider numerous wildfires as opposed to a single fire event. These

findings are of interest to the broader science community because observations are drawn from multiple fires which broaden the perspective on these compounded disturbances. The long-term perspective of our study shows that ecological legacies of prior high severity disturbance may continue to influence subsequent disturbance for many years after the initial event. This can provide insight on future disturbance interactions associated with the recent mountain pine beetle outbreak as much of the landscape impacted by the recent outbreak will enter the old mountain pine beetle phase in coming decades.

Collectively, the findings of my dissertation contribute new insight into the influence of several major disturbance types. The research in the Little Mountain Ecosystem advances our ability to measure disparate forest cover across the shrubland ecotone that might be inaccurately described by regional data. Results of the trend research contribute to the growing body of literature which indicates climate not only impacts forest demographics through extreme events, but also by less conspicuous events that might have cumulative impacts over a decadal timeframe. I developed a new method for reconstructing historic bark beetle outbreaks using multiple lines of evidence to characterize the severity of a disturbance that we did not know much about. Finally, my research contributes to our understanding of linkages between beetle outbreak and the ecological consequences of subsequent fire. Although many factors must be considered, my results indicate that beetle outbreaks have ecological legacies on ensuing forest disturbance for some time after the initial outbreak.

APPENDIX A: Supplementary Material for Mapping Forest Functional Type in a Forest-Shrubland Ecotone (Chapter 2)

Chapter 2 was published by the journal *Remote Sensing Letters*. However, due to space limitations of the journal I had to omit one of the objectives of this study which was to compare the results of our modeling framework with regional land cover data sets. I believe this comparison adds value to our analysis and is informative to readers so I chose to include it here.

A.1 METHODS

In order to compare our map with regional data, we reclassified NLCD, LANDFIRE and ReGAP data into deciduous forest, coniferous forest and non-forest (Tables A1-A3). We identified contiguous patches of forest cover using the same procedure as above. We calculated basic landscape metrics (total cover area, mean patch size and number of patches) to provide a simple, quantitative assessment of how each product characterized the forest cover of the study area.

A.2 RESULTS

The landscape metrics calculated from the regional data sources revealed high levels of disagreement between land cover products. LANDFIRE and ReGAP reported the most total area of deciduous forest with 44.3 km^2 and 41.7 km^2 respectively (Table A4). However, the LANDFIRE map has over five times the number of patches as the ReGAP map, resulting in a much smaller mean patch size. NLCD has the smallest amount of deciduous forest and the fewest patches. Our synthesis map had the most deciduous patches and the smallest mean patch size, with a total area between the high and low range of regional map products. Conversely, NLCD identifies the most coniferous forest in the study area (Table A4) with a large average patch size (0.073 km^2). ReGAP and our map report similar total area (38.8 km^2 and 34.4 km^2

respectively) of coniferous forest. However, our synthesis map has nearly five times the number of patches and therefore a much smaller mean patch size. LANDFIRE reports far less coniferous forest, yet a high number of patches.

A.3 DISCUSSION

Our results show that fine-scale mapping is necessary to capture the spatial heterogeneity of deciduous and coniferous woodlands characteristic of this ecoregion (Figure A1B). Figure A1 depicts a representative area on Little Mountain which highlights the small size of isolated forest patches of the study area (Figure A1A). The LANDFIRE map overestimates deciduous forest cover and contains many single pixels, inflating the number of patches (Figure A1C). The NLCD map underestimates deciduous forest (Figure A1D), whereas the ReGAP map overestimates deciduous forest at the expense of non-forest (Figure A1E). Native LANDFIRE data classifies significant portions of coniferous forest as shrubland, resulting in lower total area (Table A4, Figure A1C). NLCD reports a large area of coniferous forest, in part because it is the only product that does not differentiate between montane conifer species and less dense conifer woodland at lower elevations (Table A4).

The results of the land cover comparison highlight the differences in land cover data that are currently available at regional scales (Figure A1C-E, Table A4). We acknowledge our comparison is biased since our model utilized finer scale data. It is not our intent to criticize regional land cover data products, rather we identify the differences in localized areas that exhibit high levels of spatial heterogeneity. Regional land cover products were developed with more coarse data (e.g. 30 m Landsat) at much greater spatial extents than our modeling and mapping process. However, in our highly heterogeneous study area, there is little agreement between the land cover data. Our methodology is capable of detecting both total forest cover as

well as the landscape juxtaposition of forest patches that are representative of this area (Figure A1B). We conclude that ecological studies requiring highly accurate forest cover and plant functional type should consider using multi-temporal SPOT imagery to derive regionally specific land cover maps.

Table A1. LANDFIRE reclassification crosswalk table. Version LF_1.3.0 (2012) was used in the analysis.

Map Class	LANDFIRE Existing Vegetation Type Name (EVT Code)
Deciduous Forest	Rocky Mountain Aspen Forest and Woodland (2011) Rocky Mountain Gambel Oak-Mixed Montane Shrubland (2107)
Coniferous Forest	Northern Rocky Mountain Subalpine Woodland and Parkland (2046) Rocky Mountain Lodgepole Pine Forest (2050) Southern Rocky Mountain Dry-Mesic Montane Mixed Conifer Forest and Woodland (2051) Southern Rocky Mountain Ponderosa Pine Woodland (2054) Rocky Mountain Subalpine Dry-Mesic Spruce-Fir Forest and Woodland (2055) Middle Rocky Mountain Montane Douglas-fir Forest and Woodland (2166) Rocky Mountain Poor-Site Lodgepole Pine Forest (2167)

Table A2. NLCD reclassification crosswalk table. Version NLCD 2011 was used in the analysis.

Map Class	NLCD Classification Description (Class Value)
Deciduous Forest	Deciduous Forest (41) Mixed Forest (43)
Coniferous Forest	Evergreen Forest (42)

Table A3. ReGAP reclassification crosswalk table. Version 2 ReGAP data (2011) was used in the analysis.

Map Class	ReGAP Ecological System Description (Level 3 Code)
Deciduous Forest	Rocky Mountain Aspen Forest and Woodland (4111)
Coniferous Forest	Inter-Mountain Basins Aspen-Mixed Conifer Forest and Woodland (4324) Northern Rocky Mountain Dry-Mesic Montane Mixed Conifer Forest (4524) Rocky Mountain Lodgepole Pine Forest (4527) Southern Rocky Mountain Dry-Mesic Montane Mixed Conifer Forest and Woodland (4528) Rocky Mountain Subalpine Dry-Mesic Spruce-Fir Forest and Woodland (4531) Middle Rocky Mountain Montane Douglas-fir Forest and Woodland (4543) Northern Rocky Mountain Mesic Montane Mixed Conifer Forest (4609)

Table A4. Results of the land cover comparison between the synthesis map and regional data products.

Product	Deciduous Forest			Coniferous Forest		
	Total Area (km^2)	**No. of Patches**	**Mean Patch Size (km^2)**	**Total Area (km^2)**	**No. of Patches**	**Mean Patch Size (km^2)**
Synthesis Map	27.2	7110	0.004	34.5	2362	0.015
LANDFIRE	44.3	6518	0.007	13.7	2001	0.007
NLCD	15.4	812	0.019	86.7	1192	0.073
ReGAP	41.7	1223	0.034	38.8	496	0.078

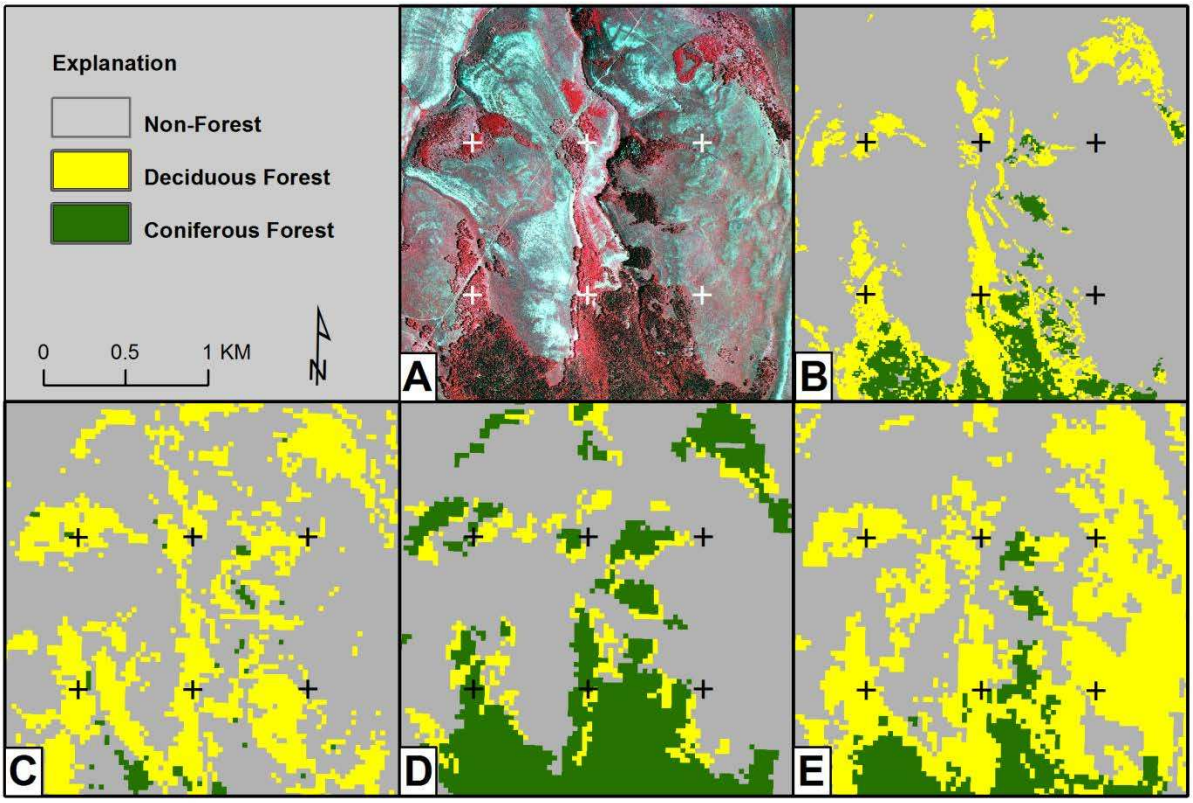

Figure A1. Comparison of forest type maps derived from each data source of a representative area of the landscape on Little Mountain. Note: each map panel is displayed at the same scale; tick marks are spaced at 30 second intervals. (A) 2009 color-infrared aerial photo (National Agriculture Imagery Program). Dark red/black hues indicate coniferous forest; red hues indicate deciduous forest; grey/light red/blue hues represent non-forest, (B) USGS synthesis map, (C) LANDFIRE map, (D) NLCD map, and (E) ReGAP map.

APPENDIX B: Supplementary Material for Modeling a Historical Mountain Pine Beetle Outbreak Using Landsat MSS and Multiple Lines of Evidence (Chapter 4)

This appendix contains information on the geometric correction, calibration, atmospheric correction and image normalization procedures applied to the Landsat MSS imagery used in the analysis in Chapter 4.

B.1 GEOMETRIC CORRECTION

Twenty GCPs were established to compare the spatial accuracy between the 2009 NAIP photo and a 2010 Landsat Thematic Mapper (TM) image of the study area. We used the AutoSync module in Erdas Imagine to georectify the image to the 2009 photo (RMSE < 0.5 pixel). The process was repeated to georectify each of the nine Landsat MSS images to the 2010 TM image. Each MSS image had an RMSE < 0.4 pixel and was resampled to 30 m during the georectification process using a nearest neighbor transformation to minimize geometric offsets in the image stack (Goodwin et al., 2008). However, the spatial resolution of the data is still considered 60 m.

B.2 CALIBRATION

Radiometric calibration of imagery is an important step for creating a consistent, high-quality temporal image series. We converted the four bands of each image from Digital Numbers to absolute units of at-sensor spectral radiance using the formula (Chander et al., 2009):

$$L_\lambda = (LMAX_\lambda - LMIN_\lambda / Q_{calmax} - Q_{calmin}) * (Q_{cal} - Q_{calmin}) + LMIN_\lambda \quad (1)$$

where

L_λ = Spectral radiance at the sensor's aperture [$W/(m^2\ sr\ \mu m)$]

Q_{cal} = Quantized calibrated pixel value [DN]

Q_{calmin} = Minimum quantized calibrated pixel value corresponding to $LMIN_\lambda$ [DN]

Q_{calmax} = Maximum quantized calibrated pixel value corresponding to $LMAX_\lambda$ [DN]

$LMIN_\lambda$ = Spectral at-sensor radiance that is scaled to Qcalmin [W/(m^2 sr µm)]

$LMAX_\lambda$ = Spectral at-sensor radiance that is scaled to Qcalmax [W/(m^2 sr µm)]

The spectral radiance values were converted to Top-Of-Atmosphere (TOA) reflectance to account for differences in sensor and viewing angle using the formula (Chander et al., 2009):

$$\rho_\lambda = \pi * L_\lambda * d^2 / ESUN_\lambda * \cos\theta_s \quad (2)$$

where

ρ_λ = Planetary TOA reflectance [unitless]

π = Mathematical constant equal to ~3.14159 [unitless]

L_λ = Spectral radiance at the sensor's aperture [W/(m^2 sr µm)]

d = Earth-Sun distance [astronomical units]

$ESUN_\lambda$ = Mean exoatmospheric solar irradiance [W/(m^2 µm)]

θ_s = Solar zenith angle [degrees]

Inputs used in the formulas above were supplied by the header file (.MTL) for each scene and Chander et al. (2009).

B.3 ATMOSPHERIC CORRECTION

Each image was snapped to the reference image (1979 image) in ArcGIS to ensure each 30 m pixel for every year was exactly congruent with the master image. An absolute normalization was applied to the 1979 master image using a dark object subtraction technique (Chavez 1988). The minimum pixel value of each band (recorded in at least 1000 pixels), representing deep glacial lakes and shadows, was identified (Chavez, 1996). The theoretical

radiance of a dark object is assumed to have 1% reflectance (Chavez, 1996; Moran et al., 1992) so the minimum identified pixel value was multiplied by 0.99 to generate the presumed dark object of each image band.

B.4 RELATIVE NORMALIZATION

The remaining images were normalized to the master image using a relative normalization technique. This procedure removes non-surface noise and improves the temporal homogeneity between images so that spectral change associated with surface phenomena can be detected (Yuan and Elvidge, 1996). Psuedo-Invariant Features (PIFs) are targets in each image that are not expected to change between image dates (Schott et al., 1988). Relative normalization is based on the assumption that a linear relationship exists between the reference image and the image to be normalized (Schott et al., 1988; Yuan and Elvidge, 1996). This technique has been applied in many studies to analyze vegetation change (Bradley and Fleishman, 2008; Schroeder et al., 2006; Vicente-Serrano et al., 2008). We identified 60 PIFs that encompassed a range of pseudo-invariant reflectance values in each band. Each PIF was 32,400 m^2 in size; equivalent to a 3x3 block of 60 m Landsat MSS pixels. The mean of the reflectance values at these sites were used to fit an ordinary least squares regression model between the image to be normalized for each year and the reference image for each of the four bands. We tested the residuals for spatial autocorrelation using the Moran's I statistic and the Likelihood Ratio Test (Legendre and Fortin, 1989). Inverse distance was used to define the neighborhood structure of the spatial weights matrix. If spatial autocorrelation was detected, a spatially autoregressive model was used to fit the data (Cressie, 1993). In all cases, the fit of lines used to spectrally align the images had R^2 values > 0.92. Statistical analysis was conducted using the r package (R Development Core Team, 2013) and the linear regression was applied to each image in Erdas Imagine.

LITERATURE CITED

Bradley, B.A., Fleishman, E., 2008. Relationships between expanding pinyon–juniper cover and topography in the central Great Basin, Nevada. J. Biogeogr. 35, 951–964. doi:10.1111/j.1365-2699.2007.01847.x

Chander, G., Markham, B.L., Helder, D.L., 2009. Remote Sensing of Environment Summary of current radiometric calibration coefficients for Landsat MSS , TM , ETM + , and EO-1 ALI sensors. Remote Sens. Environ. 113, 893–903. doi:10.1016/j.rse.2009.01.007

Chavez, P.S., 1996. Image-Based Atmospheric Corrections - Revisited and Improved. Photogramm. Eng. Remote Sens. 62, 1025–1036.

Chavez, P.S., 1988. An improved dark-object subtraction technique for atmospheric scattering correction of multispectral data. Remote Sens. Environ. 24, 459–479. doi:10.1016/0034-4257(88)90019-3

Cressie, N.A., 1993. Statistics for Spatial Data, Revised. ed. Wiley-Interscience, New York, NY. doi:978-0471002550

Goodwin, N.R., Coops, N.C., Wulder, M.A., Gillanders, S., Schroeder, T.A., Nelson, T., 2008. Estimation of insect infestation dynamics using a temporal sequence of Landsat data. Remote Sens. Environ. 112, 3680–3689. doi:10.1016/j.rse.2008.05.005

Legendre, P., Fortin, M., 1989. Spatial Pattern and Ecological Analysis. Vegetatio 80, 107–138.

Moran, M.S., Jackson, R.D., Slater, P.N., Teiuet, P.M., 1992. Evaluation of Simplified Procedures for Retrieval of Land Surface Reflectance Factors from Satellite Sensor Output. Remote Sens. Environ. 41, 169–184.

R Development Core Team, 2013. R: A language and environment for statistical computing.

Schott, J.R., Salvaggio, C., Volchok, W.J., 1988. Radiometric Scene Normalization Using Pseudoinvariant Features. Remote Sens. Environ. 26, 1–16.

Schroeder, T.A., Cohen, W.B., Song, C., Canty, M.J., Yang, Z., 2006. Radiometric correction of multi-temporal Landsat data for characterization of early successional forest patterns in western Oregon. Remote Sens. Environ. 103, 16 – 26. doi:10.1016/j.rse.2006.03.008

Vicente-Serrano, S., Perezcabello, F., Lasanta, T., 2008. Assessment of radiometric correction techniques in analyzing vegetation variability and change using time series of Landsat images. Remote Sens. Environ. 112, 3916–3934. doi:10.1016/j.rse.2008.06.011

Yuan, D., Elvidge, C.D., 1996. Comparison of relative radiometric normalization techniques. Photogramm. Remote Sens. 51, 117–126. doi:10.1016/0924-2716(96)00018-4

APPENDIX C: Supplementary Material for Investigation of Mountain Pine Beetle Outbreak and Burn Severity (Chapter 5)

This appendix contains tables of coefficients, standard errors and P values for the sequential autoregression (SAR) models for each fire analyzed in Chapter 5. The coefficients presented in this appendix are the unstandardized regression coefficients associated with the model for each fire. The regression coefficients presented in Table 5.4 have been standardized.

C.1 RESULTS

Table C1. Sequential autoregression models of burn severity (RdNBR) for the Red Bench fire.

Variable	β	SE	*P* value
Intercept	-1173.70	219.82	< 0.001
elev	0.35	0.10	< 0.001
tpi90	46.22	6.25	< 0.001
slope90	9.58	1.06	< 0.001
mpb90	318.13	19.87	< 0.001
hload	441.78	39.92	< 0.001
FM100	-53.20	8.99	< 0.001
FM1000	107.48	20.45	< 0.001

Table C2. Sequential autoregression models of burn severity (RdNBR) for the Adair-Howling fire.

Variable	β	SE	*P* value
Intercept	-537.31	163.81	0.001
elev	0.13	0.10	0.197
tpi	-6.20	1.54	< 0.001
slope	2.46	0.57	< 0.001
mpb180	488.02	75.76	< 0.001
hload90	678.75	82.74	< 0.001
FM100	2.90	3.05	0.342
FM1000	-8.20	3.84	0.033

Table C3. Sequential autoregression models of burn severity (RdNBR) for the Anaconda fire.

Variable	*β*	SE	*P* value
Intercept	-1722.74	278.46	< 0.001
elev	1.25	0.16	< 0.001
tpi45	33.26	3.03	< 0.001
slope	-0.69	0.62	0.261
mpb90	202.52	28.43	< 0.001
hload45	802.65	73.38	< 0.001
FM100	-18.13	5.88	0.002
FM1000	-4.54	18.55	0.807

Table C4. Sequential autoregression models of burn severity (RdNBR) for the Parke Peak fire.

Variable	*β*	SE	*P* value
Intercept	-54.08	346.31	0.876
elev	0.43	0.19	0.022
tpi90	7.23	11.74	0.538
slope	-1.05	1.32	0.426
mpb180	385.02	122.49	0.002
hload	81.27	87.08	0.351
FM100	-27.61	44.35	0.534
FM1000	2.38	20.84	0.909

Table C5. Sequential autoregression models of burn severity (RdNBR) for the Moose fire.

Variable	*β*	SE	*P* value
Intercept	-794.08	151.38	< 0.001
elev	1.04	0.09	< 0.001
tpi90	34.13	3.96	< 0.001
slope	-0.44	0.38	0.248
mpb180	560.23	45.28	< 0.001
hload	219.69	24.99	< 0.001
FM100	-8.38	3.84	0.029
FM1000	-27.36	7.45	< 0.001

Table C6. Sequential autoregression models of burn severity (RdNBR) for the Wolf Gun fire.

Variable	*β*	SE	*P* value
Intercept	-259.250	152.940	0.090
elev	0.008	0.076	0.917
tpi90	32.291	5.112	< 0.001
slope	2.796	0.500	< 0.001
mpb180	214.110	65.417	0.001
hload45	404.700	43.684	< 0.001
FM100	-14.264	5.892	0.015
FM1000	30.377	11.842	0.010

Table C7. Sequential autoregression models of burn severity (RdNBR) for the Wedge Canyon fire.

Variable	*β*	SE	*P* value
Intercept	-326.19	121.42	0.007
elev	0.57	0.05	< 0.001
tpi90	20.03	3.53	< 0.001
slope90	0.93	0.71	0.192
mpb90	144.80	17.37	< 0.001
hload45	309.71	30.32	< 0.001
FM100	5.53	4.32	0.200
FM1000	-31.15	12.57	0.013

Table C8. Sequential autoregression models of burn severity (RdNBR) for the Robert fire.

Variable	*β*	SE	*P* value
Intercept	583.27	142.50	< 0.001
elev	-0.10	0.05	0.026
tpi45	10.58	0.92	< 0.001
slope45	4.82	0.32	< 0.001
mpb	32.45	5.33	< 0.001
hload	280.21	18.64	< 0.001
FM100	-1.32	4.53	0.771
FM1000	-31.53	15.40	0.041

Table C9. Sequential autoregression models of burn severity (RdNBR) for the Middle Fork Complex fire.

Variable	*β*	SE	*P* value
Intercept	233.53	171.35	0.173
elev	0.26	0.06	< 0.001
tpi90	27.17	3.08	< 0.001
slope45	2.52	0.43	< 0.001
mpb90	-18.82	25.91	0.467
hload	189.88	18.72	< 0.001
FM100	1.18	5.58	0.832
FM1000	-44.34	19.38	0.022

Table C10. Sequential autoregression models of burn severity (RdNBR) for the Rampage fire.

Variable	*β*	SE	*P* value
Intercept	920.32	233.82	< 0.001
elev	0.05	0.05	0.289
tpi45	7.74	1.23	< 0.001
slope90	-2.85	0.81	< 0.001
mpb	43.69	15.51	0.005
hload	80.59	26.15	0.002
FM100	-0.27	9.98	0.978
FM1000	-42.38	27.72	0.126

Table C11. Sequential autoregression models of burn severity (RdNBR) for the Red Eagle fire.

Variable	*β*	SE	*P* value
Intercept	114.36	226.28	0.613
elev	0.28	0.06	< 0.001
tpi45	18.73	1.56	< 0.001
slope90	-6.81	0.81	< 0.001
mpb90	172.60	34.45	< 0.001
hload	150.45	28.75	< 0.001
FM100	-70.73	17.31	< 0.001
FM1000	58.14	21.51	0.007